



(12)

Rettet oversættelse af
europæisk patentskriftPatent- og
Varemærkestyrelsen

(51) Int.Cl.: **A 61 K 48/00 (2006.01)**
C 12 N 15/12 (2006.01) **A 61 P 21/00 (2006.01)**
C 12 N 15/85 (2006.01) **C 07 K 14/47 (2006.01)**

(45) Oversættelsen bekendtgjort den: **2024-09-16**

(80) Dato for Den Europæiske Patentmyndigheds
bekendtgørelse om meddelelse af patentet: **2024-03-13**

(86) Europæisk ansøgning nr.: **17783207.8**

(86) Europæisk indleveringsdag: **2017-04-14**

(87) Den europæiske ansøgnings publiceringsdag: **2019-02-20**

(86) International ansøgning nr.: **US2017027583**

(87) Internationalt publikationsnr.: **WO2017180976**

(30) Prioritet: **2016-04-15 US 201662323333 P** **2016-12-13 US 201662433548 P**

(84) Designerede stater: **AL AT BE BG CH CY CZ DE DK EE ES FI FR GB GR HR HU IE IS IT LI LT LU LV MC MK MT NL NO PL PT RO RS SE SI SK SM TR**

(73) Patenthaver: **Research Institute at Nationwide Children's Hospital, 700 Children's Drive, Room W172, Columbus, Ohio 43205, USA**

(72) Opfinder: **RODINO-KLAPAC, Louise, 4912 Bixby Ridge Drive E, Groveport, OH 43125, USA**
MENDELL, Jerry, R., 8176 Copperfield Drive, Columbus, OH 43235, USA

(74) Fuldmægtig i Danmark: **RWS Group, Europa House, Chiltern Park, Chiltern Hill, Chalfont St Peter, Bucks SL9 9FG, Storbritannien**

(54) Benævnelse: **ADENOASSOCIERET VIRUSVEKTORFREMFRØRING AF β-SARCOGLYCAN OG MIKRORNA-29 OG BEHANDLING AF MUSKELDYSTROFI**

(56) Fremdragne publikationer:
US-A- 5 672 694
US-A1- 2006 154 250
US-A1- 2011 301 226
POZSGAI ET AL: "172. Pre-Clinical Efficacy Study of Beta-Sarcoglycan Gene Transfer", MOLECULAR THERAPY, vol. 21, no. suppl. 1, 1 May 2013 (2013-05-01), page s68, XP55433494, United States
ZANOTTI SIMONA ET AL: "Opposing roles of miR-21 and miR-29 in the progression of fibrosis in Duchenne muscular dystrophy", BIOCHIMICA ET BIOPHYSICA ACTA. MOLECULAR BASIS OF DISEASE, AMSTERDAM, NL, vol. 1852, no. 7, 17 April 2015 (2015-04-17), pages 1451-1464, XP029232473, ISSN: 0925-4439, DOI: 10.1016/J.BBADIS.2015.04.013
BAODONG SUN ET AL: "Correction of Multiple Striated Muscles in Murine Pompe Disease Through Adeno-associated Virus-mediated Gene Therapy", MOLECULAR THERAPY, vol. 16, no. 8, 17 June 2008 (2008-06-17), pages 1366-1371, XP055080604, ISSN: 1525-0016, DOI: 10.1038/mt.2008.133
POZSGAI et al.: "beta-Sarcoglycan Gene Transfer Leads to Functional Improvement in a Model of LGMD2E (S61.002", Neurology, vol. 82, no. 10, suppl., 8 April 2014 (2014-04-08), page 1 of 1, XP009513811, ISSN: 0028-

3878

POZSGAI et al.: "172. Pre-Clinical Efficacy Study of Beta-Sarcoglycan Gene Transfer", Molecular Therapy, vol. 21, no. Suppl. 1, 1 May 2013 (2013-05-01), page S68, XP055433494,

DESCRIPTION

Description

FIELD OF THE INVENTION

[0001] Described herein are therapy vectors such as AAV vectors expressing β -sarcoglycan and their use for reducing and preventing fibrosis in subjects suffering from a muscular dystrophy. Also described are combination gene therapy methods comprising the administration of a first AAV vector expressing β -sarcoglycan and a second AAV vector expressing miR-29 to reduce and prevent fibrosis in patients suffering from muscular dystrophy.

BACKGROUND

[0002] Limb-girdle muscular dystrophy (LGMD) type 2E (LGMD2E) is an autosomal recessive disorder resulting from mutations in the gene encoding β -sarcoglycan (SGCB), causing loss of functional protein.¹ LGMD2E represents a relatively common and severe form of LGMD in the United States with worldwide reports of incidence of 1/200,000-1/350,000.⁽²⁾ The absence of β -sarcoglycan leads to a progressive dystrophy with chronic muscle fiber loss, inflammation, fat replacement and fibrosis, all resulting in deteriorating muscle strength and function. ^(3,4) As a complex, the sarcoglycans (α -, β -, γ -, δ -), ranging in size between 35 and 50 kD,⁽⁵⁾ are all transmembrane proteins that provide stability to the sarcolemma offering protection from mechanical stress during muscle activity.⁽³⁾ Loss of 3-sarcoglycan in LGMD2E usually results in varying degrees of concomitant loss of other sarcoglycan proteins contributing to the fragility of the muscle membrane leading to loss of myofibers.¹ Although the range of clinical phenotype of LGMD2E varies, diagnosis typically occurs before age 10 and with loss of ambulation occurring by mid to late teens.^{1,6,7} Patients present with elevated serum creatine kinase (CK), proximal muscle weakness, difficulty arising from the floor and progressive loss of ambulation. Cardiac involvement occurs in as many as fifty percent of cases

[0003] Adeno-associated virus (AAV) is a replication-deficient parvovirus, the single-stranded DNA genome of which is about 4.7 kb in length including two 145 nucleotide inverted terminal repeat (ITRs). There are multiple serotypes of AAV. The nucleotide sequences of the genomes of the AAV serotypes are known. For example, the complete genome of AAV-1 is provided in GenBank Accession No. NC_002077; the complete genome of AAV-2 is provided in GenBank Accession No. NC_001401 and Srivastava et al., J. Virol., 45: 555-564 {1983}; the complete genome of AAV-3 is provided in GenBank Accession No. NC_1829; the complete genome of

AAV-4 is provided in GenBank Accession No. NC_001829; the AAV-5 genome is provided in GenBank Accession No. AF085716; the complete genome of AAV-6 is provided in GenBank Accession No. NC_001862; at least portions of AAV-7 and AAV-8 genomes are provided in GenBank Accession Nos. AX753246 and AX753249, respectively; the AAV-9 genome is provided in Gao et al., *J. Virol.*, 78: 6381-6388 (2004); the AAV-10 genome is provided in *Mol. Ther.*, 13(1): 67-76 (2006); and the AAV-11 genome is provided in *Virology*, 330(2): 375-383 (2004). The sequence of the AAV rh.74 genome is provided in see U.S. Patent 9,434,928. Cis-acting sequences directing viral DNA replication (rep), encapsidation/packaging and host cell chromosome integration are contained within the AAV ITRs. Three AAV promoters (named p5, p19, and p40 for their relative map locations) drive the expression of the two AAV internal open reading frames encoding rep and cap genes. The two rep promoters (p5 and p19), coupled with the differential splicing of the single AAV intron (at nucleotides 2107 and 2227), result in the production of four rep proteins (rep 78, rep 68, rep 52, and rep 40) from the rep gene. Rep proteins possess multiple enzymatic properties that are ultimately responsible for replicating the viral genome. The cap gene is expressed from the p40 promoter and it encodes the three capsid proteins VP1, VP2, and VP3. Alternative splicing and non-consensus translational start sites are responsible for the production of the three related capsid proteins. A single consensus polyadenylation site is located at map position 95 of the AAV genome. The life cycle and genetics of AAV are reviewed in Muzyczka, *Current Topics in Microbiology and Immunology*, 158: 97-129 (1992).

[0004] AAV possesses unique features that make it attractive as a vector for delivering foreign DNA to cells, for example, in gene therapy. AAV infection of cells in culture is noncytopathic, and natural infection of humans and other animals is silent and asymptomatic. Moreover, AAV infects many mammalian cells allowing the possibility of targeting many different tissues *in vivo*. Moreover, AAV transduces slowly dividing and non-dividing cells, and can persist essentially for the lifetime of those cells as a transcriptionally active nuclear episome (extrachromosomal element). The AAV proviral genome is inserted as cloned DNA in plasmids, which makes construction of recombinant genomes feasible. Furthermore, because the signals directing AAV replication and genome encapsidation are contained within the ITRs of the AAV genome, some or all of the internal approximately 4.3 kb of the genome (encoding replication and structural capsid proteins, rep-cap) may be replaced with foreign DNA. To generate AAV vectors, the rep and cap proteins may be provided in trans. Another significant feature of AAV is that it is an extremely stable and hearty virus. It easily withstands the conditions used to inactivate adenovirus (56° to 65°C for several hours), making cold preservation of AAV less critical. AAV may even be lyophilized. Finally, AAV-infected cells are not resistant to superinfection.

[0005] Multiple studies have demonstrated long-term (> 1.5 years) recombinant AAV-mediated protein expression in muscle. See, Clark et al., *Hum Gene Ther*, 8: 659-669 (1997); Kessler et al., *Proc Nat. Acad Sc. USA*, 93: 14082-14087 (1996); and Xiao et al., *J Virol*, 70: 8098-8108 (1996). See also, Chao et al., *Mol Ther*, 2:619-623 (2000) and Chao et al., *Mol Ther*, 4:217-222 (2001). Moreover, because muscle is highly vascularized, recombinant AAV transduction has resulted in the appearance of transgene products in the systemic circulation following

intramuscular injection as described in Herzog et al., Proc Natl Acad Sci USA, 94: 5804-5809 (1997) and Murphy et al., Proc Natl Acad Sci USA, 94: 13921-13926 (1997). Moreover, Lewis et al., J Virol, 76: 8769-8775 (2002) demonstrated that skeletal myofibers possess the necessary cellular factors for correct antibody glycosylation, folding, and secretion, indicating that muscle is capable of stable expression of secreted protein therapeutics.

[0006] An emerging form of therapy for LGMD2E is viral-mediated gene delivery to restore wild-type protein to affected muscle resulting in restoration of muscle function. Considering that a subset of patients can develop cardiomyopathy, (8, 9, 10, 13) this would have to be considered in the long-term care of these patients. In previous reports, the Sgcb-null mouse was well characterized. Araishi et al.³ developed the β -sarcoglycan-deficient mouse with accompanying loss of all of the sarcoglycans as well as sarcospan, with at least minor preservation of merosin, the dystroglycans and dystrophin, reproducing the clinical picture seen in LGMD2E. The histological changes in this animal model were also a prototype for the clinical counterpart, including the prominence of skeletal muscle fibrosis.(14) Dressman et al. (25) injected the transverse abdominal muscle using rAAV2.CMV.SGCB. Expression persisted for 21 months and muscle fibers were protected from recurrent necrosis. The use of self-complementary AAV to enhance transgene expression,¹⁶ a muscle-specific promoter to better target skeletal muscle (20, 26) and the optimization of a human β -sarcoglycan gene (hSGCB) has also been described.

[0007] Functional improvement in patients suffering from LGMD and other muscular dystrophies require both gene restoration and reduction of fibrosis. There is a need for methods of reducing fibrosis that may be paired with gene restoration methods for more effective treatments of LGMD and other muscular dystrophies.

SUMMARY

[0008] Described herein are gene therapy vectors, e.g. AAV, expressing the β -sarcoglycan gene and methods of delivering β -sarcoglycan to the muscle to reduce and/or prevent fibrosis; and/or to increase muscular force, and/or to treat a β -sarcoglycanopathy in a mammalian subject suffering from muscular dystrophy.

[0009] Also described herein are gene therapy vectors for use delivering β -sarcoglycan in combination therapies and approaches to address the gene defect observed in LGMD2E and gene therapy vectors delivering miR-29 to further suppress fibrosis.

[0010] In one aspect, the invention provides a recombinant AAV vector comprising a polynucleotide sequence encoding β -sarcoglycan, wherein the polynucleotide sequence comprises a nucleotide sequence at least 95% identical to SEQ ID NO: 1. In some embodiments, the polynucleotide sequence encoding β -sarcoglycan comprises a sequence e.g. at least 96%, 97%, 98%, 99% or more identical to the nucleotide sequence set forth in SEQ ID NO: 1 and encodes protein that retains β -sarcoglycan activity. In some embodiments,

the polynucleotide sequence encoding β -sarcoglycan comprises the nucleotide sequence set forth in SEQ ID NO: 1. In some embodiments, the polynucleotide sequence encoding β -sarcoglycan consists the nucleotide sequence set forth in SEQ ID NO: 1.

[0011] In another aspect, the invention provides a recombinant AAV vector comprising a polynucleotide sequence encoding β -sarcoglycan that is at least 95% identical to SEQ ID NO: 2.

[0012] In another aspect, the invention provides a composition comprising the recombinant AAV vector of the invention.

[0013] In another aspect, the invention provides a composition comprising the recombinant AAV vector of the invention for use in reducing fibrosis in a subject in need thereof.

[0014] In another aspect, the invention provides a composition comprising the recombinant AAV vector of the invention for use in treating β -sarcoglycanopathy in a subject in need thereof.

[0015] In another aspect, the invention provides a composition comprising the recombinant AAV vector of the invention for the treatment of muscular dystrophy.

[0016] In another aspect, the invention provides a composition comprising the recombinant AAV vector of the invention for use in treatment of muscular dystrophy, optionally wherein the muscular dystrophy is limb-girdle muscular dystrophy (LGMD), and optionally wherein the LGMD is LGMD2E.

[0017] In another aspect, a recombinant AAV vector described herein comprises a polynucleotide sequence encoding β -sarcoglycan that has at least 96%, 97%, 98% or 99% sequence identity to the amino acid sequence of SEQ ID NO: 2, and the protein retains β -sarcoglycan activity.

[0018] In another aspect, described herein is a recombinant AAV vector comprising a polynucleotide sequence encoding functional β -sarcoglycan that comprises a nucleotide sequence that hybridizes under stringent conditions to the nucleic acid sequence of SEQ ID NO: 1, or a complement thereof.

[0019] The term "stringent" is used to refer to conditions that are commonly understood in the art as stringent. Hybridization stringency is principally determined by temperature, ionic strength, and the concentration of denaturing agents such as formamide. Examples of stringent conditions for hybridization and washing are 0.015 M sodium chloride, 0.0015 M sodium citrate at 65-68°C or 0.015 M sodium chloride, 0.0015M sodium citrate, and 50% formamide at 42°C. See Sambrook et al., Molecular Cloning: A Laboratory Manual, 2nd Ed., Cold Spring Harbor Laboratory, (Cold Spring Harbor, N.Y. 1989). More stringent conditions (such as higher temperature, lower ionic strength, higher formamide, or other denaturing agent) may also be used, however, the rate of hybridization will be affected. In instances

wherein hybridization of deoxyoligonucleotides is concerned, additional exemplary stringent hybridization conditions include washing in 6x SSC 0.05% sodium pyrophosphate at 37°C (for 14-base oligos), 48°C (for 17-base oligos), 55°C (for 20-base oligos), and 60°C (for 23-base oligos).

[0020] Other agents may be included in the hybridization and washing buffers for the purpose of reducing non-specific and/or background hybridization. Examples are 0.1% bovine serum albumin, 0.1% polyvinyl-pyrrolidone, 0.1% sodium pyrophosphate, 0.1% sodium dodecylsulfate, NaDODSO₄, (SDS), ficoll, Denhardt's solution, sonicated salmon sperm DNA (or other non-complementary DNA), and dextran sulfate, although other suitable agents can also be used. The concentration and types of these additives can be changed without substantially affecting the stringency of the hybridization conditions. Hybridization experiments are usually carried out at pH 6.8-7.4, however, at typical ionic strength conditions, the rate of hybridization is nearly independent of pH. See Anderson et al., Nucleic Acid Hybridisation: A Practical Approach, Ch. 4, IRL Press Limited (Oxford, England). Hybridization conditions can be adjusted by one skilled in the art in order to accommodate these variables and allow DNAs of different sequence relatedness to form hybrids.

[0021] In another aspect, the polynucleotide sequence may be operably linked to a muscle-specific control element. For example the muscle-specific control element is human skeletal actin gene element, cardiac actin gene element, myocyte-specific enhancer binding factor MEF, muscle creatine kinase (MCK), tMCK (truncated MCK), myosin heavy chain (MHC), MHCK7 (a hybrid version of MHC and MCK), C5-12 (synthetic promoter), murine creatine kinase enhancer element, skeletal fast-twitch troponin C gene element, slow-twitch cardiac troponin C gene element, the slow-twitch troponin I gene element, hypozia-inducible nuclear factors, steroid-inducible element or glucocorticoid response element (GRE).

[0022] In some embodiments, the muscle-specific promoter is MHCK7 (SEQ ID NO: 4). An exemplary rAAV described herein is pAAV.MHCK7.hSCGB which comprises the nucleotide sequence of SEQ ID NO: 3; wherein the MCHK7 promoter spans nucleotides 130-921, a SV40 chimeric intron spans nucleotides 931-1078, the β -sarcoglycan sequence spans nucleotides 1091-2047 and the poly A spans nucleotides 2054-2106.

[0023] In some embodiments, the muscle-specific promoter is tMCK (SEQ ID NO: 6). An exemplary rAAV described herein is pAAV.tMCK.hSCGB which comprises the nucleotide sequence of SEQ ID NO: 5; wherein the tMCK promoter spans nucleotides 141-854, an SV40 chimeric intron spans nucleotides 886-1018, the β -sarcoglycan sequence spans nucleotides 1058-2014 and the poly A spans nucleotides 2021-2073.

[0024] The AAV can be any serotype, for example AAV1, AAV2, AAV3, AAV4, AAV5, AAV6, AAV7, AAV8, AAV9, AAV-10, AAV-11, AAV-12, AAV-13 and AAV rh.74. Production of pseudotyped rAAV is disclosed in, for example, WO 01/83692. Other types of rAAV variants, for example rAAV with capsid mutations, are also contemplated. See, for example, Marsic et al., Molecular Therapy, 22(11): 1900-1909 (2014).

[0025] Compositions comprising any of the rAAV vectors described herein are also contemplated.

[0026] Methods of producing a recombinant AAV vector particle comprising culturing a cell that has been transfected with any recombinant AAV vector described herein and recovering recombinant AAV particles from the supernatant of the transfected cells are also described. Viral particles comprising any of the recombinant AAV vectors described herein are also contemplated

[0027] The invention also provides compositions of the invention for use in methods of reducing fibrosis in a mammalian subject in need thereof is also provided. In this regard, the method comprises administering a therapeutically effective amount of an AAV vector described herein (or composition comprising an AAV vector described herein) to the mammalian subject. In some embodiments, the mammalian subject suffers from muscular dystrophy. In some embodiments, administration of an AAV vector described herein (or composition comprising an AAV vector described herein) reduces fibrosis in skeletal muscle or in cardiac muscle of the subject. These methods may further comprise the step of administering a second recombinant AAV vector comprising a polynucleotide sequence comprising miR29C.

[0028] The term "muscular dystrophy" as used herein refers to a disorder in which strength and muscle bulk gradually decline. Non-limiting examples of muscular dystrophy diseases may include Becker muscular dystrophy, tibial muscular dystrophy, Duchenne muscular dystrophy, Emery-Dreifuss muscular dystrophy, facioscapulohumeral muscular dystrophy, sarcoglycanopathies, congenital muscular dystrophy such as congenital muscular dystrophy due to partial LAMA2 deficiency, merosin-deficient congenital muscular dystrophy, type 1D congenital muscular dystrophy, Fukuyama congenital muscular dystrophy, limb-girdle type 1A muscular dystrophy, limb-girdle type 2A muscular dystrophy, limb-girdle type 2B muscular dystrophy, limb-girdle type 2C muscular dystrophy, limb-girdle type 2D muscular dystrophy, limb-girdle type 2E muscular dystrophy, limb-girdle type 2F muscular dystrophy, limb-girdle type 2G muscular dystrophy, limb-girdle type 2H muscular dystrophy, limb-girdle type 2I muscular dystrophy, limb-girdle type 2J muscular dystrophy, limb-girdle type 2K muscular dystrophy, limb-girdle type 1C muscular dystrophy, rigid spine muscular dystrophy with epidermolysis bullosa simplex, oculopharyngeal muscular dystrophy, Ullrich congenital muscular dystrophy, and Ullrich scleroatonic muscular dystrophy. In some embodiments, the subject is suffering from limb-girdle muscular dystrophy. In some embodiments, the subject is suffering from limb-girdle muscular dystrophy type 2E (LGMD2E).

[0029] The term "fibrosis" as used herein refers to the excessive or unregulated deposition of extracellular matrix (ECM) components and abnormal repair processes in tissues upon injury including skeletal muscle, cardiac muscle, liver, lung, kidney, and pancreas. The ECM components that are deposited include collagen, e.g. collagen 1, collagen 2 or collagen 3, and fibronectin.

[0030] Described herein is an effective amount of an AAV vector described herein (or a composition comprising an AAV vector described herein) for use in increasing muscular force/muscle mass to the mammalian subject.

[0031] In any of the methods described herein, the subject may be suffering from muscular dystrophy such as limb-girdle muscular dystrophy or any other dystrophin-associated muscular dystrophy.

[0032] The invention also provides compositions of the invention for use in a method of treating muscular dystrophy in a mammalian subject comprising administering a therapeutically effective amount of an AAV vector described herein (or composition comprising an AAV vector described herein) to the mammalian subject. In some embodiments, the muscular dystrophy is limb-girdle muscular dystrophy. Any of the methods described herein may further comprise the step of administering a second recombinant AAV vector comprising a polynucleotide sequence comprising miR29C.

[0033] Combination therapies are also contemplated. In this regard, any of the foregoing methods described here may further comprise administering a second recombinant AAV vector comprising a polynucleotide sequence comprising miR29C. In some embodiments, the polynucleotide comprising miR29C is operably linked operably linked to a muscle-specific control element. For example the muscle-specific control element is human skeletal actin gene element, cardiac actin gene element, myocyte-specific enhancer binding factor MEF, muscle creatine kinase (MCK), tMCK (truncated MCK), myosin heavy chain (MHC), MHCK7 (a hybrid version of MHC and MCK), C5-12 (synthetic promoter), murine creatine kinase enhancer element, skeletal fast-twitch troponin C gene element, slow-twitch cardiac troponin C gene element, the slow-twitch troponin I gene element, hypoxia-inducible nuclear factors, steroid-inducible element or glucocorticoid response element (GRE). In some embodiments, the second recombinant vector comprises a polynucleotide sequence set forth in SEQ ID NO: 9 or SEQ ID NO: 8, as described in U.S. Provisional Application No. 62/323,163.

[0034] In combination therapy methods described herein in which both an rAAV vector expressing β -sarcoglycan and an rAAV vector expressing miR29c are administered to the mammalian subject, the rAAV vectors may be administered concurrently, or administered consecutively with the rAAV vector expressing β -sarcoglycan being administered immediately before or after the rAAV expressing miR29c. Alternatively, the AAV vector expressing β -sarcoglycan is administered within about 1-24 hours (e.g., 1, 2, 3, 4, 5, 6, 7, 8, 9, 10, 11, 12, 13, 14, 15, 16, 17, 18, 19, 20, 21, 22, 23 or 24 hours) after administering the rAAV expressing miR-29 or the methods described herein are carried out wherein the AAV vector expressing the β -sarcoglycan is administered within about 1-24 hours (e.g., 1, 2, 3, 4, 5, 6, 7, 8, 9, 10, 11, 12, 13, 14, 15, 16, 17, 18, 19, 20, 21, 22, 23 or 24 hours) before administering the rAAV expressing miR-29. In some embodiments, the AAV vector expressing β -sarcoglycan is administered within about 1-5 hours (e.g., 1, 2, 3, 4 or 5 hours) after administering the rAAV expressing miR-29 or the methods described herein are carried out wherein the AAV vector expressing the β -sarcoglycan is administered within about 1-5 hours (e.g., 1, 2, 3, 4 or 5 hours) before administering the rAAV expressing miR-29.

hours) before administering the rAAV expressing miR-29c.

[0035] In any of the methods described herein, the rAAV is administered by intramuscular injection or intravenous injection. In addition, in any of the method described herein, the rAAV is administered systemically, such as parental administration by injection, infusion or implantation.

[0036] The compositions of the invention are formulated for intramuscular injection or intravenous injection. In addition, the compositions of the invention are formulated for systemic administration, such as parental administration by injection, infusion or implantation.

[0037] In addition, any of the compositions formulated for administration to a subject suffering from muscular dystrophy (such as limb-girdle muscular dystrophy or any other dystrophin-associated muscular dystrophy). In some embodiments, the composition may further comprise a second recombinant AAV vector comprising a polynucleotide sequence set forth in SEQ ID NO: 9 or SEQ ID NO: 8.

[0038] In any of the uses described herein, the medicament is formulated for intramuscular injection or intravenous injection. In addition, in any of the uses described herein, the medicament is formulated for systemic administration, such as parental administration by injection, infusion or implantation. In addition, any of the medicaments may be prepared for administration to a subject suffering from muscular dystrophy (such as limb-girdle muscular dystrophy or any other dystrophin associated muscular dystrophy). In some embodiments, the medicament may further comprise a second recombinant AAV vector comprising a polynucleotide sequence set forth in SEQ ID NO: 9 or SEQ ID NO: 8.

BRIEF DESCRIPTION OF THE FIGURES

[0039]

Figures 1A-1D demonstrate that AAV mediated β -sarcoglycan expression restores dystrophin-associated proteins and protects membrane integrity. (a) Self-complementary AAV vector containing the codon-optimized human β -sarcoglycan gene (hSGCB) driven by the muscle-specific tMCK promoter. The cassette also contains a chimeric intron to augment processing and polyadenylation signal for stability. (b) Immunofluorescence staining with anti- β -SG antibody shows high levels of sarcolemmal staining of the SGCB transgene in 5-week-old mice both 6 and 12 weeks post injection, $\times 20$ images shown. Percentage of fibers expressing beta-sarcoglycan per TA muscle averaged $88.4 \pm 4.2\%$ after 6 weeks (n=9, 4 male, 5 female) and $76.5 \pm 5.8\%$ after 12 weeks (n=6, 4 male, 2 female). Protein expression confirmed in the western blot with gamma-tubulin blot shown for a loading control. (c) AAV delivery of β -sarcoglycan leads to restoration of other members of the sarcoglycan complex; α -sarcoglycan, dystrophin, $\times 20$ images. (d) scAAVrh.74.hSGCB protects sgcb/- membranes from damage. Image showing a large area of Evans blue-positive fibers (red) juxtaposed to a cluster of β -

sarcoglycan-positive fibers that have been protected from Evans blue dye incorporation, $\times 40$ image is shown.

Figures 2A-2D shows the histological analysis of β -SG-deficient treated skeletal muscle. scAAVrh.74.hSGCB treatment normalizes histological parameters of $sgcb^{-/-}$ mice. Hematoxylin & Eosin staining and Picosirius Red staining were performed on TA muscle from $sgcb^{-/-}$ mice along with normal control C57/BL6 mice and scAAVrh.74.hSGCB-treated mice followed by quantification of histological parameters and % collagen staining. (a) H&E staining shows the presence of centrally nucleated fibers, inflammatory cells and large fiber diameter distribution in β -SG-deficient muscle and an improvement in histopathology following gene transfer. (b) Picosirius Red staining shows a decrease in red collagen staining in treated muscle. (c) Quantification of centrally nucleated fibers showing a decrease following treatment ($P<0.0005$, one-way ANOVA) and (d) representation of fiber size distribution and increase in average fiber size of TA muscle from C57/BL6 controls and $sgcb^{-/-}$ mice compared with treated mice ($P<0.0001$, one-way ANOVA). (e) Quantification of % collagen in TA muscle from C57/BL6 controls and $sgcb^{-/-}$ mice compared with $sgcb^{-/-}$ -treated mice ($P<0.0001$, one-way ANOVA). 100 μ m scale bar shown for $\times 20$ images. *** $P<0.001$; **** $P<0.0001$.

Figures 3A-3C shows that scAAVrh.74.hSGCB intramuscular delivery corrects tetanic force and resistance to contraction-induced injury. The TA muscle of $sgcb^{-/-}$ mice treated with 3×10^{10} vg of scAAVrh.74.hSGCB via an IM injection was harvested 6 weeks post gene transfer, and subjected to a protocol to assess tetanic force and an eccentric contraction protocol to assess resistance to contraction-induced injury. (a) AAVrh.74.hSGCB-treated TA's demonstrated significant improvement in both absolute tetanic force ($P<0.01$, paired t-test) and (b) normalized specific force ($P<0.05$, paired t-test), which was not different from wild-type force (C57BL6). (c) AAVrh.74.hSGCB treated TA's exhibited significant improvement in resistance to contraction-induced injury compared with untreated $sgcb^{-/-}$ controls ($P<0.01$, two-way ANOVA). Force retention following 10 contractions is shown. * $P<0.05$; ** $P<0.01$.

Figures 4A-4C shows the results of the analysis of aged mice treated intramuscularly with scAAVrh.74.tMCK.hSGCB. (a) Immunofluorescence staining of TA muscle from 6-month-old treated $sgcb^{-/-}$ mice 12 weeks post injection ($n=5$, 5 male) shows sarcolemmal expression of the SGCB transgene at levels averaging 80% in injected mice compared with untreated ($n=4$, 4 male), (b) Picosirius red staining of the treated and untreated TA muscle. (c) Quantitation of collagen present in the Picosirius red stained tissue shows a significant reduction in the amount of collagen following treatment with rAAVrh.74.tMCK.hSGCB ($P<0.0001$, one-way ANOVA). 100 μ m scale bar shown for $\times 20$ images. **** $P<0.0001$.

Figures 5A-5C show the results of vascular delivery of scAAVrh.74.hSGCB. Four ($n=5$, 5 male) and five ($n=4$, 2 male, 2 female) weeks β -SG-deficient mice were treated with vector via the femoral artery to deliver the vector to the lower limb muscles. At a dose of 5×10^{11} vg, β -SG expression was $90.6 \pm 2.8\%$ in the TA and $91.8 \pm 4.7\%$ in the GAS of treated mice accompanied by improvements in histopathology that resulted in significant improvement in specific force

compared with untreated animals even following an injury paradigm, (a) β -SG protein expression from three representative mice. Muscle from a β -SG KO untreated mouse is shown for comparison in the inset (lower right), $\times 20$ Images are shown. Expression in treated muscles confirmed via western blot and gamma-tubulin is shown as a loading control. (b) Histopathology is significantly improved following high dose treatment. Upper panels-treated TA and gastrocnemius muscles. Bottom panels-untreated β -SG-deficient control muscle. 100 μ m scale bar shown for $\times 20$ images. (c) Percentage of specific force retained in EDL muscle following 10 cycles of eccentric contraction-induced injury. Treatment with 5×10^{11} vg of AAVrh.74.hSGCB led to significant improvement in force that was equivalent to WT (normal) control muscle ($P < 0.05$, one-way ANOVA). * $P < 0.05$.

Figures 6A-6B show reduction of fibrosis in ILP-treated β -SG KO mice. (a) Picosirius red staining shows reduced fibrosis in treated mice indicated by a decrease in collagen deposition compared with untreated $sgcb^{-/-}$ mice. (b) Quantification of collagen levels in the TA and GAS muscles from BL6 WT, untreated $sgcb^{-/-}$ mice, and treated mice confirm reduction in collagen levels in treated mice ($P < 0.001$, one-way ANOVA). 100 μ m scale bar shown for $\times 20$ images. *** $P < 0.001$.

Figures 7A and 7B show vector biodistribution and protein expression. (a) Histogram of average distribution of vector in harvested tissues from ILP-treated mice given in copies of transcript per microgram of DNA added to qPCR. Left limb was treated. (b) No protein expression via western blot seen in off target organs.

Figure 8A-D provide histological and functional deficits in $sgcb^{-/-}$ mice at 7 months of age. Trichome staining in the diaphragm (A) and heart (C) of SGCB $^{-/-}$ mice shows extensive fibrosis (red). The force output from the diaphragm is significantly reduced in the diaphragm (B) and the cardiac ejection fraction is also reduced in $sgcb^{-/-}$ mice (D).

Figure 9 provides a schematic of therapeutic β -sarcoglycan transgene cassette. Self-complementary AAV vector containing the codon-optimized human β -sarcoglycan gene (hSGCB). A muscle specific MHCK7 promoter drives expression. The cassette also contains a chimeric intron to augment processing and polyadenylation signal for stability.

Figure 10 provides immunofluorescence staining for β -sarcoglycan in various skeletal muscles demonstrates robust expression with rare negative fibers after 1, 4, or 6 months of treatment (1 month shown).

Figure 11 provides immunofluorescence staining for β -sarcoglycan in diaphragm and heart demonstrates robust expression with rare negative fibers after 1, 4, or 6 months of treatment (1 month shown).

Figure 12A-D depicts restoration of SGCB expression following intravenous delivery of scAAVrh.74.MHCK7.hSGCB. (A) scAAVrh.74.MHCK7.hSGCB cassette. (b) Immunofluorescence imaging 6 months post-injection of skeletal muscles, diaphragm, and heart from $sgcb^{-/-}$ mice intravenously injected with 1e12 vg total dose

scAAVrh.74.MHCK7.hSGCB. Representative images of skeletal muscles displaying an average of $98.13 \pm 0.31\%$ transduction. 20X images are shown. Representative images of heart tissue displaying high levels of hSGCB transgene expression. 10X images are shown. (c) Western blotting of all muscles from one treated *sgcb*^{-/-} mouse confirming hSGCB transgene expression. (d) Western blotting for hSGCB expression in hearts of five *sgcb*^{-/-} treated mice with densitometry quantification showing overexpression of hSGCB up to 72.0% of BL6 WT levels.

Figure 13A-D depicts the effect of systemic treatment with scAAVrh74.MHCK7.hSGCB on muscle pathology, (a) H&E stain of diaphragm and QUAD muscle from C57BL/6 WT, *sgcb*^{-/-}, and scAAVrh.74.MHCK7.hSGCB treated mice showing normalized histopathology. (b) Quantification of reduction in centrally nucleated fibers in *sgcb*^{-/-} treated muscle compared to untreated *sgcb*^{-/-} muscle (TA, GAS, GLUT, diaphragm, $p<0.0001$) (QUAD, PSOAS, TRI, $p<0.05$). (c) Normalization of fiber distribution in GAS, PSOAS, and TRI, and (d) increase in average fiber size in treated muscles compared to untreated *sgcb*^{-/-} muscles ($p<0.001$) (ONE-WAY ANOVA) ($n=5$ per group).

Figure 14A and 14B depict reduced collagen deposition in intravenous treated β -SG KO mice. (a) Picosirius red staining showed reduced fibrosis in treated mice indicated by a decrease in collagen deposition compared to untreated *sgcb*^{-/-} mice in diaphragm and GAS. (b) Quantification of collagen levels in the diaphragm and GAS muscles from C57BL/6 WT mice ($n=4$), untreated *sgcb*^{-/-} mice ($n=4$), and treated *sgcb*^{-/-} mice ($n=5$) confirm reduction in collagen levels in both treated muscles ($p<0.0001$, ONE-WAY ANOVA). 100 μ m scale bar shown for 20X images.

Figure 15 demonstrates delivery of scAAVrh.74.MHCK7.hSGCB via the tail vein of *sgcb*^{-/-} mice completely restores force in the diaphragm, following 6 months of treatment (IV administration (1e12vg)). Diaphragm muscle strips were harvested from treated and control SGCB^{-/-} mice and WT mice and subjected to force measurements, treatment restored force to WT levels.

Figure 16 provides a schematic of rAAV vector scAACrh.74.CMV.miR29c and the nucleotide sequence of the miR-29c in a natural miR-30 backbone.

Figure 17 demonstrates that following 3 months of treatment with AAVrh.74.CMV.miR29C, TA muscles were harvested from treated and control SGCB^{-/-} mice and WT mice and analyzed for fibrosis (collagen levels) ($n=5$ per group). Using sirius red staining and quantification, collagen levels were reduced following treatment (see figure 18). Results indicated that transcript levels of Col1A, Col3A, and Fbn were normalized and muscle fiber size was increased.

Figure 18 provides representative images of scanned full sections of untreated and AAVrh.74.CMV.miR29C treated tibialis anterior muscles stained with Sirius Red which stains for collagen 1 and 3. Quantification is shown in Figure 17

Figure 19A and 19B demonstrate correction of kyphoscoliosis in thoracic spine. (a) Kyphoscoliosis in *sgcb*^{-/-} mice as evidenced by X-ray radiography. (b) The Kyphotic Index (KI)

score of *sgcb*^{-/-} mice (3.69) is low compared to C57BL/6 WT (6.01) (p<0.01), but increases upon treatment with scAAVrh.74.MHCK7.hSGCB (5.39) (p<0.05 compared to *sgcb*^{-/-}) (ONE-WAY ANOVA) (n=6 per group).

Figure 20A-D provide the assessment of cardiomyopathy in heart muscle. (a) H&E and picrosirius red stains of 7 month old BL6 WT, *sgcb*^{-/-}, and AAV.MHCK7.hSGCB treated *sgcb*^{-/-} hearts 6 months post-treatment indicating myocardial degeneration in untreated *sgcb*^{-/-} muscle and improvement following treatment. (b) Cardiac MRI analysis showing reduction in *sgcb*^{-/-} hearts in stroke volume (p<0.01), cardiac output, and ejection fraction (p<0.05) (ONE-WAY ANOVA) and improvements 6 months after treatment (n=6 per group). (c) Western blotting of two C57BL/6 WT hearts, two *sgcb*^{-/-} hearts, and five AAV.MHCK7.hSGCB treated *sgcb*^{-/-} hearts showing decreased cardiac troponin I levels in diseased mice. (d) Densitometry quantification showing reduction of cardiac troponin I (cTrpI) to 60.38% of BL6 WT levels and an overexpression of up to 135.8% of BL6 WT levels.

Figure 21A-B demonstrates diaphragm function correction and increased open-field cage activity. (a) Diaphragm muscle strips were harvested to measure force and resistance to fatigue in BL6 WT mice (n=5), *sgcb*^{-/-} mice (n=4), and AAV.MHCK7.hSGCB treated *sgcb*^{-/-} mice (n=5) all at 7 months of age. Six months of treatment restored force to WT levels (p<0.01 compared to *sgcb*^{-/-}) and improved resistance to fatigue, (b) Overall ambulation in x and y planes is significantly decreased in *sgcb*^{-/-} mice (p<0.0001) and slightly improved in MCHK7 treated mice (p<0.05). Vertical activity rearing onto hindlimbs also decreased in *sgcb*^{-/-} mice (p<0.01) and significantly increased in MCHK7 treated mice (p<0.05) (ONE-WAY ANOVA) (n=6 per group).

Figure 22A-B provide biodistribution and off-target transgene expression analysis of systemic scAAVrh.74.MHCK7.hSGCB delivery. (a) Distribution histogram of average vg copies of transcript per microgram DNA added to qPCR reaction in various tissues from two *sgcb*^{-/-} mice after IV delivery of scAAVrh.74.MHCK7.hSGCB at 1e12 vg total dose. (b) Biodistribution westerns on muscles and organs from scAAVrh.74.MHCK7.hSGCB systemically injected *sgcb*^{-/-} mice indicating no expression of hSGCB transgene in any non-muscle samples.

DETAILED DESCRIPTION

[0040] The present disclosure is based on the discovery that administration of an AAV vector comprising a polynucleotide expressing β -sarcoglycan results in a reduction or complete reversal of muscle fibrosis in a limb-girdle muscular dystrophy animal model. As demonstrated in the Examples, administration of the AAV vector described herein resulted in the reversal of dystrophic features including fewer degenerating fibers, reduced inflammation and improved

functional recovery by protection against eccentric contraction with increased force generation.

[0041] As used herein, the term "AAV" is a standard abbreviation for adeno-associated virus. Adeno-associated virus is a single-stranded DNA parvovirus that grows only in cells in which certain functions are provided by a co-infecting helper virus. There are currently thirteen serotypes of AAV that have been characterized. General information and reviews of AAV can be found in, for example, Carter, 1989, *Handbook of Parvoviruses*, Vol. 1, pp. 169-228, and Berns, 1990, *Virology*, pp. 1743-1764, Raven Press, (New York). However, it is fully expected that these same principles will be applicable to additional AAV serotypes since it is well known that the various serotypes are quite closely related, both structurally and functionally, even at the genetic level. (See, for example, Blacklowe, 1988, pp. 165-174 of *Parvoviruses and Human Disease*, J. R. Pattison, ed.; and Rose, *Comprehensive Virology* 3:1-61 (1974)). For example, all AAV serotypes apparently exhibit very similar replication properties mediated by homologous rep genes; and all bear three related capsid proteins such as those expressed in AAV2. The degree of relatedness is further suggested by heteroduplex analysis which reveals extensive cross-hybridization between serotypes along the length of the genome; and the presence of analogous self-annealing segments at the termini that correspond to "inverted terminal repeat sequences" (ITRs). The similar infectivity patterns also suggest that the replication functions in each serotype are under similar regulatory control.

[0042] An "AAV vector" as used herein refers to a vector comprising one or more polynucleotides of interest (or transgenes) that are flanked by AAV terminal repeat sequences (ITRs). Such AAV vectors can be replicated and packaged into infectious viral particles when present in a host cell that has been transfected with a vector encoding and expressing rep and cap gene products.

[0043] An "AAV virion" or "AAV viral particle" or "AAV vector particle" refers to a viral particle composed of at least one AAV capsid protein and an encapsidated polynucleotide AAV vector. If the particle comprises a heterologous polynucleotide (i.e. a polynucleotide other than a wild-type AAV genome such as a transgene to be delivered to a mammalian cell), it is typically referred to as an "AAV vector particle" or simply an "AAV vector". Thus, production of AAV vector particle necessarily includes production of AAV vector, as such a vector is contained within an AAV vector particle.

AAV

[0044] Recombinant AAV genomes comprise nucleic acid molecule as defined in the invention and one or more AAV ITRs flanking a nucleic acid molecule. AAV DNA in the rAAV genomes may be from any AAV serotype for which a recombinant virus can be derived including, but not limited to, AAV serotypes AAV-1, AAV-2, AAV-3, AAV-4, AAV-5, AAV-6, AAV-7, AAV-8, AAV-9, AAV-10, AAV-11, AAV-12, AAV-13 and AAV rh.74. Production of pseudotyped rAAV is disclosed in, for example, WO 01/83692. Other types of rAAV variants, for example rAAV with capsid mutations, are also contemplated. See, for example, Marsic et al., *Molecular Therapy*, 22(11):

1900-1909 (2014). As noted in the Background section above, the nucleotide sequences of the genomes of various AAV serotypes are known in the art. To promote skeletal muscle specific expression, AAV1, AAV5, AAV6, AAV8 or AAV9 may be used.

[0045] DNA plasmids described herein comprise rAAV genomes. The DNA plasmids are transferred to cells permissible for infection with a helper virus of AAV (e.g., adenovirus, E1-deleted adenovirus or herpesvirus) for assembly of the rAAV genome into infectious viral particles. Techniques to produce rAAV particles, in which an AAV genome to be packaged, rep and cap genes, and helper virus functions are provided to a cell are standard in the art. Production of rAAV requires that the following components are present within a single cell (denoted herein as a packaging cell): a rAAV genome, AAV rep and cap genes separate from (i.e., not in) the rAAV genome, and helper virus functions. The AAV rep and cap genes may be from any AAV serotype for which recombinant virus can be derived and may be from a different AAV serotype than the rAAV genome ITRs, including, but not limited to, AAV serotypes AAV-1, AAV-2, AAV-3, AAV-4, AAV-5, AAV-6, AAV-7, AAV-8, AAV-9, AAV-10, AAV-11, AAV-12, AAV-13 and AAV rh.74. Production of pseudotyped rAAV is disclosed in, for example, WO 01/83692.

[0046] A method of generating a packaging cell is to create a cell line that stably expresses all the necessary components for AAV particle production. For example, a plasmid (or multiple plasmids) comprising a rAAV genome lacking AAV rep and cap genes, AAV rep and cap genes separate from the rAAV genome, and a selectable marker, such as a neomycin resistance gene, are integrated into the genome of a cell. AAV genomes have been introduced into bacterial plasmids by procedures such as GC tailing (Samulski et al., 1982, Proc. Natl. Acad. S6. USA, 79:2077-2081), addition of synthetic linkers containing restriction endonuclease cleavage sites (Laughlin et al., 1983, Gene, 23:65-73) or by direct, blunt-end ligation (Senapathy & Carter, 1984, J. Biol. Chem., 259:4661-4666). The packaging cell line is then infected with a helper virus such as adenovirus. The advantages of this method are that the cells are selectable and are suitable for large-scale production of rAAV. Other examples of suitable methods employ adenovirus or baculovirus rather than plasmids to introduce rAAV genomes and/or rep and cap genes into packaging cells.

[0047] General principles of rAAV production are reviewed in, for example, Carter, 1992, Current Opinions in Biotechnology, 1533-539; and Muzyczka, 1992, Curr. Topics in Microbial. and Immunol., 158:97-129). Various approaches are described in Ratschin et al., Mol. Cell. Biol. 4:2072 (1984); Hermonat et al., Proc. Natl. Acad. Sci. USA, 81:6466 (1984); Tratschin et al., Mol. Cell. Biol. 5:3251 (1985); McLaughlin et al., J. Virol., 62:1963 (1988); and Lebkowski et al., 1988 Mol. Cell. Biol., 7:349 (1988). Samulski et al. (1989, J. Virol., 63:3822-3828); U.S. Patent No. 5,173,414; WO 95/13365 and corresponding U.S. Patent No. 5,658,776 ; WO 95/13392; WO 96/17947; PCT/US98/18600; WO 97/09441 (PCT/US96/14423); WO 97/08298 (PCT/US96/13872); WO 97/21825 (PCT/US96/20777); WO 97/06243 (PCT/FR96/01064); WO 99/11764; Perrin et al. (1995) Vaccine 13:1244-1250; Paul et al. (1993) Human Gene Therapy 4:609-615; Clark et al. (1996) Gene Therapy 3:1124-1132; U.S. Patent. No. 5,786,211; U.S. Patent No. 5,871,982; and U.S. Patent. No. 6,258,595.

[0048] Described herein are packaging cells that produce infectious rAAV. Packaging cells may be stably transformed cancer cells such as HeLa cells, 293 cells and PerC.6 cells (a cognate 293 line). Packaging cells may be cells that are not transformed cancer cells, such as low passage 293 cells (human fetal kidney cells transformed with E1 of adenovirus), MRC-5 cells (human fetal fibroblasts), WI-38 cells (human fetal fibroblasts), Vero cells (monkey kidney cells) and FRhL-2 cells (rhesus fetal lung cells).

[0049] Recombinant AAV (*i.e.*, infectious encapsidated rAAV particles) of the invention comprise a rAAV genome. Embodiments include, but are not limited to, the rAAV named pAAV.MHCK7.hSCGB which comprises the polynucleotide sequence set forth in SEQ ID NO: 3; and pAAV.tMCK.hSCGB which comprises the polynucleotide sequence set forth in SEQ ID NO: 5.

[0050] The rAAV may be purified by methods standard in the art such as by column chromatography or cesium chloride gradients. Methods for purifying rAAV vectors from helper virus are known in the art and include methods disclosed in, for example, Clark et al., *Hum. Gene Ther.*, 10(6): 1031-1039 (1999); Schenpp and Clark, *Methods Mol. Med.*, 69 427-443 (2002); U.S. Patent No. 6,566,118 and WO 98/09657.

[0051] In another embodiment, the invention contemplates compositions comprising rAAV of the present invention. Compositions described herein comprise rAAV in a pharmaceutically acceptable carrier. The compositions may also comprise other ingredients such as diluents and adjuvants. Acceptable carriers, diluents and adjuvants are nontoxic to recipients and are preferably inert at the dosages and concentrations employed, and include buffers such as phosphate, citrate, or other organic acids; antioxidants such as ascorbic acid; low molecular weight polypeptides; proteins, such as serum albumin, gelatin, or immunoglobulins; hydrophilic polymers such as polyvinylpyrrolidone; amino acids such as glycine, glutamine, asparagine, arginine or lysine; monosaccharides, disaccharides, and other carbohydrates including glucose, mannose, or dextrans; chelating agents such as EDTA; sugar alcohols such as mannitol or sorbitol; salt-forming counterions such as sodium; and/or nonionic surfactants such as Tween, pluronic or polyethylene glycol (PEG).

[0052] Titers of rAAV to be administered in methods described herein will vary depending, for example, on the particular rAAV, the mode of administration, the treatment goal, the individual, and the cell type(s) being targeted, and may be determined by methods standard in the art. Titers of rAAV may range from about 1×10^6 , about 1×10^7 , about 1×10^8 , about 1×10^9 , about 1×10^{10} , about 1×10^{11} , about 1×10^{12} , about 1×10^{13} to about 1×10^{14} or more DNase resistant particles (DRP) per ml. Dosages may also be expressed in units of viral genomes (vg).

[0053] Methods of transducing a target cell with rAAV, *in vivo or in vitro*, are contemplated. The *in vivo* methods comprise the step of administering an effective dose, or effective multiple doses, of a composition comprising a rAAV of the invention to an animal (including a human being) in need thereof. If the dose is administered prior to development of a disorder/disease, the administration is prophylactic. If the dose is administered after the development of a

disorder/disease, the administration is therapeutic. In embodiments of the invention, an effective dose is a dose that alleviates (eliminates or reduces) at least one symptom associated with the disorder/disease state being treated, that slows or prevents progression to a disorder/disease state, that slows or prevents progression of a disorder/disease state, that diminishes the extent of disease, that results in remission (partial or total) of disease, and/or that prolongs survival. An example of a disease contemplated for prevention or treatment with methods described herein is muscular dystrophy, such as limb-girdle muscular dystrophy

[0054] Combination therapies are also contemplated. Combination as used herein includes both simultaneous treatment or sequential treatments. Combinations of methods described herein with standard medical treatments (e.g., corticosteroids) are specifically contemplated, as are combinations with novel therapies.

[0055] A therapeutically effective amount of the rAAV vector is a dose of rAAV ranging from about 1e13 vg/kg to about 5e14 vg/kg, or about 1e13 vg/kg to about 2e13 vg/kg, or about 1e13 vg/kg to about 3e13 vg/kg, or about 1e13 vg/kg to about 4e13 vg/kg, or about 1e13 vg/kg to about 5e13 vg/kg, or about 1e13 vg/kg to about 6e13 vg/kg, or about 1e13 vg/kg to about 7e13 vg/kg, or about 1e13 vg/kg to about 8e13 vg/kg, or about 1e13 vg/kg to about 9e13 vg/kg, or about 1e13 vg/kg to about 1e14 vg/kg, or about 1e13 vg/kg to about 2e14 vg/kg, or 1e13 vg/kg to about 3e14 vg/kg, or about 1e13 to about 4e14 vg/kg, or about 3e13 vg/kg to about 4e13 vg/kg, or about 3e13 vg/kg to about 5e13 vg/kg, or about 3e13 vg/kg to about 6e13 vg/kg, or about 3e13 vg/kg to about 7e13 vg/kg, or about 3e13 vg/kg to about 8e13 vg/kg, or about 3e13 vg/kg to about 9e13 vg/kg, or about 3e13 vg/kg to about 1e14 vg/kg, or about 3e13 vg/kg to about 2e14 vg/kg, or 3e13 vg/kg to about 3e14 vg/kg, or about 3e13 to about 4e14 vg/kg, or about 3e13 vg/kg to about 5e14 vg/kg, or about 5e13 vg/kg to about 6e13 vg/kg, or about 5e13 vg/kg to about 7e13 vg/kg, or about 5e13 vg/kg to about 8e13 vg/kg, or about 5e13 vg/kg to about 9e13 vg/kg, or about 5e13 vg/kg to about 1e14 vg/kg, or about 5e13 vg/kg to about 2e14 vg/kg, or 5e13 vg/kg to about 3e14 vg/kg, or about 5e13 to about 4e14 vg/kg, or about 5e13 vg/kg to about 5e14 vg/kg, or about 1e14 vg/kg to about 2e14 vg/kg, or 1e14 vg/kg to about 3e14 vg/kg, or about 1e14 to about 4e14 vg/kg, or about 1e14 vg/kg to about 5e14 vg/kg. The invention also comprises compositions comprising these ranges of rAAV vector.

[0056] For example, a therapeutically effective amount of rAAV vector is a dose of 1e13 vg/kg, about 2e13 vg/kg, about 3e13 vg/kg, about 4e13 vg/kg, about 5e13 vg/kg, about 6e13 vg/kg, about 7e13 vg/kg, about 8e13 vg/kg, about 9e13 vg/kg, about 1e14 vg/kg, about 2e14 vg/kg, about 3e14 vg/kg, about 4e14 vg/kg and 5e14 vg/kg. The invention also comprises compositions comprising these doses of rAAV vector.

[0057] Administration of an effective dose of the compositions may be by routes standard in the art including, but not limited to, intramuscular, parenteral, intravenous, oral, buccal, nasal, pulmonary, intracranial, intraosseous, intraocular, rectal, or vaginal. Route(s) of administration and serotype(s) of AAV components of the rAAV (in particular, the AAV ITRs and capsid protein) of the invention may be chosen and/or matched by those skilled in the art taking into

account the infection and/or disease state being treated and the target cells/tissue(s) that are to express the β -sarcoglycan.

[0058] An effective dose of rAAV and compositions of the invention may be administered, for example, by local administration or systemic administration. For example, systemic administration is administration into the circulatory system so that the entire body is affected. Systemic administration includes enteral administration such as absorption through the gastrointestinal tract and parental administration through injection, infusion or implantation.

[0059] In particular, actual administration of rAAV of the present invention may be accomplished by using any physical method that will transport the rAAV recombinant vector into the target tissue of an animal. Administration according to the invention includes, but is not limited to, injection into muscle, the bloodstream and/or directly into the liver. Simply resuspending a rAAV in phosphate buffered saline has been demonstrated to be sufficient to provide a vehicle useful for muscle tissue expression, and there are no known restrictions on the carriers or other components that can be co-administered with the rAAV (although compositions that degrade DNA should be avoided in the normal manner with rAAV). Capsid proteins of a rAAV may be modified so that the rAAV is targeted to a particular target tissue of interest such as muscle. See, for example, WO 02/053703. Pharmaceutical compositions can be prepared as injectable formulations or as topical formulations to be delivered to the muscles by transdermal transport. Numerous formulations for both intramuscular injection and transdermal transport have been previously developed and can be used in the practice of the invention. The rAAV can be used with any pharmaceutically acceptable carrier for ease of administration and handling.

[0060] For purposes of intramuscular injection, solutions in an adjuvant such as sesame or peanut oil or in aqueous propylene glycol can be employed, as well as sterile aqueous solutions. Such aqueous solutions can be buffered, if desired, and the liquid diluent first rendered isotonic with saline or glucose. Solutions of rAAV as a free acid (DNA contains acidic phosphate groups) or a pharmacologically acceptable salt can be prepared in water suitably mixed with a surfactant such as hydroxypropylcellulose. A dispersion of rAAV can also be prepared in glycerol, liquid polyethylene glycols and mixtures thereof and in oils. Under ordinary conditions of storage and use, these preparations contain a preservative to prevent the growth of microorganisms. In this connection, the sterile aqueous media employed are all readily obtainable by standard techniques well-known to those skilled in the art.

[0061] The pharmaceutical forms suitable for injectable use include sterile aqueous solutions or dispersions and sterile powders for the extemporaneous preparation of sterile injectable solutions or dispersions. In all cases the form must be sterile and must be fluid to the extent that easy syringability exists. It must be stable under the conditions of manufacture and storage and must be preserved against the contaminating actions of microorganisms such as bacteria and fungi. The carrier can be a solvent or dispersion medium containing, for example, water, ethanol, polyol (for example, glycerol, propylene glycol, liquid polyethylene glycol and the like), suitable mixtures thereof, and vegetable oils. The proper fluidity can be maintained,

for example, by the use of a coating such as lecithin, by the maintenance of the required particle size in the case of a dispersion and by the use of surfactants. The prevention of the action of microorganisms can be brought about by various antibacterial and antifungal agents, for example, parabens, chlorobutanol, phenol, sorbic acid, thimerosal and the like. In many cases it will be preferable to include isotonic agents, for example, sugars or sodium chloride. Prolonged absorption of the injectable compositions can be brought about by use of agents delaying absorption, for example, aluminum monostearate and gelatin.

[0062] Sterile injectable solutions are prepared by incorporating rAAV in the required amount in the appropriate solvent with various other ingredients enumerated above, as required, followed by filter sterilization. Generally, dispersions are prepared by incorporating the sterilized active ingredient into a sterile vehicle which contains the basic dispersion medium and the required other ingredients from those enumerated above. In the case of sterile powders for the preparation of sterile injectable solutions, the preferred methods of preparation are vacuum drying and the freeze drying technique that yield a powder of the active ingredient plus any additional desired ingredient from the previously sterile-filtered solution thereof.

[0063] Transduction with rAAV may also be carried out *in vitro*. In one embodiment, desired target muscle cells are removed from the subject, transduced with rAAV and reintroduced into the subject. Alternatively, syngeneic or xenogeneic muscle cells can be used where those cells will not generate an inappropriate immune response in the subject.

[0064] Suitable methods for the transduction and reintroduction of transduced cells into a subject are known in the art. In one embodiment, cells can be transduced *in vitro* by combining rAAV with muscle cells, e.g., in appropriate media, and screening for those cells harboring the DNA of interest using conventional techniques such as Southern blots and/or PCR, or by using selectable markers. Transduced cells can then be formulated into pharmaceutical compositions, and the composition introduced into the subject by various techniques, such as by intramuscular, intravenous, subcutaneous and intraperitoneal injection, or by injection into smooth and cardiac muscle, using e.g., a catheter.

[0065] Transduction of cells with rAAV of the invention results in sustained expression of β -sarcoglycan. Described herein are methods of administering/delivering rAAV which express β -sarcoglycan to a mammalian subject, preferably a human being. These methods include transducing tissues (including, but not limited to, tissues such as muscle, organs such as liver and brain, and glands such as salivary glands) with one or more rAAV of the present invention. Transduction may be carried out with gene cassettes comprising tissue specific control elements. For example, described are methods of transducing muscle cells and muscle tissues directed by muscle specific control elements, including, but not limited to, those derived from the actin and myosin gene families, such as from the myoD gene family [See Weintraub et al., Science, 251: 761-766 (1991)], the myocyte-specific enhancer binding factor MEF-2 [Cserjesi and Olson, Mol Cell Biol 11: 4854-4862 (1991)], control elements derived from the human skeletal actin gene [Muscat et al., Mol Cell Biol, 7: 4089-4099 (1987)], the cardiac actin gene, muscle creatine kinase sequence elements [See Johnson et al., Mol Cell Biol, 9:3393-3399

(1989)] and the murine creatine kinase enhancer (mCK) element, control elements derived from the skeletal fast-twitch troponin C gene, the slow-twitch cardiac troponin C gene and the slow-twitch troponin I gene: hypoxia-inducible nuclear factors (Semenza et al., Proc Natl Acad Sci USA, 88: 5680-5684 (1991)), steroid-inducible elements and promoters including the glucocorticoid response element (GRE) (See Mader and White, Proc. Natl. Acad. Sci. USA 90: 5603-5607 (1993)), and other control elements.

[0066] Muscle tissue is an attractive target for *in vivo* DNA delivery, because it is not a vital organ and is easy to access. The invention contemplates sustained expression of miRNAs from transduced myofibers.

[0067] By "muscle cell" or "muscle tissue" is meant a cell or group of cells derived from muscle of any kind (for example, skeletal muscle and smooth muscle, e.g. from the digestive tract, urinary bladder, blood vessels or cardiac tissue). Such muscle cells may be differentiated or undifferentiated, such as myoblasts, myocytes, myotubes, cardiomyocytes and cardiomyoblasts.

[0068] The term "transduction" is used to refer to the administration/delivery of a polynucleotide of interest (e.g., a polynucleotide sequence encoding β -sarcoglycan) to a recipient cell either *in vivo* or *in vitro*, via a replication-deficient rAAV described resulting in expression of β -sarcoglycan by the recipient cell.

[0069] Thus, also described herein is an effective dose (or doses administered essentially simultaneously or doses given at intervals) of rAAV encoding β -sarcoglycan for administration to a mammalian subject in need thereof

[0070] The invention is further described in the following Examples, which do not limit the scope of the invention described in the claims.

EXAMPLES

Materials and Methods

[0071] *Animal models* - All procedures were approved by The Research Institute at Nationwide Children's Hospital Institutional Animal Care and Use Committee (protocol AR12-00040). B6.129-Sgcb^{tm1Kcam/1J} heterozygous mice were purchased from the Jackson Laboratory (Bar Harbor, ME, USA; Strain # 006832). Sgcb^{-/-} mice were generated by breeding heterozygous mice. KO mice were bred and maintained as homozygous animals in standardized conditions in the Animal Resources Core at the Research Institute at Nationwide Children's Hospital. Mice were maintained on Teklad Global Rodent Diet (3.8z5 fiber, 18.8% protein, 5% fat chow) with a 12:12-h dark: light cycle. Identification of SGCB^{-/-} mice was performed by genotyping using

PCR. All animals were housed in standard mouse cages with food and water ad libitum.

[0072] *Beta-sarcoglycan gene construction.* The full-length human beta-sarcoglycan cDNA (GenBank Accession No. NM_0034994.3) was codon optimized and synthesized by GenScript Inc, Piscataway, NJ, USA. Codon optimization through GenScript uses an algorithm that takes into account parameters that include transcription, mRNA processing and stability, translation and protein folding to design a cDNA sequence that results in maximum expression in muscle tissue (www.genscript.com).

[0073] For the pAAV.tMCK.hSGCB construct, the cDNA was then cloned into a plasmid containing AAV2 ITRs and the cassette included a consensus Kozak sequence (CCACC), an SV40 chimeric intron and a synthetic polyadenylation site (53 bp). The recombinant tMCK promoter was a gift from Dr Xiao Xiao (University of North Carolina). It is a modification of the previously described CK6 promoter²⁷ and includes a modification in the enhancer upstream of the promoter region containing transcription factor binding sites. The enhancer is composed of two E-boxes (right and left). The tMCK promoter modification includes a mutation converting the left E-box to a right E-box (2R modification) and a 6-bp insertion (S5 modification). The pAAV.tMCK.hSGCB vector was constructed by ligation of 1040 bp KpnI/XbaI fragment from pUC57-BSG (Genscript Inc.) into the KpnI/XbaI sites of pAAV.tMCK.hSGCA.26

[0074] The pAAV.MHCK7.hSGCB vector was constructed by removing the tMCK promoter and SV40 chimeric intron with NotI/KpnI sites and inserting a PCR amplified fragment containing the MHCK7 promoter and identical SV40 chimeric intron with NotI/KpnI sites. MHCK7 is an MCK based promoter which utilizes a 206-bp enhancer taken from ~1.2kb 5' of the transcription start site within the endogenous muscle creatine kinase gene with a proximal promoter (enh358MCK, 584-bp)^{3,12}. The MHCK7 promoter itself contains this modified CK7 cassette from the MCK family of genes ligated to a 188-bp α-MyHC (α-myosin heavy chain) enhancer 5' of the CK portion to enhance cardiac expression¹². The creatine kinase portion of the promoter (CK) is 96% identical between tMCK and MHCK7. Finally, the pAAV.MHCK7.hSGCB vector was constructed by ligation of the 960 bp NotI/KpnI MHCK7+Intron fragment from pAAV.MHCK7.DYSF5'DV44 into the NotI/KpnI sites of pAAV.tMCK.hSGCB (Pozgai et al., Gene Ther. 23: 57-66, 2016)

[0075] *rAAV production.* A modified cross-packaging approach, previously reported by Rodino-Klapac et al. (J. Trans. Med. 5:45, 2007), was used to produce the rAAV vector. Here, a triple transfection method with CaPO₄ precipitation in HEK293 cells allows for AAV2 ITRs to be packaged into a different AAV capsid serotype. (28,29) The production plasmids were (i) pAAV.tMCK.hSGCB or pAAV.MHCK7.hSGCB, (ii) rep2-caprh.74 modified AAV helper plasmids encoding cap serotype 8-like isolate rh.74 and (iii) an adenovirus type 5 helper plasmid (pAdhelper) expressing adenovirus E2A, E4 ORF6 and VA I/II RNA genes. Vectors were purified and encapsidated vg titer (utilizing a Prism 7500 Taqman detector system; PE Applied Biosystems, Carlsbad, CA, USA) was determined as previously described. The primer and fluorescent probe targeted the tMCK promoter and were as follows: tMCK forward primer, 5'-

ACC CGA GAT GCC TGG TTA TAA TT-3' (SEQ ID NO: 10); tMCK reverse primer, 5'-TCC ATG GTG TAC AGA GCC TAA GAC-3' (SEQ ID NO: 11); and tMCK probe, 5'-FAM-CTG CTG CCT GAG CCT GAG CGG TTA C-TAMRA-3' (SEQ ID NO: 12). The primer and fluorescent probe targeted the MHCK7 promoter and were as follows: MHCK7 forward primer, 5'-CCA ACA CCT GCT GCC TCT AAA-3' (SEQ ID NO: 16); MHCK7 reverse primer, 5'-GTC CCC CAC AGC CTT GTT C-3' (SEQ ID NO: 17); and MHCK7 probe, 5'-FAM-TGG ATC CCC-Zen-TGC ATG CGA AGA TC-3IABKFQ-3' (SEQ ID NO: 18).

[0076] *Intramuscular Gene delivery.* For intramuscular injection, mice were anesthetized and maintained under 1-4% isoflurane (in O₂). The anterior compartment of the lower left limb of 4- to 6-week-old SGCB^{-/-} mice was cleaned with 95% EtOH then the transverse abdominal (TA) muscle was injected with 3×10^{11} vg of scAAVrh.74.tMCK.hSGCB diluted in saline in a 30- μ l volume using a 30 gauge ultra-fine insulin syringe. The contralateral muscle was left untreated to serve as a control. TA muscle from both limbs was removed at either 6 (n = 9, 4 male, 5 female) or 12 (n = 6, 4 male, 2 female) weeks post injection to assess gene transfer efficiency. In experiments involving 6-month-old mice (n = 5, 5 male), treatment consisted of intramuscular injection into the left TA with 3×10^{11} vg scAAVrh.74.tMCK.hSCGB. For isolated limb perfusion experiments, sgcb^{-/-} mice were perfused at 4 (n = 5, 5 male) and 5 (n = 4, 2 male, 2 female) weeks of age with 5×10^{11} vg of scAAVrh.74.tMCK.hSCBB by injection into the femoral artery as previously described. 19 Animals were euthanized and muscles were analyzed 8 weeks post gene transfer.

[0077] *Systemic Gene Delivery:* Systemic delivery was achieved through injection of vector into the tail vein of sgcb^{-/-} mice. Mice were injected with 1×10^{12} vg of scAAVrh.74.MHCK7.hSGCB diluted in saline in a 212 μ L volume using a 30 gauge ultra-fine insulin syringe. Mice were restrained in a holding tube placing the tail back through tail slot to warm it up in order dilate the blood vessels for ease of injection. After locating the artery down the center line of the tail, the injection was performed in one of the purple/blue lateral veins that run alongside the tail artery. All treated mice were injected at 4-5 weeks of age and euthanized 6-months post-injection.

[0078] *EDL force generation and protection from eccentric contractions.* A physiological analysis of the EDL muscles from mice treated by isolated perfusion (ILP) was performed. The EDL muscle from both lower hind limbs of treated mice was dissected at the tendons and subjected to a physiology protocol to assess function that was previously described by our laboratory and others (19,31) with some adaptations. During the eccentric contraction protocol, a 5% stretch-re-lengthening procedure executed between 500 and 700 ms (5% stretch over 100 ms, followed by return to optimal length in 100 ms). Following the tetanus and eccentric contraction protocol, the muscle was removed, wet-weighed, mounted on chuck using gum tragacanth, and then frozen in methyl-butane cooled in liquid nitrogen.

[0079] *TA force generation and protection from eccentric contractions.* A protocol to assess

functional outcomes in the TA muscle was performed on muscles extracted from mice treated by IM injection. This TA procedure is outlined in several previous studies.(32,33) After the eccentric contractions, the mice were then euthanized and the TA muscle was dissected out, weighed and frozen for analysis. Analysis of the data was performed blindly but not randomly.

[0080] Immunofluorescence. Cryostat sections (12 μ m) were incubated with a monoclonal human beta-sarcoglycan primary antibody (Leica Biosystems, New Castle, UK; Cat. No. NCL-L-b-SARC) at a dilution of 1:50 in a block buffer (1 \times TBS, 10% Goat Serum, 0.1% Tween) for 1 h at room temperature in a wet chamber. Sections were then washed with TBS three times, each for 20 min and re-blocked for 30 min. AlexaFluor 594 conjugated goat anti-mouse secondary IgG1 antibody (Life Technologies, Grand Island, NY, USA; Cat. No. A21125) was applied at a 1:250 dilution for 45 min. Sections were washed in TBS three times for 20 min and mounted with Vectashield mounting medium (Vector Laboratories, Burlingame, CA, USA). Four random \times 20 images covering the four different quadrants of the muscle section were taken using a Zeiss AxioCam MRC5 camera. Percentage of fibers positive for beta-sarcoglycan staining (450% of muscle membrane staining intensity) was determined for each image and averaged for each muscle.

[0081] Western blot analysis. Tissue sections from the left treated TA muscle and the right contralateral TA muscle (20-20 micron thick) were collected into a micro-centrifuge and homogenized with 100 μ l homogenization buffer (125 mM Tris-HCl, 4% SDS, 4 M urea) in the presence of 1 protease inhibitor cocktail tablet (Roche, Indianapolis, IN, USA). After homogenization, the samples were centrifuged at 10,000 rpm for 10 min at 4°C. Protein was quantified on NanoDrop (Thermo Scientific, Waltham, MA, USA). Protein samples (20 μ g) were electrophoresed on a 3-8% polyacrylamide Tris-acetate gel (NuPage, Invitrogen, Carlsbad, CA, USA) for 1 h 5 min at 150 V and then transferred onto a PVDF membrane (Amersham Biosciences, Piscataway, NJ, USA) for 1 h 15 min at 35 V. The membrane was blocked in 5% non-fat dry milk in TBST for 1 h, and then incubated with a rabbit polyclonal human beta-sarcoglycan antibody (Novus Biologicals, Littleton, CO, USA; Cat. No. NBP-1-90300 1:100 or 1:250 dilution) and a 1:5000 of a monoclonal mouse gamma-tubulin antibody (Sigma-Aldrich, St Louis, MO, USA; Cat. No. T6557) or a 1:5000 dilution of a mouse monoclonal mouse α -actinin antibody (Sigma-Aldrich, St Louis, MO, USA; Cat. No. A7811). A 1:500 dilution of a rabbit polyclonal mouse cardiac troponin I antibody (Abcam, Cambridge, MA; Cat. No. ab47003) and a 1:1000 dilution of a rabbit monoclonal mouse vinculin antibody (Invitrogen, Frederick, MD; Cat. No. 70062) were used. Anti-mouse (Millipore, Billerica, MA, USA; Cat. No. AP308P) and anti-rabbit (Life Technologies; Cat. No. 656120) secondary-HRP antibodies were used for ECL immunodetection.

[0082] EBD assay. A dose of 3×10^{10} vg of scAAVrh.74.tMCK.hSGCB was delivered to 4-week-old sgcb^{-/-} mice to the left TA through an intramuscular injection. Four weeks post injection, mice were injected in the intraperitoneal cavity on the right side at 5 μ l/g body weight of a filter sterilized 10 mg/ml EBD in 1x phosphate buffer solution. Mice were then killed 24 h post injection and tissues were harvested and sectioned. Sections were fixed in cold acetone for 10 min and then the immunofluorescence protocol was used to stain for human beta-

sarcoglycan.

[0083] *Morphometric analysis.* Muscle fiber diameters and percentage of myofibers with centrally located nuclei were determined from TA and GAS muscles stained with hematoxylin and eosin (H&E). Four random \times 20 images per section per animal were taken with a Zeiss AxioCam MRC5 camera. Centrally nucleated fibers were quantified using the NIH ImageJ software (Bethesda, MD, USA). Fiber diameters were measured as the shortest diameter through the muscle fiber using Zeiss Axiovision LE4 software (Carl Zeiss Microscopy, Munich, Germany).

[0084] *Biodistribution qPCR analysis.* Taqman quantitative PCR was performed to quantify the number of vector genome copies present in targeted and untargeted contralateral muscle as well as non-targeted organs as previously described.(18,30) A vector-specific primer probe set was used to amplify a sequence of the intronic region directly downstream from the tMCK promoter that is unique and located within the scAAVrh.74.tMCK.hSGCB transgene cassette. The following primers and probe were used in this study: tMCK and MHCK7 intron Forward Primer 5'-GTG AGG CAC TGG GCA GGT AA -3' (SEQ ID NO: 13); tMCK and MHCK7 intron Reverse Primer 5'-ACC TGT GGA GAG AAA GGC AAA G -3' (SEQ ID NO: 14); and tMCK and MHCK7 intron Probe 5'-6FAM-ATC AAG GTT ACA AGA CAG-GTT TAA GGA GAC CAA TAG AAA -tamra-3' (IDT) (SEQ ID NO: 15). Copy number is reported as vector genomes per microgram of genomic DNA. *Immunohistochemistry for immune cell staining.* Immunohistochemistry was used to identify immune cells. Frozen tissue sections on Fisherbrand Superfrost charged microscope slides were incubated with rat anti-mouse monoclonal antibodies using an anti-rat Ig HRP Detection kit (BD Pharmagen, San Jose, CA, USA; Cat: 551013): CD3 (Cat: 555273), CD4 (Cat: 550280), CD8 (Cat: 550281) and Mac-3 for macrophages (Cat: 550292). All primary antibodies were diluted at 1:20 with phosphate-buffered saline. Positive immune staining was visualized using DAB chromagen diluted in DAB buffer with Streptavidin-HRP peroxidase ectastain ABC Peroxidase. Ten random \times 40 images were taken for each muscle and each corresponding stain. The number of mono-nuclear cells was counted and expressed as total number per mm².

[0085] *Picosirius red stain and collagen quantification.* Frozen sections placed onto Fisherbrand Superfrost charged microscope slides were fixed in 10% Neutral Buffered Formalin for 5 min, then rinsed in distilled water. Slides were then incubated in Solution A (Phosphomolydbic acid) from the Picosirius Red Stain Kit (Polysciences Inc., Warrington, PA, USA; Catalog # 24901) for 2 min. After a thorough rinse in distilled water, the slides were placed in Solution B (Direct Red 80/2 4 6-Trinitrophenol) for 15 min, followed by an additional rinse in distilled water and then incubation in Solution C (0.1 N hydrochloride acid) for 2 min. Slides were counterstained for 2.5 min with 1% Fast Green in 1% Glacial Acetic Acid from Poly Scientific (Catalog #S2114) using a 1:10 dilution in DI water. Finally, the slides were rinsed again in distilled water, dehydrated in graded ethanol, cleared in xylene and mounted with coverslips using Cytoseal 60 media from Thermo-Scientific (Waltham, MA, USA; Cat#8310). Images were taken using the AxioVision 4.9.1 software (Carl Zeiss Microscopy). For analysis of Sirius red staining and % collagen quantification, the contrast between the red and the green

colors was enhanced using Adobe Photoshop. The color deconvolution plugin in the ImageJ software program was selected and the RGB color deconvolution option was used. The Red image includes all connective tissue from the Sirius Red stain. The Green image includes all muscle from the Fast Green counterstain. Only the Red image and the original image were used. A threshold was then applied to the images to obtain black and white images with areas positive for collagen in black and negative areas in white. Using the measure function, the area of collagen was calculated. The total tissue area was then determined by converting the originally image to '8-bit' and adjusting the threshold to 254, which will be one unit below completely saturating the image. The total tissue area was then measured as done previously and total area was recorded. The percentage of collagen was then calculated by dividing the area of collagen by the total tissue area. The mean percentage for each individual was then calculated.

[0086] Diaphragm Tetanic Contraction for Functional Assessment: Mice were euthanized and the diaphragm was dissected with rib attachments and central tendon intact, and placed in K-H buffer as previously described by Beaström et al. (Am. J. Pathol. 179: 2464-74, 2011), Rafael-Forney et al. (Circulation 124: 582-8, 2011 and Moorwood et al. (J. Visualized Experiments 71:e50036, [year?]) A 2-4 mm wide section of diaphragm was isolated. Diaphragm strips were tied firmly with braided surgical silk (6/0; Surgical Specialties, Reading, PA) at the central tendon, and sutured through a portion of rib bone affixed to the distal end of the strip. Each muscle was transferred to a water bath filled with oxygenated K-H solution that was maintained at 37°C. The muscles were aligned horizontally and tied directly between a fixed pin and a dual-mode force transducer-servomotor (305C; Aurora Scientific, Aurora, Ontario, Canada). Two platinum plate electrodes were positioned in the organ bath so as to flank the length of the muscle. The muscle was stretched to optimal length for measurement of twitch contractions, and then allowed to rest for 10 minutes before initiation of the tetanic protocol. Once the muscle is stabilized, the muscle is set to an optimal length of 1g and is subjected to a warm-up which consists of three 1Hz twitches every 30 seconds followed by three 150Hz twitches every minute. After a 3 min rest period, the diaphragm is stimulated at 20, 50, 80, 120, 150, 180Hz, allowing a 2 min rest period between each stimulus, each with a duration of 250ms to determine maximum tetanic force. Muscle length and weight was measured. The force was normalized for muscle weight and length.

[0087] Cardiac Magnetic Resonance Imaging : Cardiac function was analyzed using a 9.4T horizontal-bore magnetic resonance imaging (MRI) system and mouse volume coil (Bruker BioSpin, Billerica, MA, USA). Mice were anaesthetized with 2.5% isoflurane mixed with carbogen (1 L/min) for 3 minutes prior to placement on the imaging bed. Upon placement of mice in imaging apparatus and initiation of imaging, isoflurane/carbogen mixture was dropped to 1.5% for the remainder of the study. EKG and respiration were monitored using an MRI-compatible system (Model 1025, Small Animal Instruments, Stonybrook, NY, USA). Gated cardiac short-axis FLASH cine T1-weighted images were acquired over the entire left ventricle (LV) of the mouse (TR = 8 ms; TE = 2.8 ms; α = 180°; matrix = 256 \times 256; FOV = 3.0 \times 3.0 cm; slice thickness = 1 mm, nslices=7, up to 20 frames per cardiac cycle). For image analysis, the end-diastolic and end-systolic timepoint of each short-axis image were identified and the

endocardial and epicardial cardiac boundaries were manually traced. The papillary muscles were excluded from the endocardial boundary of the LV. From these measured areas, end-diastolic volume (EDV), end-systolic volume (ESV), stroke volume (SV), cardiac output (CO), ejection fraction (EF), and average LV mass were calculated.

[0088] Immunofluorescence: Cryostat sections (12 μ m) from the tibialis anterior (TA), gastrocnemius (GAS), quadriceps (QUAD), psoas major (PSOAS), gluteal (GLUT), triceps (TRI), and diaphragm muscles along with the heart were subjected to immunofluorescence staining for the hSGCB transgene via our previously used protocol as described in Pozgai et al., Gene Therap. 23: 57-66, 2016. Sections were incubated with a mouse monoclonal human beta-sarcoglycan primary antibody (Leica Biosystems, New Castle, UK; Cat. No. NCL-L-b-SARC) at a dilution of 1:100. Four random 20X images covering the four different quadrants of the muscle section were taken using a Zeiss AxioCam MRC5 camera. Percentage of fibers positive for beta-sarcoglycan staining (>50% of muscle membrane staining) was determined for each image and averaged for each muscle.

[0089] Morphometric Analysis: Hematoxylin and eosin (H&E) staining was performed on 12 μ m thick cryosections of muscle from 7 month old C57BL6 WT mice (n=5), *sgcb*^{-/-} mice (n=5), and rAAV.MHCK7.hSGCB 6 month treated *sgcb*^{-/-} mice (n=5) for analysis. The percentage of myofibers with central nuclei was determined in the TA, GAS, QUAD, PSOAS, GLUT, TRI, and diaphragm muscles. Additionally, muscle fiber diameters were measured in the GAS, PSOAS, and TRI muscles. Four random 20X images per muscle per animal were taken with a Zeiss AxioCam MRC5 camera. Centrally nucleated fibers were quantified using the NIH ImageJ software and fiber diameters were measured using Zeiss Axiovision LE4 software.

[0090] X-Ray Images: Whole body x-rays were performed on anesthetized 7 month old C57BL6 WT mice (n=6), untreated *sgcb*^{-/-} mice (n=6), and rAAV.MHCK7.hSGCB 6 month treated *sgcb*^{-/-} mice (n=6) using the Faxitron MX-20 digital x-ray system at 26kV for 3 secs (Faxitron X-Ray Corp, Lincolnshire, USA).

[0091] Laser Monitoring of Open Field Cage Activity: An open-field activity chamber was used to determine overall activity of experimental mice. Mice at 7 months old from the C57BL6 WT (n=6) and untreated *sgcb*^{-/-} (n=6) control groups along with the rAAV.MHCK7.hSGCB 6 month treated *sgcb*^{-/-} mice (n=6) were subjected to analysis following a previously described protocol (Kobayashi et al., Nature 456: 511-5, 2008, Beaström et al., Am. J. Pathol. 179: 2464-74, 2011) with several modifications. All mice were tested at the same time of day in the early morning near then end of the night cycle when mice are most active. All mice were tested in an isolated room, under dim light and with the same handler each time. To reduce anxiety and keep behavioral variables at a minimum, which could potentially affect normal activity of the mice and consequently the results of the assay, the mice tested were not individually housed (Voikar et al., Genes Brain Behav. 4: 240-52, 2005). Mice were activity monitored using the Photobeam Activity System (San Diego Instruments, San Diego, CA). This system uses a grid of invisible infrared light beams that traverse the animal chamber front to back and left to right

to monitor the position and movement of the mouse within an X-Y-Z plane. Activity was recorded for 1 hour cycles at 5-minute intervals. Mice were acclimatized to the activity test room for an initial 1 hour session several days prior to beginning data acquisition. Mice were tested in individual chambers in sets of 4. Testing equipment was cleaned between each use to reduce mouse reactionary behavioral variables that could alter our results. Data collected was converted to a Microsoft Excel worksheet and all calculations were done within the Excel program. Individual beam breaks for movement in the X and Y planes were added up for each mouse to represent total ambulation, and beam breaks in the Z plane were added up to obtain vertical activity within the 1 hour time interval.

Example 1

scAAVrh.74.tMCK.hSGCB construction and vector potency

[0092] The transgene cassette containing a codon-optimized full-length human SCGB cDNA as shown in Figures 1A was constructed. The cassette includes a consensus Kozak sequence (CCACC), an SV40 chimeric intron, a synthetic polyadenylation site, and the muscle-specific tMCK promoter (20) used to drive expression of the cassette. The cassette was packaged into a self-complementary (sc) AAVrh.74 vector that is 93% homologous to AAV8. AAVrh.74 has been shown in mice and non-human primates to be safe and effective, particularly in crossing the vascular barrier when delivered to muscle through the circulation.(17, 18, 21) Vector potency was established by intramuscular injection into the left TA muscle in the Sgcb-null mouse. Delivery of 3×10^{10} vg transduced $70.5 \pm 2.5\%$ of muscle fibers and 1×10^{11} vg transduced $89.0 \pm 4.0\%$ of muscle fibers, 3 weeks post gene transfer.

Example 2

Intramuscular delivery of scAAVrh.74.tMCK.hSGCB

[0093] Following vector potency, studies were extended to analyze the efficacy of therapy 6 and 12 weeks post gene transfer. As a result of the high levels of expression following the short 3-week potency study, a dose of 3×10^{10} vg total was selected for subsequent studies to use the lowest effective dose. Five-week-old sgcb^{-/-} mice were treated with 3×10^{10} vg of scAAVrh.74.tMCK.hSCGB intramuscularly to the left transverse abdominal (TA) and β -sarcoglycan expression was demonstrated using immunofluorescence in $88.4 \pm 4.2\%$ of muscle fibers 6 weeks post injection (n=9), and in $76.5 \pm 5.8\%$ of muscle fibers 12 weeks post injection (n=6), and expression was confirmed via western blotting (Figure 1B). β -Sarcoglycan expression was accompanied by restoration of components of the dystrophin-associated

protein complex (α -sarcoglycan and dystrophin) (Figure 1C). Using Evans blue dye (EBD) as a marker for membrane permeability (22, 23) we found all fibers expressing exogenous β -sarcoglycan were protected from leakage and EBD inclusion (Figure 1D). Muscle from $sgcb^{-/-}$ mice exhibit a severe muscular dystrophy with centrally nucleated fibers, frequent muscle fiber necrosis, fibrotic tissue and significant fiber size variability represented by both atrophic and hypertrophic fibers. (3, 4) As seen in Figure 2A, hematoxylin & eosin staining shows an overall improvement in the dystrophic phenotype of diseased muscle including a reduction in central nuclei ($sgcb^{-/-}$ untreated- $76.8\pm2.3\%$ vs AAV.hSCGB treated- $38.86\pm3.5\%$; $P<0.0001$) (Figure 2C). Normalization of fiber size distribution, with an increase in the average fiber diameter following treatment was also observed ($sgcb^{-/-}$ untreated- 32.6 ± 0.31 μm vs AAV.hSGCB treated- 35.56 ± 0.22 μm ; $P<0.0001$) (Figure 2D).

[0094] The histopathological hallmark of the $scgb^{-/-}$ mouse is fibrosis characterized by widespread replacement of muscle tissue primarily with collagens along with other extracellular matrix components such as fibronectin, elastin, laminin and decorin.(14) This replacement of muscle tissue by connective tissue challenges the potential value of gene replacement and may limit the degree of improvement. (24) To test this, mice treated for 12 weeks were assayed for reduction in fibrosis. The TA muscle was specifically assessed since its inherent degree of fibrosis was established in the KO model and because it represents a potential target following vascular ILP gene delivery. Picosirius red staining for collagen, types I and III, of TA muscles showed a significant reduction (52.74%) in the amount of collagen present within scAAVrh.74.tMCK.hSGCB-treated muscle compared with untreated $sgcb^{-/-}$ mouse muscle ($20.7\pm0.57\%$ vs $43.8\pm2.3\%$, AAV.hSGCB treated vs $sgcb^{-/-}$ untreated, respectively; $P<0.0001$) (Figures 2b and e). Untreated $sgcb^{-/-}$ muscle from 5-week-old mice at the age of injection had $24.05\pm1.5\%$ collagen deposition, indicating there was a slight (14.0%) reduction in the amount of collagen following the 12 weeks of treatment.

Example 3

Functional correction in skeletal muscle following scAAVrh.74.tMCK.hSGCB gene transfer

[0095] To determine whether hSGCB gene transfer can improve muscle function, we assessed the functional properties of the TA muscle from $sgcb^{-/-}$ mice treated with scAAVrh.74.tMCK.hSCGB. Following intramuscular delivery of 3×10^{10} vg of scAAVrh.74.tMCK.hSCGB to the TA of 4-week-old $sgcb^{-/-}$ mice, 6 weeks post treatment the TA muscles were subjected to *in situ* force measurements ($n=4$). Treated muscles were compared with untreated contralateral muscles and those from C57BL/6 WT mice. scAAVrh.74.tMCK.hSCGB-treated muscle showed significant improvement in both absolute

tetanic force and normalized specific force (Figures 3A and B). Treated muscles had an average absolute force of 1436.9 ± 199.5 mN compared with 770.9 ± 118.3 mN for untreated $sgcb^{-/-}$ controls ($P < 0.01$). Similarly, treated TA muscles produced an average specific force of 254.01 ± 6.9 mN/mm² and untreated muscles produced 124.2 ± 13.9 mN/mm² of force ($P < 0.01$). Finally, muscles treated with scAAVrh.74.tMCK.hSCGB showed greater resistance to contraction-induced injury compared with the untreated control muscles (Figure 3C). Treated TA muscles lost $34.0 \pm 5.1\%$ of force from that produced after the first contraction whereas untreated diseased muscle lost $54.1 \pm 3.8\%$ ($P < 0.01$) of force following the eccentric contraction protocol. These data show that hSGCB gene transfer does provide a functional benefit to diseased muscle deficient for β -sarcoglycan.

Example 4

Treatment of aged muscle with scAAVrh.74.tMCK.hSGCB

[0096] Studies of disease progression in this mouse model of LGMD2E have shown that although the most severe tissue remodeling in muscle occurs between 6 and 20 weeks, the histopathology of the muscle continues to worsen with age, resembling the disease progression in patients.(3, 4, 14) Consequently, to mimic a clinical setting where treatment would occur at an older age with more advanced muscle deterioration and endomysial fibrosis, we treated 6-month-old $sgcb^{-/-}$ mice ($n=5$) intramuscularly in the TA with 3×10^{10} vg of scAAVrh.74.tMCK.hSCGB. Following 12 weeks of treatment, at 9 months of age, $80.1 \pm 4.8\%$ of muscle fibers were transduced (Figure 4A). Picosirius red stain for collagen types I and III showed a 42.2% reduction in the amount of collagen present in treated mice compared with untreated $sgcb^{-/-}$ mouse muscle (AAV.hSGCB treated- $20.0 \pm 0.80\%$ vs $sgcb^{-/-}$ untreated- $34.6 \pm 1.4\%$, $P < 0.0001$) (Figures 4B and C). At the age of treatment, 6-month-old $sgcb^{-/-}$ mice have $30.8 \pm 2.0\%$ collagen deposition ($n=4$, 4 male); thus, these results indicate that scAAVrh.74.tMCK.hSCGB treatment not only prevents, but also has the potential to reverse existing fibrosis.

Example 5

ILP of scAAVrh.74.tMCK.hSGCB in $sgcb^{-/-}$ mice

[0097] The ability to target multiple muscles in one limb allows for a more clinically relevant delivery method for translation to LGMD2E patients. Delivery of 5×10^{11} vg of scAAVrh.74.tMCK.hSGCB by ILP in 4- to 6-week-old $sgcb^{-/-}$ mice ($n=9$, 7 male, 2 female) was

analyzed 2 months post gene transfer. β -Sarcoglycan expression reached $91.8 \pm 4.7\%$ of fibers in the gastrocnemius (GAS) muscle and $90.6 \pm 2.8\%$ in TA (Figure 5A). ILP delivery of scAAVrh.74.tMCK.hSGCB resulted in significant protection from eccentric contraction-induced injury ($P < 0.05$), that was not different from WT, compared with untreated contralateral muscles (Figure 5C). Vascular delivery also restored muscle histopathological parameters (Figure 5B). Central nuclei were decreased in the TA ($sgcb^{-/-}$ untreated- $76.9 \pm 2.8\%$ vs AAV.hSGCB treated- $23.2 \pm 5.7\%$, $P < 0.001$) and GAS ($sgcb^{-/-}$ untreated- $78.2 \pm 2.4\%$ vs AAV.hSGCB treated- $16.8 \pm 6.6\%$, $P < 0.001$). Gene transfer also led to an increase in the average fiber size in the TA ($sgcb^{-/-}$ untreated- $30.53 \pm 0.52 \mu\text{m}$ vs AAV.hSGCB treated- $41.9 \pm 0.46 \mu\text{m}$; $P < 0.0001$) and GAS ($sgcb^{-/-}$ untreated- $38.9 \pm 0.37 \mu\text{m}$ vs AAV.hSGCB treated- $33.3 \pm 0.44 \mu\text{m}$; $P < 0.0001$), with normalization of fiber diameter distribution, a substantial decrease (~60%) in the number of CD3 cells, CD4 cells and macrophages (Table 1) was observed.

Table 1. immune response in scAAVrh.74.tMCK.hS-GCB ILP-treated mice

Cell type	Treated Left TA cells/mm ²	Untreated Right TA cells/mm ²	Uninjected SGCB -/- TA cells/mm ²
CD3	15.6 ± 3.2	37.85 ± 6.2	29.8 ± 1.7
CD4	20.9 ± 4.7	58.1 ± 2.9	49.0 ± 0.8
CD8	8.2 ± 1.8	12.7 ± 2.4	15.5 ± 5.8
Macrophage	28.2 ± 5.0	75.2 ± 5.6	100.2 ± 5.9

Abbreviations: ANOVA, analysis of variance; ILP, isolated-limb perfusion; SGCB, β -sarcoglycan; TA, tibialis anterior. Quantification of immune cells present in uninjected SGCB-/- mice, and scAAVrh.74.tMCK.hSGCB treated and untreated muscle. Data shown are following ILP delivery of virus and represent the mean number of cells/mm³ \pm s.e.m., $n = 8$ per group. A one-way ANOVA was used to compare values from the three different cohorts. Levels of immune cells were decreased with a statistically significant difference ($P < 0.01$) between the treated left TA and untreated right TA and/or the treated left TA and uninjected TA in all stains except for CD8.

[0098] Picosirius red staining of TA and GAS muscles also showed a significant reduction in the amount of collagen compared with untreated $sgcb^{-/-}$ muscle following vascular delivery (Figure 6a). Collagen levels in the TA were reduced to $21.6 \pm 1.3\%$ in treated muscle compared with $40.2 \pm 1.5\%$ in untreated $sgcb^{-/-}$ mice at the age of end point ($P < 0.0001$). As indicated previously, $sgcb^{-/-}$ mice at the age of injection presented with $24.1 \pm 1.5\%$ collagen in TA muscle, indicating again a slight reduction (10.0%) in collagen deposition following 8 weeks of treatment. Similarly, staining of the GAS muscle showed that treated mice had $22.9 \pm 0.99\%$ collagen compared with $37.9 \pm 1.3\%$ in untreated $sgcb^{-/-}$ mice at the end point ($P < 0.0001$). Qualitative PCR was performed to detect collagen transcript levels in muscle, which correlate

with the results of the Sirius red staining. Taken together, these data show that AAV-mediated delivery of human β -sarcoglycan reduces muscle fibrosis, improves muscle function and reverses dystrophic pathology of $sgcb^{-/-}$ diseased muscle.

Example 6

Safety and biodistribution of rAAVrh.74.tMCK.hSGCB

[0099] Initially, normal WT mice injected with 3×10^{10} vg of scAAVrh.74.tMCK.hSGCB intramuscularly into the TA showed no signs of toxicity by H&E stain indicating no adverse effects due to the virus. Following the ILP vascular delivery of 5×10^{11} vg total dose of scAAVrh.74.tMCK.hSGCB as described in the previous section, the safety was assessed in a small group of mice in this cohort (n=4). First, targeted muscles with significant gene expression were analyzed, as well as off target organs including heart, lung, liver, kidney, spleen, gonads and diaphragm histologically. Paraffin sections were formally reviewed by a veterinary pathologist and there was no evidence of toxicity in any organ noted (data not shown). Protein expression and vector biodistribution were also assessed in all of the above tissues and organs with western blotting and qPCR, respectively. Vector genome copies were detected in all organs tested; however, no protein expression was detected in any sample other than treated muscle (Figure 7). Finally, an analysis of wet weights of treated and untreated muscle shows no significant difference or trend when comparing the average weights from either cohort (data not shown). These data provide evidence that the muscle-specific tMCK promoter restricted expression to skeletal muscle and the vector is non-toxic.

Example 7

Histological and Functional Deficits in the heart and diaphragm of SGCB-/- mice

[0100] WT and 7 month old SGCB-/- mice (n=6 per strain) that were untreated were analyzed by cardiac MRI and diaphragm physiology to look for deficits. Following these analyses the animals were sacrificed and evaluated for histopathology (Figure 8). Trichrome staining showed extensive fibrosis (red staining) in both the diaphragm (Figure 8A) and heart (Figure 8C). This was accompanied by functional deficits of specific force in the diaphragm (116.24 mN/mm² SGCB-/- vs. 236.67 mN/mm² WT, Figure 8B) and significant deficit in ejection fraction measured by MRI (WT, 78% vs. SGCB-/- 65%, Figure 8D).

Example 8

scAAVrh.74.MHCK7.hSGCB construction and vector potency

[0101] The transgene cassette containing a codon-optimized full-length human SCGB cDNA as shown in Figure 9A was constructed. The cassette includes a consensus Kozak sequence (CCACC), an SV40 chimeric intron, a synthetic polyadenylation site, and the muscle-specific MHCK7 used to drive expression of the cassette. This is an MCK based promoter which utilizes a 206-bp enhancer taken from ~1.2kb 5' of the transcription start site within the endogenous muscle creatine kinase gene with a proximal promoter (enh358MCK, 584-bp)^{3,12}. The cassette was packaged into a self-complementary (sc) AAVrh.74 vector that is 93% homologous to AAV8. AAVrh.74 has been shown in mice and non-human primates to be safe and effective, particularly in crossing the vascular barrier when delivered to muscle through the circulation. (17, 18, 21) Vector potency was established by intramuscular injection into the left TA muscle in the Sgcb-null mouse. Delivery of 3×10^{10} vg transduced >90% of muscle fibers 4 weeks post gene transfer.

Example 9**Systemic Delivery of scAAV.MHCK7.hSGCB**

[0102] We delivered vector through a tail vein injection to 14 SGCB-/- mice at a dose of 1×10^{12} vg total dose (5×10^{13} vg/kg) to assess transgene expression and efficacy of our vector when delivered systemically at a long-term time point of 6 months. Mice were injected at 4 weeks of age and a full necropsy was performed at 6 months post-injection (1 mouse was taken down at 1 month and 2 mice were taken down at 4 months as intermediate assessments for expression). All skeletal muscles discussed above along with the diaphragm and heart were extracted for analysis. Organs were also removed for toxicology and biodistribution analysis. Immunofluorescence staining for human beta-sarcoglycan was used to determine hSGCB transgene expression in 5 limb muscles, both left and right, in addition to the diaphragm and heart of 6 of the KO mice given a systemic injection of hSGCB vector. These muscles included the TA, gastrocnemius (GAS), quadriceps (QUAD), gluteal (GLUT) (not shown), psoas major (PSOAS), and triceps (TRI) (Figure 10). A qualitative analysis of heart tissue was also used to assess the relative level of transgene expression in cardiac muscle upon delivery.

[0103] Four 20X images were taken of each muscle and the percent of hSGCB positive fibers was determined for each image resulting in the average percent transduction for each muscle from each mouse. The results shown in Figure 10 and Figure 11 demonstrate ≥98% transduction in all muscles analyzed including the diaphragm and heart. Mice deficient for β-sarcoglycan were completely absent of the protein when analyzed by immunofluorescence.

The therapeutic dose of 1×10^{12} vg total dose resulted in an average of $97.96 \pm 0.36\%$ (\pm SEM) vector transduction across all skeletal muscles including the diaphragm, and approximately 95% or greater in cardiac muscle (data not shown).

Example 10

Long-term systemic delivery of scAAVrh.74.MHCK7.hSGCB in SGCB^{-/-} mice

[0104] To build upon the results of the one-month potency assay described in Example 9, longer-term (6-month duration) systemic delivery of the β -sarcoglycan transgene cassette to $sgcb^{-/-}$ mice was investigated. Four-to-five week old $sgcb^{-/-}$ mice were treated with 1×10^{12} vg total dose scAAVrh.74.MHCK7.hSGCB intravenously in the tail vein ($n=5$). Mice were necropsied 6 months post-injection and hSGCB transgene expression was demonstrated using immunofluorescence in six skeletal muscles, both left and right, in addition to the diaphragm and heart of all treated mice. Skeletal muscles analyzed included the TA, GAS, QUAD, gluteal (GLUT), PSOAS, and TRI. Average hSGCB expression resulting from systemic delivery in treated mice was $98.13 \pm 0.31\%$ (\pm SEM) across all skeletal muscles including the diaphragm, with expression in the heart exceeding > 95%. Representative images are shown in **Figure 12b**. The expression levels in each individual muscle type averaged from all treated mice are shown in **Table 2**. Western blotting in **Figure 12c** confirms transgene expression in all muscles. The expression values in Table 2 are presented for various muscles as the average of left and right muscles from systemically injected mice ($n=5$). Values indicated as AVG \pm SEM. In addition, quantification of hSGCB transgene expression in hearts from treated mice via western blotting and densitometry indicate overexpression of hSGCB up to 72.0% above BL6 WT levels of expression (**Figure 12d**), correlating to the high levels quantified in skeletal muscle.

Table 2. β -sarcoglycan Immunofluorescence Expression

Muscle	Delivery Route	Dose (vg Total Dose)	Endpoint (Months)	% Fibers Expressing SGCB
TA	IV	1e12	6	98.88 ± 0.55
GAS	IV	1e12	6	98.24 ± 0.82
QD	IV	1e12	6	99.32 ± 0.19
GLUT	IV	1e12	6	97.50 ± 0.39
PSOAS	IV	1e12	6	98.75 ± 0.23
TRI	IV	1e12	6	97.21 ± 1.35
Diaphragm	IV	1e12	6	97.00 ± 1.26
Heart	IV	1e12	6	$\geq 95\%$

[0105] An important characteristic of *sgcb*^{-/-} muscle described in previous reports (Araishi et al, Hum. Mol. Genet 8: 1589-98, 1999, Durbeej et al., Mol. Cell. 5:141-51, 2000) and illustrated by the hematoxylin & eosin staining of the GAS and diaphragm in Figure 13a is severe dystrophic pathology including central nucleation, necrosis, inflammatory infiltration, and fibrosis. Gene transfer significantly improved this pathology, alleviating many of these dystrophic features (Figure 13a). Quantification of histological parameters showed a significant reduction in central nucleation in the various skeletal muscles analyzed as a result of gene transfer (Figure 13b). With the expected low levels of central nucleation in BL6 WT mice across all muscles averaging $1.89 \pm 0.39\%$, as note here, taking into account all muscles analyzed, an average of $66.85 \pm 1.86\%$ central nuclei in untreated *sgcb*^{-/-} mice compared to $36.30 \pm 5.16\%$ in AAV.MHCK7.hSGCB treated *sgcb*^{-/-} muscle ($p<0.0001$) Table 3 below provides central nuclei counts and fiber diameters given for various muscles as the average (\pm SEM) of left and right muscles from BL6 WT, *sgcb*^{-/-}, and systemically injected mice (n=5 per group). Of note, the most significant wave of degeneration/regeneration occurs at 3 weeks in *sgcb*^{-/-} muscle indicated by centrally placed nuclei. Animals were treated following this insult and therefore a complete reversal of centralized nuclei was not anticipated. A more in depth analysis of muscle histopathology revealed a normalization of fiber size distribution accompanied by an increase in average fiber diameter in diseased mice treated with vector compared with untreated *sgcb*^{-/-} mice in all three muscles examined (GAS: *sgcb*^{-/-} untreated - $28.37 \pm 0.23\mu\text{m}$ vs. AAV.hSGCB treated - $36.04 \pm 0.17\mu\text{m}$; $p<0.0001$) (PSOAS: *sgcb*^{-/-} untreated - $24.75 \pm 0.23\mu\text{m}$ vs. AAV.hSGCB treated - $38.43 \pm 0.28\mu\text{m}$; $p<0.0001$) (TRI: *sgcb*^{-/-} untreated - $28 \pm 0.31\mu\text{m}$ vs. AAV.hSGCB treated - $35.56 \pm 0.22\mu\text{m}$; $p<0.0001$) (Figures 13c, 13d, Table 3).

Table 3. Analysis of Percent Central Nucleation

Animal Group	Dose (vg Total Dose)	Muscle	% Central Nuclei (Avg \pm SEM)	Combined Avg %CN (\pm SEM)	Fiber Diameter μm (Avg \pm SEM)
			(Avg \pm SEM)		
C57BL6 WT	N/A	TA	1.78 ± 0.86	1.89 ± 0.39	N/A
		GAS	0.83 ± 0.41		39.69 ± 0.18
		QD	0.98 ± 0.31		N/A
		GLUT	2.50 ± 0.68		N/A
		PSOAS	1.26 ± 0.28		40.96 ± 0.22
		TRI	2.13 ± 0.36		41.53 ± 0.24
		DIA	3.75 ± 1.30		N/A

Animal Group	Dose (vg Total Dose)	Muscle	% Central Nuclei	Combined Avg %CN (±SEM)	Fiber Diameter μm
			(Avg ±SEM)		(Avg ±SEM)
<i>Sgcb</i> ^{-/-}	N/A	TA	70.45 ± 3.04	66.85 ± 1.86	N/A
		GAS	67.26 ± 1.81		28.37 ± 0.23
		QD	63.57 ± 2.09		N/A
		GLUT	61.34 ± 2.05		N/A
		PSOAS	62.73 ± 5.20		24.75 ± 0.22
		TRI	67.11 ± 2.83		28.74 ± 0.22
		DIA	75.47 ± 3.79		N/A
AAV.MHCK7.hSGCB Treated	1.00E+12	TA	43.85 ± 3.89	36.30 ± 5.16	N/A
		GAS	38.71 ± 3.50		36.04 ± 0.18
		QD	46.10 ± 6.26		N/A
		GLUT	42.11 ± 5.48		N/A
		PSOAS	21.00 ± 4.69		38.43 ± 0.28
		TRI	48.39 ± 6.20		39.92 ± 0.27
		DIA	11.59 ± 2.08		N/A

[0106] Due to the significant role fibrosis plays in the pathogenesis of LGMD2E and effectiveness of therapies, it was critical to demonstrate the same efficacy in reducing fibrosis. That was saw with localized β -sarcoglycan gene transfer. now following systemic delivery of scAAVrh.74.MHCK7.hSGCB. Using the Picosirius red stain for collagen types I and III, we analyzed the levels of collagen in the gastrocnemius and diaphragm muscles was analyzed in 7 month old BL6 WT mice (n=4), untreated *sgcb*^{-/-} mice (n=4), and treated *sgcb*^{-/-} mice (n=5) 6 months post-injection. Treated muscles displayed significantly less collagen deposition

compared to untreated *sgcb*^{-/-} muscles (Figure 14a). Vector transduced GAS muscle contained $17.55 \pm 0.59\%$ collagen compared to $43.55 \pm 3.33\%$ collagen in untreated *sgcb*^{-/-} GAS muscles ($p<0.0001$). Furthermore, treated diaphragm muscle exhibited $21.67 \pm 1.09\%$ collagen compared to $44.05 \pm 2.39\%$ in untreated *sgcb*^{-/-} muscle ($p<0.0001$) (Figure 14b) demonstrating the ability of hSGCB gene transfer to mitigate the fibrotic component of the LGMD2E phenotype.

Example 11

Restoration of diaphragm function following systemic delivery

[0107] To determine whether hSGCB gene transfer can improve muscle function, we assessed the functional properties of the diaphragm muscle from SGCB^{-/-} mice treated with scAAVrh.74.MHCK7.hSCGB (see Griffin et al. for methods). A functional deficit in diaphragms of SGCB^{-/-} mice was first established. KO diaphragms demonstrated a 50.9% reduced specific force output (116.24 mN/mm^2) compared to BL6 WT mice (116.24 mN/mm^2 vs. 236.67 mN/mm^2) and greater loss of force following a rigorous fatigue protocol (23% loss in SGCB^{-/-}; 7% loss in BL6 WT). Tail vein delivery of scAAVrh.74.MHCK7.hSGCB resulting in nearly 100% hSGCB expression in the diaphragm lead to restoration of diaphragm function with specific force output improved to 226.07 mN/mm^2 and a greater resistance to fatigue with only a 12% loss of force ($n=5$) (Figure 15).

Example 12

Delivery of scAAVrh.74.CMV.miR29C reduces fibrosis in SGCB^{-/-} mice

[0108] The extensive fibrosis we identified in both skeletal muscle (Figures 2, 4, and 6) as well as the heart and diaphragm (Figure 8) demonstrated a need to treat collagen deposition (fibrosis) in LGMD2E. We previously found that Mir29C was most severely reduced (of Mir29A, B, and C) in Duchenne muscular dystrophy. He hypothesized that Mir-29C would also be reduced in Beta-sarcoglycan deficient mice (a mouse model for LGMD2E). We proved this to be true (Figure 15). Mir29C levels were decreased, fibrosis (collagen) levels were increased, and three components of fibrosis (Co1A, Col3A, and Fbn) were increased at the RNA level. To test whether we could prevent fibrosis with Mir29C, The gene therapy vector scrAAVrh.74.CMV.miR29c (3×10^{11} vgs) was injected into the tibialis anterior muscle of 4 week old SGCB^{-/-} mice ($n=5$). The scrAAVrh.74.CMV.miR29c is shown in Figure 16 and described in U.S. Provisional Application No. 62/323,163. Following 2 months of treatment with

AAVrh.74.CMV.miR29C, TA muscles were harvested from treated and control SGCB-/- mice and WT mice and analyzed for fibrosis (collagen levels) (n=5 per group). Using sirius red staining and quantification, collagen levels were reduced following treatment (see figure 17). Transcript levels of Col1A, Col3A, and Fbn were normalized and muscle fiber size was increased. Representative images of scanned full sections of untreated and AAVrh.74.CMV.miR29C treated tibialis anterior muscles stained with Sirius Red which stains for collagen 1 and 3 are shown in figure 118. This demonstrates proof of principle that scAAVrh.74.CMV.miR29C reduces fibrosis in SGCB-/- mice and could be used in combination with gene replacement with scAAVrh.74.tMCK.hSGCB or scAAVrh.74.MHCK7.hSGCB.

Example 13

Intravenous Gene Transfer to SGCB-/- Mice Reduces Kyphoscoliosis of Thoracic Spine

[0109] Degeneration of torso muscles due to the worsening histopathology in patients suffering from LGMD2E patients can be attributed to kyphosis. Kyphoscoliosis of the thoracic spine due to weakening of muscles supporting the spinal column can result in the diaphragm being pushed forward, further compromising lung capacity and diaphragm function. As a result of the severity of the phenotype in the *sgcb*^{-/-} mouse with the gross anatomical appearance of kyphoscoliosis, full body x-ray radiography was used to determine the degree of kyphosis in 7-month old BL6 WT mice (n=6), *sgcb*^{-/-} mice (n=6), and treated *sgcb*-1- mice 6 months post-injection (n=6). The kyphotic index (KI) score determines a quantitative value for the level of kyphoscoliosis (Laws et al. J. Appl. Physiol. 97: 1970-7, 2004). As depicted in the WT panel in Figure 19a, the KI score is a ratio of length from forelimb to hindlimb compared to the length of the midline to the apex of the curvature in the spine. While *sgcb*^{-/-} mice present with a severely curved spine and lower KI score of 3.64 ± 0.16 (n=6), BL6 WT mice have a significantly straighter spine resulting in a higher KI score of 6.01 ± 0.41 (n=6) ($p<0.01$) (Figure 19b). Treated *sgcb*^{-/-} mice exhibit a significant reduction in the degree of kyphosis in the spine with an increase in the KI score to 5.39 ± 0.58 (n=6) ($p<0.05$) (Figure 19b). These data indicated that intravenous delivery of scAAVrh.74.MHCK7.hSGCB is beneficial for the overall integrity of the spine and can alleviate the kyphosis and joint contractures present in the disease. This data demonstrated the alleviation of kyphosis and increased physical activity in *sgcb*^{-/-} mice following systemic delivery of the rAAV vector of the invention. This data is additional evidence that the gene therapy of the invention improves the quality of life for LGMD2E patients.

Example 14

Assessment of Cardiomyopathy

[0110] The histological destruction of limb and diaphragm muscle is also detected in the myocardium of 7 month old *sgcb*^{-/-} mice particularly with the presence of myocardial necrosis and fibrosis as evident by H&E and picrosirius red staining (Figure 20a). The presentation of impaired heart function often in the form of dilated cardiomyopathy with reduced cardiac output and lower ejection fraction (Semplicini et al., Neurology 84: 1772-81, 2015, Fanin et al., Neuromuscul Disorder 13:303-9, 2003). Cardiac magnetic resonance imaging (MRI), was used to evaluate several functional parameters of the heart in order to establish functional deficits in the myocardium of *sgcb*^{-/-} mice compared to BL6 WT mice to use as a functional outcome measure. Imaging of control mice at 7 months of age showed a reduction of 29.4% in stroke volume from 0.041 ± 0.0019 mL in *sgcb*^{-/-} hearts to 0.029 ± 0.0024 mL in BL6 WT hearts ($p<0.01$), a 31.7% lower cardiac output from 14.70 ± 0.74 mL/min in *sgcb*^{-/-} hearts to 12.72 ± 0.97 mL/min in BL6 WT hearts, and finally a 14.3% lower ejection fraction, $66.21 \pm 3.83\%$ in *sgcb*^{-/-} hearts compared to $76.90 \pm 1.67\%$ in BL6 WT hearts ($p<0.05$) (Figure 20b). This indicates a modest decline in overall cardiac function at this age and a trend towards the development of cardiomyopathy. Restoring hSGCB expression in hearts of KO mice through systemic delivery partially corrected these deficits, improving stroke volume to 0.032 ± 0.0027 mL, cardiac output to 14.66 ± 0.75 mL/min, and ejection fraction to $68.16 \pm 2.31\%$ (Figure 19b). As a correlate to the histological and functional disruption of cardiac tissue reported here, western blotting for cardiac troponin I (cTrpI) expression, an important regulator of cardiac function and an indicator (biomarker) of cardiac damage, is reduced in diseased *sgcb*^{-/-} hearts to 60.38% of the levels seen in BL6 WT mice (Figure 20c). Levels of cTrpI are restored following treatment to levels of 35.80% of the expression seen in WT hearts (Figure 20d).

Example 15

Functional restoration in diaphragm muscle with increase in physical activity

[0111] The significant involvement of diaphragm dysfunction and respiratory failure in LGMD2E mandate functional benefit to the diaphragm essential for validation of clinical systemic therapy. With the use of an ex vivo experimental protocol on strips taken from diaphragm muscle, it was assessed whether restoring β -sarcoglycan provides a functional benefit to this severely compromised muscle. In accordance with the significant histopathology identified in 7 month old diaphragms from diseased mice, *sgcb*^{-/-} diaphragms ($n=4$) exhibited a functional deficit with a significant (51%) reduction in specific force output compared to BL6 WT mice ($n=5$) (116.24 ± 10.49 mN/mm² vs. 236.67 ± 15.87 mN/mm², respectively, $p<0.001$), as well as a greater loss of force from that produced after the first contraction following a rigorous fatigue protocol ($23 \pm 1.0\%$ loss in *sgcb*^{-/-}; $7.0 \pm 3.0\%$ loss in BL6 WT, $p<0.05$) (Figure 6a). Six months following tail

vein delivery of scAAVrh.74.MHCK7.hSGCB, a dramatic improvement in specific force output was observed. The specific force output increased to $226.07 \pm 27.12 \text{ mN/mm}^2$ (n=5) (p<0.05 compared to *sgcb*^{-/-}) and better protection of the muscle from repeated fatigue was observed with only a $12.0 \pm 4.0\%$ loss of force (p<0.05 compared to *sgcb*^{-/-}) (Figure 21a). Overall, these data support our previous findings in the TA muscle and show that restoring β -sarcoglycan provides functional recovery in diaphragm muscle.

[0112] Symptoms of increased fatigue and reduced overall activity are frequently reported in many neuromuscular diseases, partially attributed to the occurrence of kyphosis. As a result and taking into account the phenotype of LGMD2E, it was hypothesized that KO mice would naturally be less active compared to healthy WT mice, and moreover systemic delivery of rAAV.MHCK7.hSGCB to *sgcb*^{-/-} mice would result in more physically active mice. In order to test this hypothesis and additional potential functional benefits of gene transfer, a laser-monitoring of open-field cage activity protocol similar to that described in Kobayashi et al., *Nature* 456: 511-5, 2008 and Beaström et al., *Am. J. Pathol.* 179: 2464-74, 2011, was performed on all groups of mice. The graphs in Figure 21b depict a significant decrease (55.5%) in KO mice compared to WT, in both total ambulation (horizontal movement in the x and y planes) and hindlimb vertical rearing. The average number of horizontal ambulatory laser beam breaks over a 1 hour period in WT mice was 7355 ± 400.8 (n=6) compared to 3271 ± 483.8 (n=6) in KO mice (p<0.0001). Furthermore, the average number of vertical rearing beam breaks recorded in WT mice was 626.7 ± 53.76 as opposed to 264.5 ± 63.36 in KO mice (p<0.01) (Figure 21b). In accordance with the initial hypothesis, rAAV.MHCK7.hSGCB treated mice were visibly more active compared to KO which was illustrated in the quantification of activity, where total ambulation increased by 22% to 5143 ± 293.2 beam breaks (p<0.05) and hind limb vertical rearing increased dramatically by 77% to 615.3 ± 95.93 beam breaks (p<0.05) in treated mice (n=6) (Figure 21b).

Example 16

Safety and biodistribution analysis of rAAVrh.74.MHCK7.hSGCB

[0113] Potential toxicity or safety concerns of hSGCB gene therapy was assessed in *sgcb*^{-/-} mice at 6 months following systemic delivery of scAAVrh.74.MHCK7.hSGCB at 1.0×10^{12} vg total dose (5×10^{13} vg/kg). Vector biodistribution and off-target transgene expression were analyzed on tissue samples (TA, TRI, diaphragm, heart, gonad, lungs, kidney, liver, and spleen) from vector dosed *sgcb*^{-/-} animals using qPCR and Western blotting, respectively. Using vector specific primer probe sets, MHCK7.hSGCB vector genomes were detected at varying levels in all collected tissues. As expected, the highest levels were seen in the liver as well as skeletal muscle and the heart, indicating that the test article was efficiently delivered into all intended muscles of vector dosed mice (Figure 22a). Furthermore, western blotting to

detect hSGCB protein expression confirmed the functionality of the muscle specific MHCK7 promoter and the expression of transgene restricted to cardiac and skeletal muscle. Beta-sarcoglycan protein expression was observed in varying amounts in all skeletal muscle samples as well as heart samples, and importantly was not detected in any non-muscle tissue (Figure 22b), supported by the fact that beta-sarcoglycan is known to be a muscle specific protein. Finally, hematoxylin & eosin staining was performed on cryosections of muscle tissue and all offsite organs harvested from five *sgcb*^{-/-} mice along with five C57BL6 WT mice treated systemically with our vector at the therapeutic dose used in this study. These sections were then formally reviewed for toxicity by a veterinary pathologist and no adverse effects were detected in any sample from any of the mice. Taken together, these data indicate that this test article was well tolerated by the test animals.

[0114] The fact that such high levels of transduction in all muscles throughout the body was achieved with no adverse effects using a relatively low dose (1×10^{12} vg total dose; 5×10^{13} vg/kg) provides great promise for translation to LGMD2E patients. From a clinical perspective, the dose used in the experiments described herein is much lower than the dose used for systemic delivery of an SMN1 expressing AAV therapy delivered to babies with SMA, which is currently in clinical trial (Mendell et al., Mol. Ther. 24: S 190, 2016). The highly efficient restoration of β -sarcoglycan expression using the MHCK7 promoter accompanied with functional benefits is very encouraging at dosing levels that could be applied clinically, and given the high incidence of heart involvement in the β -sarcoglycan deficiency in the LGMD2E patients, systemic delivery provides a great benefit to these patients.

[0115] References:

- 1 Bonnemann CG, Modi R, Noguchi S, Mizuno Y, Yoshida M, Gussoni E et al. Beta-sarcoglycan (A3b) mutations cause autosomal recessive muscular dystrophy with loss of the sarcoglycan complex. *Nat Genet* 1995; 11: 266-273.
- 2 Moore SA, Shilling CJ, Westra S, Wall C, Wicklund MP, Stolle C et al. Limb-girdle muscular dystrophy in the United States. *J Neuropathol Exp Neurol* 2006; 65: 995-1003.
- 3 Araishi K, Sasaoka T, Imamura M, Noguchi S, Hama H, Wakabayashi E et al. Loss of the sarcoglycan complex and sarcospan leads to muscular dystrophy in beta-sarcoglycan-deficient mice. *Hum Mol Genet* 1999; 8: 1589-1598.
- 4 Durbeej M, Cohn RD, Hrstka RF, Moore SA, Allamand V, Davidson BL et al. Disruption of the beta-sarcoglycan gene reveals pathogenetic complexity of limb-girdle muscular dystrophy type 2E. *Mol Cell* 2000; 5: 141-151.
- 5 Bonnemann CG, Passos-Bueno MR, McNally EM, Vainzof M, de Sa Moreira E, Marie SK et al. Genomic screening for beta-sarcoglycan gene mutations: missense mutations may cause severe limb-girdle muscular dystrophy type 2E (LGMD 2E). *Hum Mol Genet* 1996; 5: 1953-1961.
- 6 Angelini C, Fanin M, Freda MP, Duggan DJ, Siciliano G, Hoffman EP. The clinical spectrum of sarcoglycanopathies. *Neurology* 1999; 52: 176-179.
- 7 Sandona D, Betto R. Sarcoglycanopathies: molecular pathogenesis and therapeutic prospects. *Exp Rev Mol Med* 2009; 11: e28.

8. 8 Fanin M, Melacini P, Boito C, Pegoraro E, Angelini C. LGMD2E patients risk developing dilated cardiomyopathy. *Neuromusc Disord* 2003; 13: 303-309.
9. 9 Sveen ML, Thune JJ, Kober L, Vissing J. Cardiac involvement in patients with limb-girdle muscular dystrophy type 2 and Becker muscular dystrophy. *Arch Neurol* 2008; 65: 1196-1201.
10. 10 Melacini P, Fanin M, Duggan DJ, Freda MP, Berardinelli A, Danieli GA et al. Heart involvement in muscular dystrophies due to sarcoglycan gene mutations. *Muscle Nerve* 1999; 22: 473-479.
11. 11 Narayanaswami P, Weiss M, Selcen D, David W, Raynor E, Carter G et al. Evidence-based guideline summary: diagnosis and treatment of limb-girdle and distal dystrophies: report of the guideline development subcommittee of the American Academy of Neurology and the practice issues review panel of the American Association of Neuromuscular & Electrodiagnostic Medicine. *Neurology* 2014; 83: 1453-1463.
12. 12 Wong-Kisiel LC, Kuntz NL. Two siblings with limb-girdle muscular dystrophy type 2E responsive to deflazacort. *Neuromusc Disord* 2010; 20: 122-124.
13. 13 Barresi R, Di Blasi C, Negri T, Brugnoni R, Vitali A, Felisari G et al. Disruption of heart sarcoglycan complex and severe cardiomyopathy caused by beta sarcoglycan mutations. *J Med Genet* 2000; 37: 102-107.
14. 14 Gibertini S, Zanotti S, Savadori P, Curcio M, Saredi S, Salerno F et al. Fibrosis and inflammation are greater in muscles of beta-sarcoglycan-null mouse than mdx mouse. *Cell Tissue Res* 2014; 356: 427-443.
15. 15 McCarty DM, Fu H, Monahan PE, Toulson CE, Naik P, Samulski RJ. Adeno-associated virus terminal repeat (TR) mutant generates self-complementary vectors to overcome the rate-limiting step to transduction in vivo. *Gene Ther* 2003; 10: 2112-2118.
16. 16 McCarty DM, Monahan PE, Samulski RJ. Self-complementary recombinant adeno-associated virus (scAAV) vectors promote efficient transduction independently of DNA synthesis. *Gene Ther* 2001; 8: 1248-1254.
17. 17 Chicoine LG, Rodino-Klapac LR, Shao G, Xu R, Bremer WG, Camboni M et al. Vascular delivery of rAAVrh74.MCK.GALGT2 to the gastrocnemius muscle of the rhesus macaque stimulates the expression of dystrophin and laminin alpha2 surrogates. *Mol Ther* 2014; 22: 713-724.
18. 18 Rodino-Klapac LR, Montgomery CL, Bremer WG, Shontz KM, Malik V, Davis N et al. Persistent expression of FLAG-tagged micro dystrophin in nonhuman primates following intramuscular and vascular delivery. *Mol Ther* 2010; 18: 109-117.
19. 19 Rodino-Klapac LR, Janssen PM, Montgomery CL, Coley BD, Chicoine LG, Clark KR et al. A translational approach for limb vascular delivery of the micro-dystrophin gene without high volume or high pressure for treatment of Duchenne muscular dystrophy. *J Transl Med* 2007; 5: 45.
20. 20 Wang B, Li J, Fu FH, Chen C, Zhu X, Zhou L et al. Construction and analysis of compact muscle-specific promoters for AAV vectors. *Gene Ther* 2008; 15: 1489-1499.
21. 21 Chicoine LG, Montgomery CL, Bremer WG, Shontz KM, Griffin DA, Heller KN et al. Plasmapheresis eliminates the negative impact of AAV antibodies on micro-dystrophin gene expression following vascular delivery. *Mol Ther* 2014; 22: 338-347.
22. 22 Matsuda R, Nishikawa A, Tanaka H. Visualization of dystrophic muscle fibers in mdx

mouse by vital staining with Evans blue: evidence of apoptosis in dystrophin-deficient muscle. *J Biochem* 1995; 118: 959-964.

23. 23 Straub V, Rafael JA, Chamberlain JS, Campbell KP. Animal models for muscular dystrophy show different patterns of sarcolemmal disruption. *J Cell Biol* 1997; 139: 375-385.

24. 24 Mendell JR, Sahenk Z, Malik V, Gomez AM, Flanigan KM, Lowes LP et al. A phase 1/2a follistatin gene therapy trial for becker muscular dystrophy. *Mol Ther* 2015; 23: 192-201.

25. 25 Dressman D, Araishi K, Imamura M, Sasaoka T, Liu LA, Engvall E et al. Delivery of alpha- and beta-sarcoglycan by recombinant adeno-associated virus: efficient rescue of muscle, but differential toxicity. *Hum Gene Ther* 2002; 13: 1631-1646.

26. 26 Rodino-Klapac LR, Lee JS, Mulligan RC, Clark KR, Mendell JR. Lack of toxicity of alpha-sarcoglycan overexpression supports clinical gene transfer trial in LGMD2D. *Neurology* 2008; 71: 240-247.

27. 27 Shield MA, Haugen HS, Clegg CH, Hauschka SD. E-box sites and a proximal regulatory region of the muscle creatine kinase gene differentially regulate expression in diverse skeletal muscles and cardiac muscle of transgenic mice. *Mol Cell Biol* 1996; 16: 5058-5068.

28. 28 Rabinowitz JE, Rolling F, Li C, Conrath H, Xiao W, Xiao X et al. Cross-packaging of a single adeno-associated virus (AAV) type 2 vector genome into multiple AAV serotypes enables transduction with broad specificity. *J Virol* 2002; 76: 791-801.

29. 29 Grieger JC, Choi VW, Samulski RJ. Production and characterization of adeno-associated viral vectors. *Nat Protoc* 2006; 1: 1412-1428.

30. 30 Clark KR, Liu X, McGrath JP, Johnson PR. Highly purified recombinant adeno-associated virus vectors are biologically active and free of detectable helper and wild-type viruses. *Hum Gene Ther* 1999; 10: 1031-1039.

31. 31 Liu M, Yue Y, Harper SQ, Grange RW, Chamberlain JS, Duan D. Adeno-associated virus-mediated microdystrophin expression protects young mdx muscle from contraction-induced injury. *Mol Ther* 2005; 11: 245-256.

32. 32 Hakim CH, Grange RW, Duan D. The passive mechanical properties of the extensor digitorum longus muscle are compromised in 2- to 20-mo-old mdx mice. *J Appl Physiol* 2011; 110: 1656-1663.

33. 33 Wein N, Vulin A, Falzarano MS, Szigyarto CA, Maiti B, Findlay A et al. Translation from a DMD exon 5 IRES results in a functional dystrophin isoform that attenuates dystrophinopathy in humans and mice. *Nat Med* 2014; 20: 992-1000.

REFERENCES CITED IN THE DESCRIPTION

Cited references

This list of references cited by the applicant is for the reader's convenience only. It does not form part of the European patent document. Even though great care has been taken in compiling the references, errors or omissions cannot be excluded and the EPO disclaims all liability in this regard.

Patent documents cited in the description

- US9434928B [0003]
- WO0183692A [0024] [0044] [0045]
- US62323163 [0033] [0108]
- US5173414A [0047]
- WO9513365A [0047]
- US5658776A [0047]
- WO9513392A [0047]
- WO9617947A [0047]
- US9818600W [0047]
- WO9709441A [0047]
- US9614423W [0047]
- WO9708298A [0047]
- US9613872W [0047]
- WO9721825A [0047]
- US9620777W [0047]
- WO9706243A [0047]
- FR9601064W [0047]
- WO9911764A [0047]
- US5786211A [0047]
- US5871982A [0047]
- US6258595B [0047]
- US6566118B [0050]
- WO9809657A [0050]
- WO02053703A [0059]

Non-patent literature cited in the description

- **SRIVASTAVA et al.** *J. Virol.*, 1983, vol. 45, 555-564 [0003]
- **GAO et al.** *J. Virol.*, 2004, vol. 78, 6381-6388 [0003]
- *Mol. Ther.*, 2006, vol. 13, 167-76 [0003]

- Virology, 2004, vol. 330, 2375-383 [0003]
- MUZYCZKA Current Topics in Microbiology and Immunology, 1992, vol. 158, 97-129 [0003]
- CLARK et al. Hum Gene Ther, 1997, vol. 8, 659-669 [0005]
- KESSLER et al. Proc Natl Acad Sci USA, 1996, vol. 93, 14082-14087 [0005]
- XIAO et al. J Virol, 1996, vol. 70, 8098-8108 [0005]
- CHAO et al. Mol Ther, 2000, vol. 2, 619-623 [0005]
- CHAO et al. Mol Ther, 2001, vol. 4, 217-222 [0005]
- HERZOG et al. Proc Natl Acad Sci USA, 1997, vol. 94, 5804-5809 [0005]
- MURPHY et al. Proc Natl Acad Sci USA, 1997, vol. 94, 13921-13926 [0005]
- LEWIS et al. J Virol, 2002, vol. 76, 8769-8775 [0005]
- SAMBROOK et al. Molecular Cloning: A Laboratory Manual Cold Spring Harbor Laboratory 19890000 [0019]
- ANDERSON et al. Nucleic Acid Hybridisation: A Practical Approach IRL Press Limited [0020]
- MARSIC et al. Molecular Therapy, 2014, vol. 22, 111900-1909 [0024] [0044]
- CARTER Handbook of Parvoviruses, 1989, vol. 1, 169-228 [0041]
- BERNNS Virology Raven Press 199000001743-1764 [0041]
- BLACKLOWE Parvoviruses and Human Disease 19880000165-174 [0041]
- ROSE Comprehensive Virology, 1974, vol. 3, 1-61 [0041]
- SAMULSKI et al. Proc. Natl. Acad. S6. USA, 1982, vol. 79, 2077-2081 [0046]
- LAUGHLIN et al. Gene, 1983, vol. 23, 65-73 [0046]
- SENAPATHY CARTER J. Biol. Chem., 1984, vol. 259, 4661-4666 [0046]
- CARTER Current Opinions in Biotechnology, 1992, 1533-539 [0047]
- MUZYCZKA Curr. Topics in Microbial. and Immunol., 1992, vol. 158, 97-129 [0047]
- RATTSCHIN et al. Mol. Cell. Biol., 1984, vol. 4, 2072- [0047]
- HERMONAT et al. Proc. Natl. Acad. Sci. USA, 1984, vol. 81, 6466- [0047]
- TRATSCHIN et al. Mol. Cell. Biol., 1985, vol. 5, 3251- [0047]
- MCLAUGHLIN et al. J. Virol., 1988, vol. 62, 1963- [0047]
- LEBKOWSKI et al. Mol. Cell. Biol., 1988, vol. 7, 349- [0047]
- SAMULSKI et al. J. Virol., 1989, vol. 63, 3822-3828 [0047]
- PERRIN et al. Vaccine, 1995, vol. 13, 1244-1250 [0047]
- PAUL et al. Human Gene Therapy, 1993, vol. 4, 609-615 [0047]
- CLARK et al. Gene Therapy, 1996, vol. 3, 1124-1132 [0047]
- CLARK et al. Hum. Gene Ther., 1999, vol. 10, 61031-1039 [0050]
- SCHENPP CLARK Methods Mol. Med., 2002, vol. 69, 427-443 [0050]
- WEINTRAUB et al. Science, 1991, vol. 251, 761-766 [0065]
- CSERJESIOLSON Mol Cell Biol, 1991, vol. 11, 4854-4862 [0065]
- MUSCAT et al. Mol Cell Biol, 1987, vol. 7, 4089-4099 [0065]
- JOHNSON et al. Mol Cell Biol, 1989, vol. 9, 3393-3399 [0065]
- SEMENZA et al. Proc Natl Acad Sci USA, 1991, vol. 88, 5680-5684 [0065]
- MADERWHITE Proc. Natl. Acad. Sci. USA, 1993, vol. 90, 5603-5607 [0065]
- POZGAI et al. Gene Ther., 2016, vol. 23, 57-66 [0074]
- RODINO-KLAPAC et al. J. Trans. Med., 2007, vol. 5, 45- [0075]

- BEASTROM et al. Am. J. Pathol., 2011, vol. 179, 2464-74 [0086] [0112]
- RAFAEL-FORNEY et al. Circulation, 2011, vol. 124, 582-8 [0086]
- POZGAI et al. Gene Therap., 2016, vol. 23, 57-66 [0088]
- KOBAYASHI et al. Nature, 2008, vol. 456, 511-5 [0091] [0112]
- BEASTROM et al. Am. J. Pathol., 2011, vol. 179, 2464-74 [0091]
- VOIKAR et al. Genes Brain Behav., 2005, vol. 4, 240-52 [0091]
- ARAISHI et al. Hum. Mol. Genet, 1999, vol. 8, 1589-98 [0105]
- DURBEEJ et al. Mol. Cell., 2000, vol. 5, 141-51 [0105]
- LAWS et al. J. Appl. Physiol., 2004, vol. 97, 1970-7 [0109]
- SEMPLICINI et al. Neurology, 2015, vol. 84, 1772-81 [0110]
- FANIN et al. Neuromuscul Disorder, 2003, vol. 13, 303-9 [0110]
- MENDELL et al. Mol. Ther., 2016, vol. 24, 190- [0114]
- BONNEMANN CGMODI RNOGUCHI SMIZUNO YYOSHIDA MGUSSONI E et al. Beta-sarcoglycan (A3b) mutations cause autosomal recessive muscular dystrophy with loss of the sarcoglycan complex. Nat Genet, 1995, vol. 11, 266-273 [0115]
- MOORE SASHILLING CJWESTRA SWALL CWICKLUND MPSTOLLE C et al. Limb-girdle muscular dystrophy in the United States. J Neuropathol Exp Neurol, 2006, vol. 65, 995-1003 [0115]
- ARAISHI KSASAOKA TIMAMURA MNOGUCHI SHAMA HWAKABAYASHI E et al. Loss of the sarcoglycan complex and sarcospan leads to muscular dystrophy in beta-sarcoglycan-deficient mice. Hum Mol Genet, 1999, vol. 8, 1589-1598 [0115]
- DURBEEJ MCOHN RDHRSTKA RFMOORE SAALLAMAND VDAVIDSON BL et al. Disruption of the beta-sarcoglycan gene reveals pathogenetic complexity of limb-girdle muscular dystrophy type 2E. Mol Cell, 2000, vol. 5, 141-151 [0115]
- BONNEMANN CGPASSOS-BUENO MRMCNALLY EMVAINZOF MDE SA MOREIRA EMARIE SK et al. Genomic screening for beta-sarcoglycan gene mutations: missense mutations may cause severe limb-girdle muscular dystrophy type 2E (LGMD 2E). Hum Mol Genet, 1996, vol. 5, 1953-1961 [0115]
- ANGELINI CFANIN MFREDA MPDUGGAN DJSICILIANO GHOFFMAN EP The clinical spectrum of sarcoglycanopathies. Neurology, 1999, vol. 52, 176-179 [0115]
- SANDONA DBETTO RSarcoglycanopathies: molecular pathogenesis and therapeutic prospects. Exp Rev Mol Med, 2009, vol. 11, e28- [0115]
- FANIN MMELACINI PBOITO CPEGORARO EANGELINI CLGMD2E patients risk developing dilated cardiomyopathy. Neuromusc Disord, 2003, vol. 13, 303-309 [0115]
- SVEEN MLTHUNE JJKOBER LVISSING J. Arch Neurol, 2008, vol. 65, 1196-1201 [0115]
- MELACINI PFANIN MDUGGAN DJFREDA MPBERARDINELLI ADANIELI GA et al. Heart involvement in muscular dystrophies due to sarcoglycan gene mutations. Muscle Nerve, 1999, vol. 22, 473-479 [0115]
- NARAYANASWAMI PWEISS MSELKEN DDAVID WRAYNOR ECARTER G et al. Evidence-based guideline summary: diagnosis and treatment of limb-girdle and distal dystrophies: report of the guideline development subcommittee of the American Academy of Neurology and the practice issues review panel of the American Association of Neuromuscular & Electrodiagnostic Medicine. Neurology, 2014, vol. 83, 1453-1463 [0115]

- WONG-KISIEL LCKUNTZ NLTwo siblings with limb-girdle muscular dystrophy type 2E responsive to deflazacort. *Neuromusc Disord*, 2010, vol. 20, 122-124 [0115]
- BARRESI RDI BLASI CNEGRI TBRUGNONI RVITALI AFELISARI G et al. Disruption of heart sarcoglycan complex and severe cardiomyopathy caused by beta sarcoglycan mutations. *J Med Genet*, 2000, vol. 37, 102-107 [0115]
- GIBERTINI SZANOTTI SAVADORI PCURCIO MSAREDI SSALERNO F et al. Fibrosis and inflammation are greater in muscles of beta-sarcoglycan-null mouse than mdx mouse. *Cell Tissue Res*, 2014, vol. 356, 427-443 [0115]
- MCCARTY DMFU HMONAHAN PETOULSON CENA IK PSAMULSKI RJ. Adeno-associated virus terminal repeat (TR) mutant generates self-complementary vectors to overcome the rate-limiting step to transduction in vivo. *Gene Ther*, 2003, vol. 10, 2112-2118 [0115]
- MCCARTY DMMONAHAN PESAMULSKI RJ. Self-complementary recombinant adeno-associated virus (scAAV) vectors promote efficient transduction independently of DNA synthesis. *Gene Ther*, 2001, vol. 8, 1248-1254 [0115]
- CHICOINE LGRODINO-KLAPAC LRSHAO GXU RBREMER WGAMBONI M et al. Vascular delivery of rAAVrh74.MCK.GALGT2 to the gastrocnemius muscle of the rhesus macaque stimulates the expression of dystrophin and laminin alpha2 surrogates. *Mol Ther*, 2014, vol. 22, 713-724 [0115]
- RODINO-KLAPAC LRMONTGOMERY CLBREMER WGSHONTZ KMMALIK VDAVIS N et al. Persistent expression of FLAG-tagged micro dystrophin in nonhuman primates following intramuscular and vascular delivery. *Mol Ther*, 2010, vol. 18, 109-117 [0115]
- RODINO-KLAPAC LRJANSSEN PMMONTGOMERY CLCOLEY BDCHICOINE LGCLARK KR et al. A translational approach for limb vascular delivery of the micro-dystrophin gene without high volume or high pressure for treatment of Duchenne muscular dystrophy. *J Transl Med*, 2007, vol. 5, 45- [0115]
- WANG BLI JFU FHCHEN CZHU XZHOU L et al. Construction and analysis of compact muscle-specific promoters for AAV vectors. *Gene Ther*, 2008, vol. 15, 1489-1499 [0115]
- CHICOINE LGMONTGOMERY CLBREMER WGSHONTZ KMGRiffin DAHELLER KN et al. Plasmapheresis eliminates the negative impact of AAV antibodies on micro-dystrophin gene expression following vascular delivery. *Mol Ther*, 2014, vol. 22, 338-347 [0115]
- MATSUDA RNISHIKAWA ATANAKA H. Visualization of dystrophic muscle fibers in mdx mouse by vital staining with Evans blue: evidence of apoptosis in dystrophin-deficient muscle. *J Biochem*, 1995, vol. 118, 959-964 [0115]
- STRAUB VRAFAEL JACHAMBERLAIN JSCAMPBELL KP. Animal models for muscular dystrophy show different patterns of sarcolemmal disruption. *J Cell Biol*, 1997, vol. 139, 375-385 [0115]
- MENDELL JRSAHENK ZMALIK VGOMEZ AMFLANIGAN KMLOWES LP et al. A phase 1/2a follistatin gene therapy trial for becker muscular dystrophy. *Mol Ther*, 2015, vol. 23, 192-201 [0115]
- DRESSMAN DARAISHI KIMAMURA MSASAOKA TLIU LAENGVALL E et al. Delivery of alpha- and beta-sarcoglycan by recombinant adeno-associated virus: efficient rescue of muscle, but differential toxicity. *Hum Gene Ther*, 2002, vol. 13, 1631-1646 [0115]

- RODINO-KLAPAC LRLEE JSMULLIGAN RCCLARK KRMENDELL JR.Lack of toxicity of alpha-sarcoglycan overexpression supports clinical gene transfer trial in LGMD2D.*Neurology*, 2008, vol. 71, 240-247 [0115]
- SHIELD MAHAUGEN HSCLEGG CHHAUSCHKA SDE-box sites and a proximal regulatory region of the muscle creatine kinase gene differentially regulate expression in diverse skeletal muscles and cardiac muscle of transgenic mice.*Mol Cell Biol*, 1996, vol. 16, 5058-5068 [0115]
- RABINOWITZ JEROLLING FLI CCONRATH HXIAO WXIAO X et al.Cross-packaging of a single adeno-associated virus (AAV) type 2 vector genome into multiple AAV serotypes enables transduction with broad specificity.*J Virol*, 2002, vol. 76, 791-801 [0115]
- GRIEGER JCCHOI VWSAMULSKI RJ.Production and characterization of adeno-associated viral vectors.*Nat Protoc*, 2006, vol. 1, 1412-1428 [0115]
- CLARK KRLIU XMCGRATH JPJOHNSON PR.Highly purified recombinant adeno-associated virus vectors are biologically active and free of detectable helper and wild-type viruses.*Hum Gene Ther*, 1999, vol. 10, 1031-1039 [0115]
- LIU MYUE YHARPER SQGRANGE RWCHAMBERLAIN JSDUAN D.Adeno-associated virus-mediated microdystrophin expression protects young mdx muscle from contraction-induced injury.*Mol Ther*, 2005, vol. 11, 245-256 [0115]
- HAKIM CHGRANGE RWDUAN D.The passive mechanical properties of the extensor digitorum longus muscle are compromised in 2- to 20-mo-old mdx mice.*J Appl Physiol*, 2011, vol. 110, 1656-1663 [0115]
- WEIN NVULIN AFALZARANO MSSZIGYARTO CAMAITI BFINDLAY A et al.Translation from a DMD exon 5 IRES results in a functional dystrophin isoform that attenuates dystrophinopathy in humans and mice.*Nat Med*, 2014, vol. 20, 992-1000 [0115]

Patentkrav

1. Rekombinant AAV-vektor, som omfatter en polynukleotidsekvens, der koder for β -sarcoglycan, hvor polynukleotidsekvensen omfatter en nukleotidsekvens, der er mindst 95 % identisk med SEQ ID NO: 1.
2. Rekombinant AAV-vektor, som omfatter en polynukleotidsekvens, der koder for β -sarcoglycan, der er mindst 95 % identisk med SEQ ID NO: 2.
3. Rekombinant AAV-vektor ifølge krav 1 eller 2, hvor polynukleotidsekvensen, der koder for β -sarcoglycan, omfatter nukleotidsekvensen som vist i SEQ ID NO: 1.
4. Rekombinant AAV-vektor ifølge krav 2, hvor polynukleotidsekvensen koder for β -sarcoglycan ifølge SEQ ID NO: 2.
5. Rekombinant AAV-vektor ifølge et hvilket som helst af kravene 1-4, hvor vektoren er serotype AAV1, AAV2, AAV4, AAV5, AAV6, AAV7, AAV8, AAV9, AAV10, AAV11, AAV12, AAV13 eller AAV rh.74.
6. Rekombinant AAV-vektor ifølge et hvilket som helst af kravene 1-5, hvor polynukleotidsekvensen er operabelt koblet til et muskelspecifikt kontrolelement.
7. Rekombinant AAV-vektor ifølge krav 6, hvor det muskelspecifikke kontrolelement er den trunkerede MCK-promotor (tMCK).
8. Rekombinant AAV-vektor ifølge krav 6, hvor det muskelspecifikke kontrolelement er MHCK7-promotoren.
9. Rekombinant AAV-vektor ifølge et hvilket som helst af kravene 1-8, som omfatter nukleotidsekvensen som vist i SEQ ID NO: 3.

10. Rekombinant AAV-vektor ifølge et hvilket som helst af kravene 1-8, som omfatter nukleotidsekvensen som vist i SEQ ID NO: 5.

5

11. Sammensætning, som omfatter den rekombinante AAV-vektor ifølge et hvilket som helst af kravene 1-10.

12. Sammensætning, som omfatter den rekombinante AAV-vektor
10 ifølge et hvilket som helst af kravene 1-10, til anvendelse til
reducering af fibrose hos et individ, der har brug for det.

13. Sammensætning, som omfatter den rekombinante AAV-vektor
15 ifølge et hvilket som helst af kravene 1-10, til anvendelse til
behandling af β -sarcoglycanopati hos et individ, der har brug
for det.

14. Sammensætning til anvendelse ifølge krav 12 eller 13, hvor
individet lider af muskeldystrofi, eventuelt hvor
20 muskeldystrofien er limb-girdle muskeldystrofi.

15. Sammensætning, som omfatter den rekombinante AAV-vektor ifølge et hvilket som helst af kravene 1-10, til anvendelse til
behandling af muskeldystrofi.

25

16. Sammensætning til anvendelse ifølge et hvilket som helst af kravene 12-15, hvor individet er et menneske.

17. Sammensætning, som omfatter den rekombinante AAV-vektor
30 ifølge et hvilket som helst af kravene 1-10, til anvendelse til
behandling af muskeldystrofi, eventuelt hvor muskeldystrofien
er limb-girdle muskeldystrofi (LGMD), og eventuelt hvor LGMD er
LGMD2E.

35 18. Sammensætning til anvendelse ifølge et hvilket som helst af kravene 12-17 eller sammensætning ifølge krav 11, som yderligere omfatter en anden rekombinant AAV-vektor, som omfatter miR-29-nukleotidsekvensen.

19. Sammensætning til anvendelse ifølge krav 18 eller
sammensætning ifølge krav 11, hvor den anden rekombinante AAV-
vektor omfatter nukleotidsekvensen som vist i SEQ ID NO: 9 eller
5 nukleotidsekvensen som vist i SEQ ID NO: 8.

20. Sammensætning til anvendelse ifølge et hvilket som helst
af kravene 12-19, hvor sammensætningen er formuleret til
intramuskulær injektion eller intravenøs injektion og/eller
10 formuleret til systemisk administration.

21. Sammensætning til anvendelse ifølge krav 20 eller
sammensætning ifølge krav 20, hvor den systemiske administration
er parenteral administration ved injektion, infusion eller
15 implantation.

DRAWINGS

Drawing

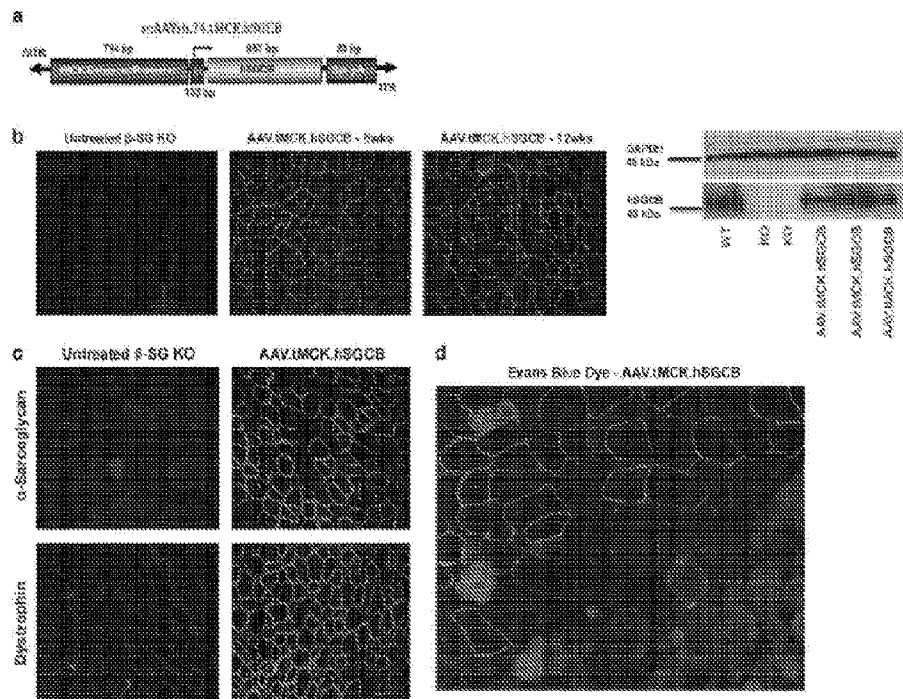


Figure 1. AAV-mediated β -sarcoglycan expression restores dystrophin-associated proteins and protects membranes integrity. **(a)** Self-complementary AAV vector containing the codon-optimized human β -sarcoglycan gene (hSGCB) driven by the muscle-specific MCK promoter. The cassette also contains a cleavage site to augment processing and polyadenylation signal for stability. **(b)** Immunofluorescence staining with anti- β -SG antibody shows high levels of sarcoglycan staining of the SGCB transgene in 5-week-old mice both 6 and 12 weeks post injection. $\times 20$ images shown. Percentage of fibers expressing beta-sarcoglycan per TA muscle averaged $22.4 \pm 8.2\%$ after 6 weeks ($n=9$, 4 male, 5 female) and $70.5 \pm 5.5\%$ after 12 weeks ($n=6$, 4 male, 2 female). Protein expression confirmed in the western blot with gamma-tubulin blot shown for a loading control. **(c)** AAV delivery of β -sarcoglycan leads to restoration of other members of the sarcoglycan complex, α -sarcoglycan, dystrophin. $\times 20$ images. **(d)** scAAV:hSGCB protects $\text{sg}\beta^{-/-}$ membranes from damage. Image showing a large area of Evans blue-positive fibers (red) juxtaposed to a cluster of β -sarcoglycan-positive fibers that have been protected from Evans blue dye incorporation. $\times 40$ image is shown.

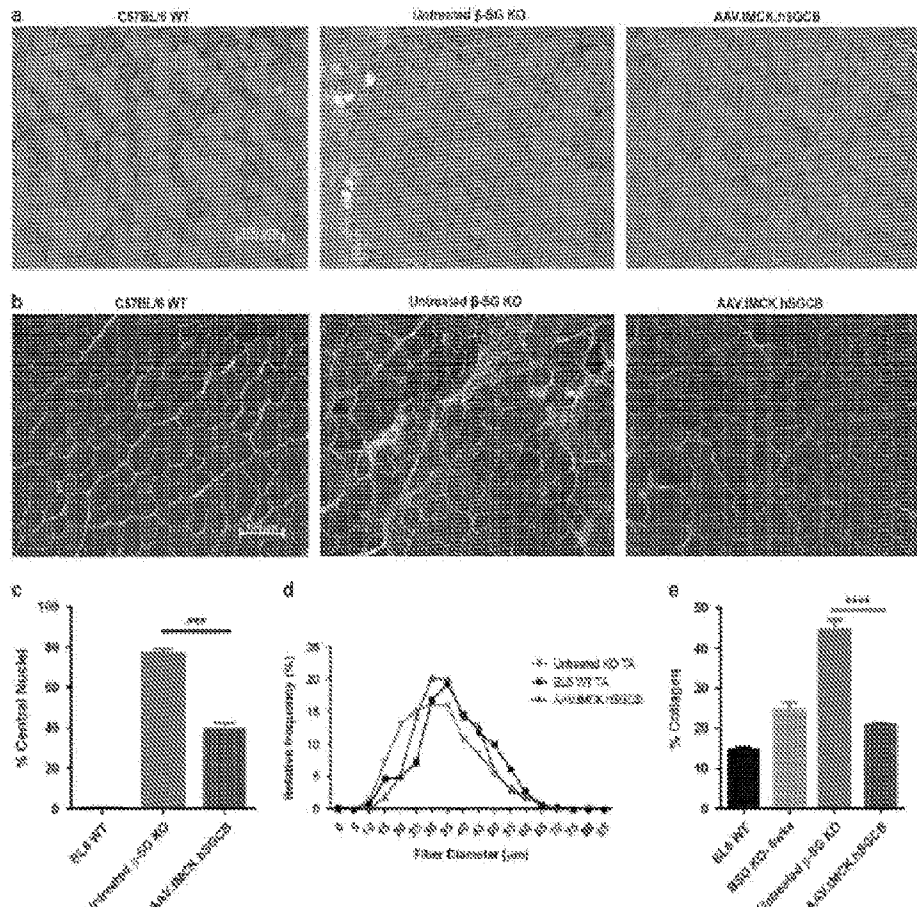


Figure 2. Histological analysis of p65-deficient treated skeletal muscle. AdAAV.p65CB treatment normalizes histological parameters of *tgfb3^{-/-}* mice. Hematoxylin & Eosin staining and Picosirius Red staining were performed on TA muscle from *tgfb3^{-/-}* mice along with normal control C57BL/6 mice and AdAAV.p65CB-treated mice followed by quantification of histological parameters and % collagen staining. (a) H&E staining shows the presence of centrally nucleated fibers, inflammatory cells and large fiber diameter distribution in p65-deficient muscle and an improvement in histopathology following gene transfer. (b) Picosirius Red staining shows a decrease in red collagen staining in treated muscle. (c) Quantification of centrally nucleated fibers showing a decrease following treatment ($P < 0.0005$, one-way ANOVA) and (d) representation of fiber size distribution and increase in average fiber size of TA muscle from C57BL/6 controls and *tgfb3^{-/-}* mice compared with treated mice ($P < 0.0001$, one-way ANOVA). (e) Quantification of % collagen in TA muscle from C57BL/6 controls and *tgfb3^{-/-}* mice compared with *tgfb3^{-/-}* treated mice ($P < 0.0001$, one-way ANOVA). 100 μ m scale bar shown for > 20 images. *** $P < 0.001$; **** $P < 0.0001$.

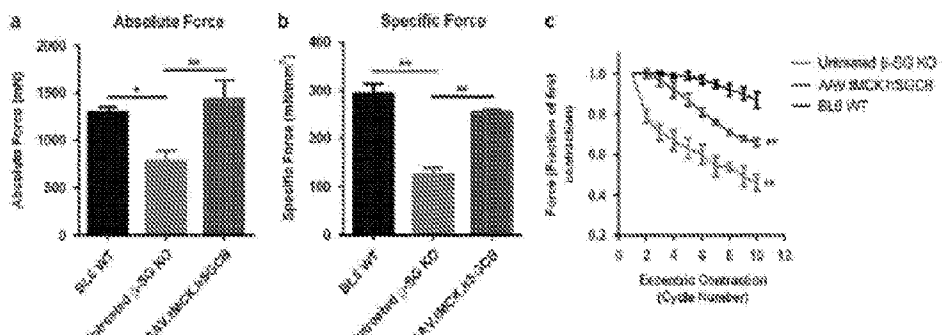


Figure 3. scAAVrh74.hSGCB intramuscular delivery corrects tetanic force and resistance to contraction-induced injury. The TA muscle of *sgcb*^{−/−} mice treated with 3×10^{11} vg of scAAVrh74.hSGCB via an iIC injection was harvested 6 weeks post gene transfer, and subjected to a protocol to assess tetanic force and an eccentric contraction protocol to assess resistance to contraction-induced injury. (a) AAVrh74.hSGCB-treated TAs demonstrated significant improvement in both absolute tetanic force ($P < 0.01$, paired t -test) and (b) normalized specific force ($P < 0.05$, paired t -test), which was not different from wild-type force (1.57/8.0). (c) AAVrh74.hSGCB-treated TAs exhibited significant improvement in resistance to contraction-induced injury compared with untreated *sgcb*^{−/−} controls ($P < 0.01$, two-way ANOVA). Force relaxation following 10 contractions is shown. * $P < 0.05$; ** $P < 0.01$.

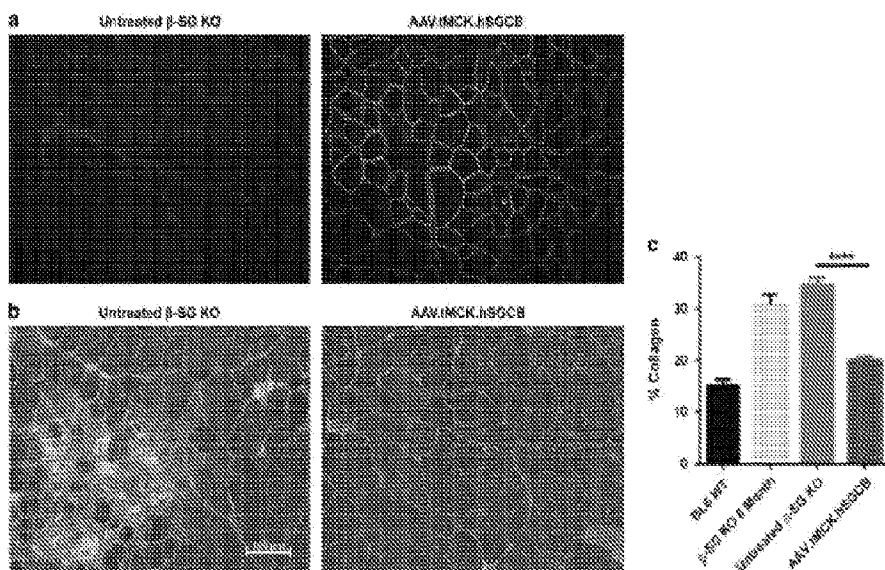


Figure 4. Analysis of aged mice injected intramuscularly with scAAVrh74.hMCK-hSGCB. (a) Immunofluorescence staining of TA muscle from 6-month-old injected *sgcb*^{−/−} mice 12 weeks post injection ($n = 5$, 3 male). Shows ectopic expression of the hSGCB transgene at levels averaging 20% in injected mice compared with untreated ($n = 4$, 4 male). (b) Picrosirius red staining of the treated and untreated TA muscle. (c) Quantification of collagen present in the Picrosirius red stained tissue shows a significant reduction in the amount of collagen following treatment with scAAVrh74.hMCK-hSGCB ($P < 0.0001$, one-way ANOVA). 100 μ m scale bar shown for $\times 20$ images. **** $P < 0.0001$.

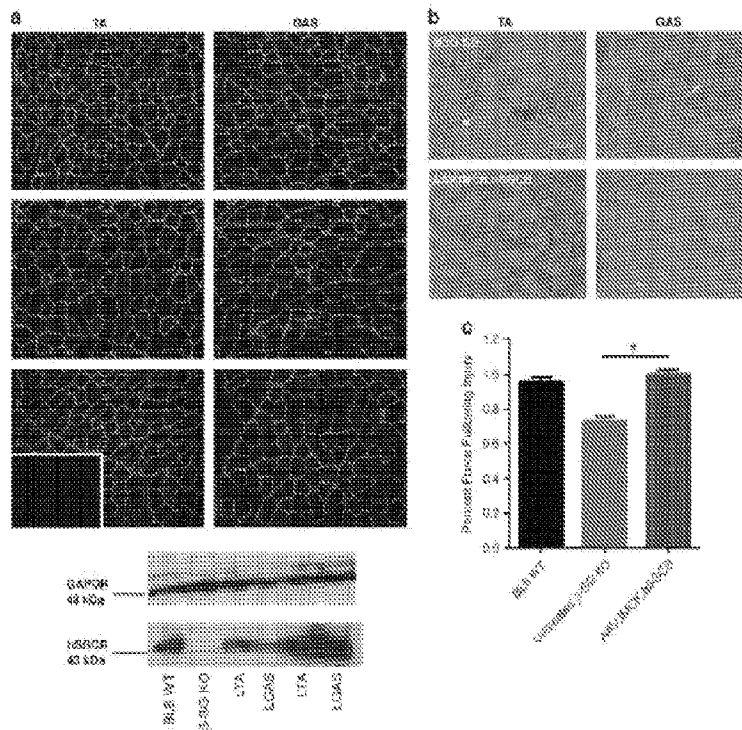


Figure 5. Vascular delivery of AdAVh74.hSGCB. Four ($n=3$, 3 male) and five ($n=4$, 2 male, 2 female) weeks β -SG-deficient mice were treated with vector via the femoral artery to deliver the vector to the lower limb muscles. At a dose of 5×10^7 vg, β -SG expression was $59.6 \pm 3.8\%$ in the TA and $31.3 \pm 4.7\%$ in the GAS of treated mice accompanied by improvements in histopathology that resulted in significant improvement in specific force compared with untreated animals even following an injury paradigm. (a) β -SG protein expression from three representative mice. Muscle from a β -SG KO untreated mouse is shown for comparison in the inset (lower right). $\times 20$ images are shown. Expression in treated muscles confirmed via western blot and gamma-tubulin is shown as a loading control. (b) Histopathology is significantly improved following high dose treatment. Upper panels-treated TA and gastrocnemius muscles. Bottom panels-untreated β -SG-deficient control muscle, 100 μ m scale bar shown for $\times 20$ images. (c) Percentage of specific force retained in EDL muscle following 10 cycles of eccentric contraction-induced injury. Treatment with 5×10^7 vg of AdAVh74.hSGCB led to significant improvement in force that was equivalent to WT (normal) control muscle ($P < 0.05$, one-way ANOVA). * $P < 0.05$.

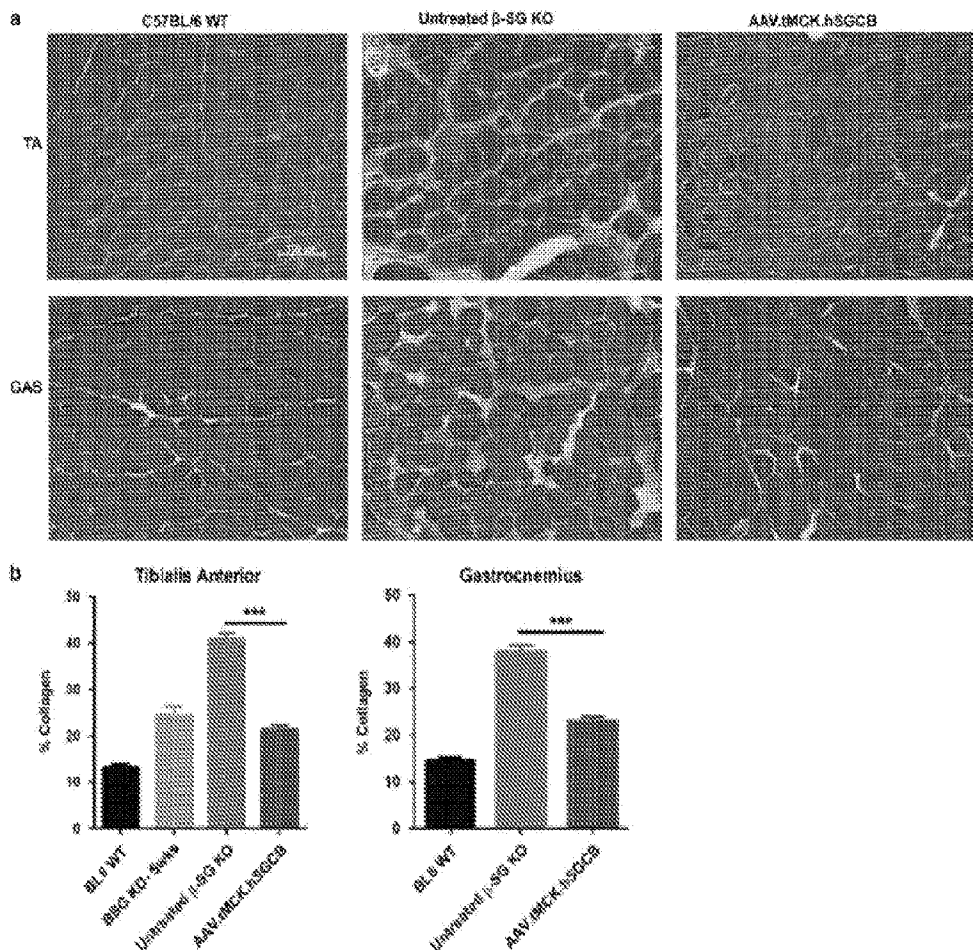


Figure 6. Reduction of fibrosis in ILP-treated β -SG KO mice. (a) Picrosirius red staining shows reduced fibrosis in treated mice indicated by a decrease in collagen deposition compared with untreated β -SG^{−/−} mice. (b) Quantification of collagen levels in the TA and GAS muscles from BL/6 WT, untreated β -SG^{−/−} mice, and treated mice confirm reduction in collagen levels in treated mice ($P < 0.001$, one-way ANOVA). 100 μ m scale bar shown for $\times 20$ images. *** $P < 0.001$.

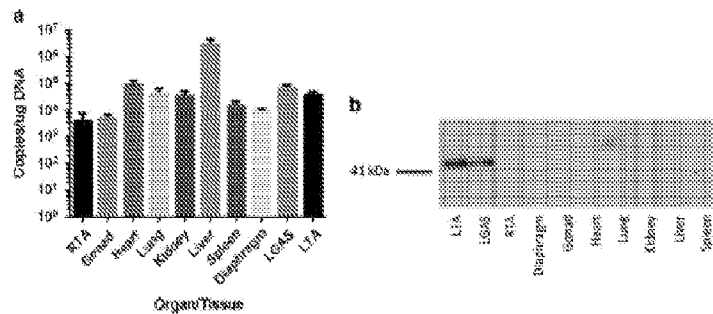


Figure 7. Vector biodistribution and protein expression. (a) Histogram of average distribution of vector in harvested tissues from ILP-treated mice given in copies of transcript per microgram of DNA added to qPCR. Left limb was treated. (b) No protein expression via western blot seen in off target organs.

Figure 8A

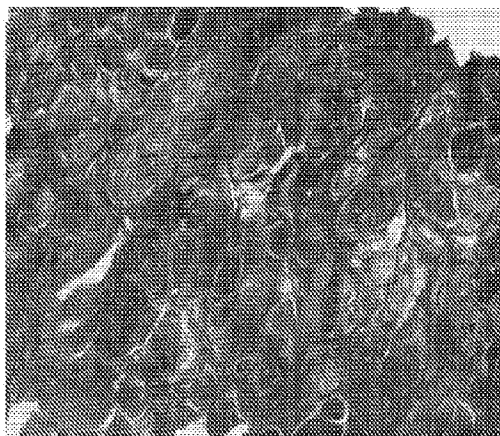


Figure 8B

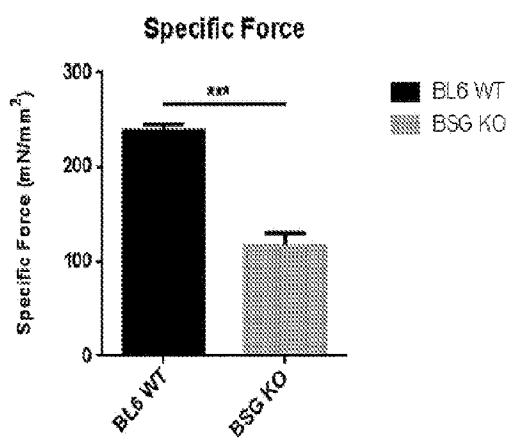


Figure 8C

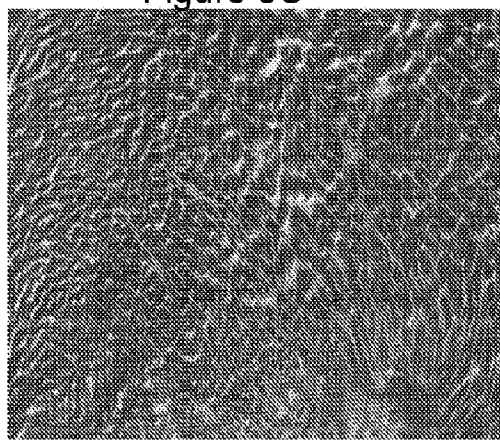


Figure 8D

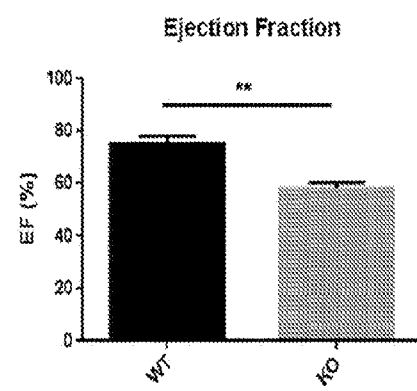
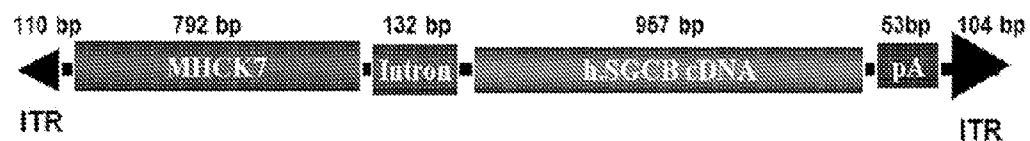


Figure 9

scAAVrh.74.MHCK7.hSGCB



scAAV.MHCK7.hSGCB cassette

Figure 10

Delivery of scAAVrh.74.MHCK7.hSGCB via the tail vein of SGCB^{-/-} mice results in nearly 100% transduction of muscle fibers in every muscle

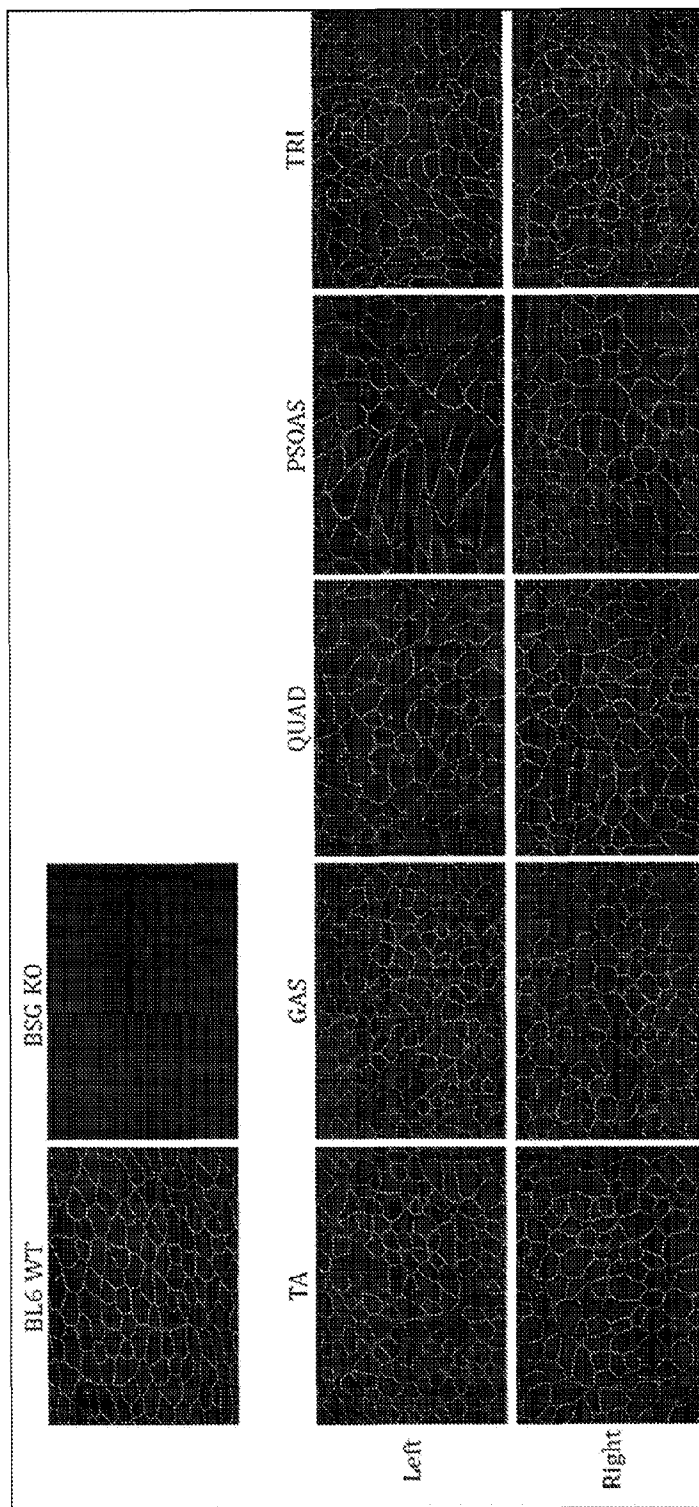


Figure 11

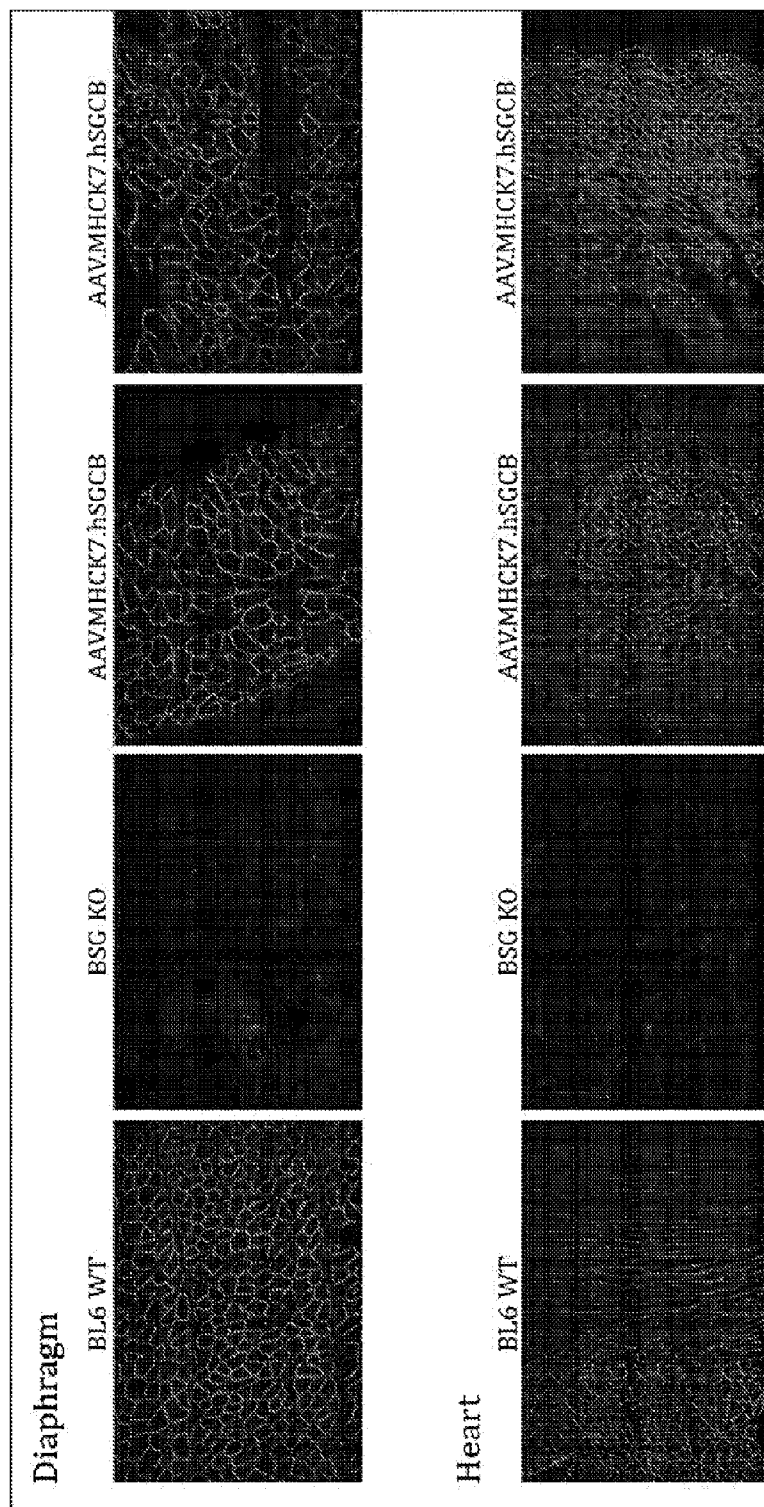


Figure 12B

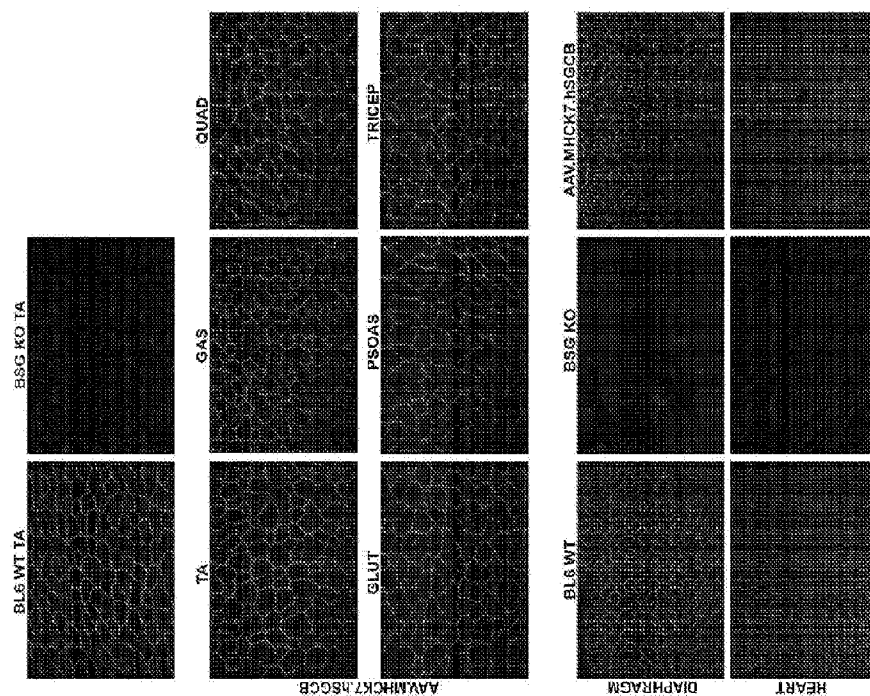


Figure 12A

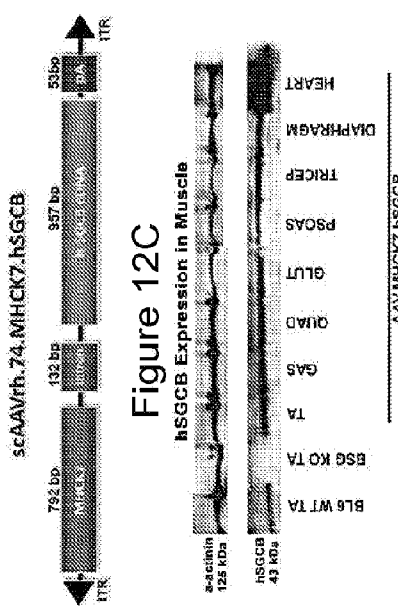


Figure 12C

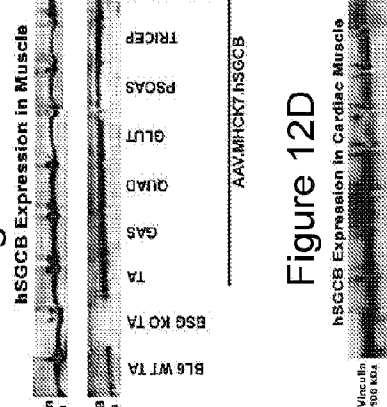
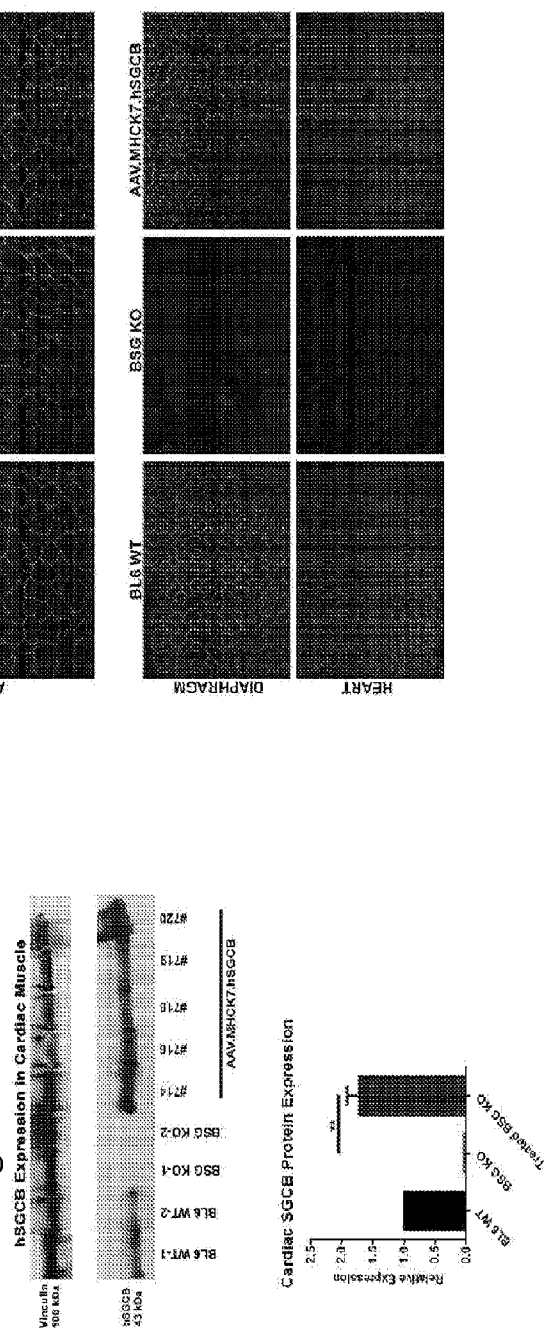


Figure 12D



Cardiac SGCB Protein Expression

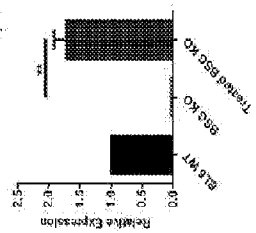


Figure 13A

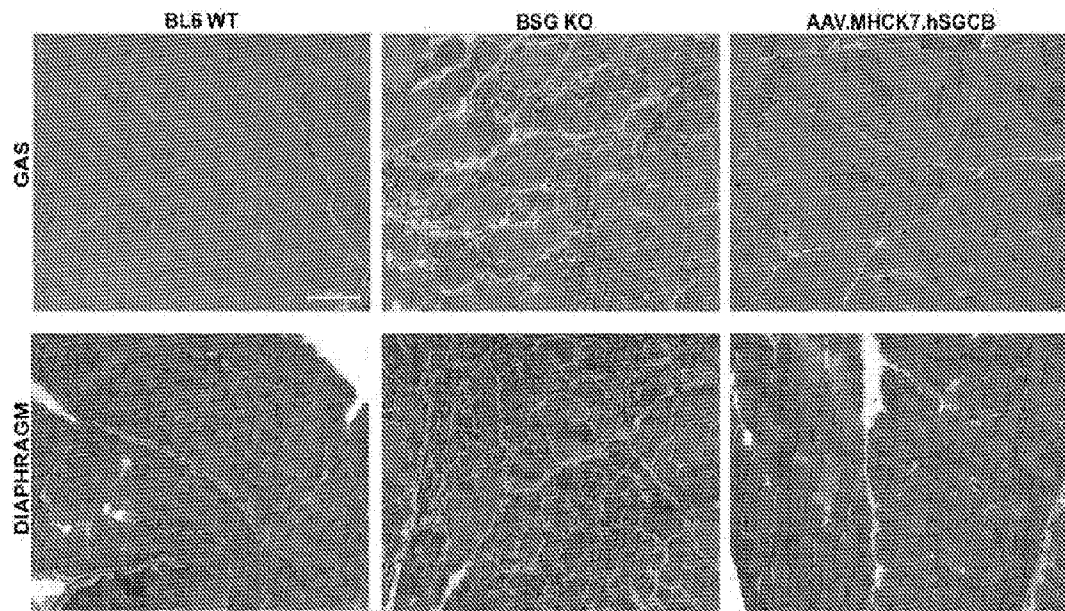


Figure 13B

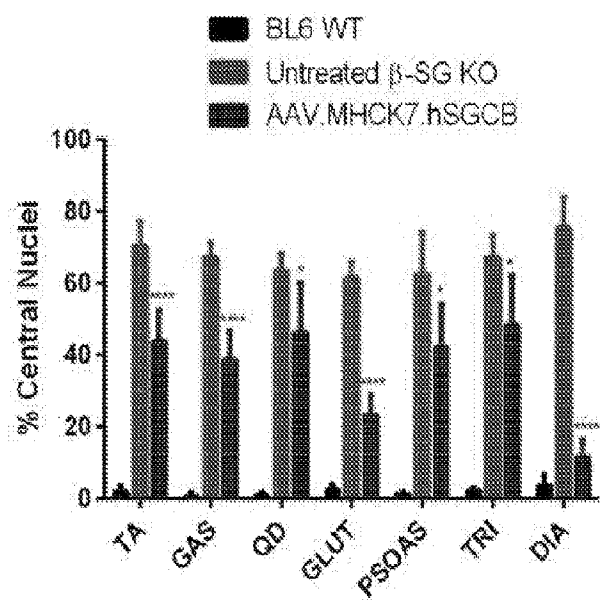


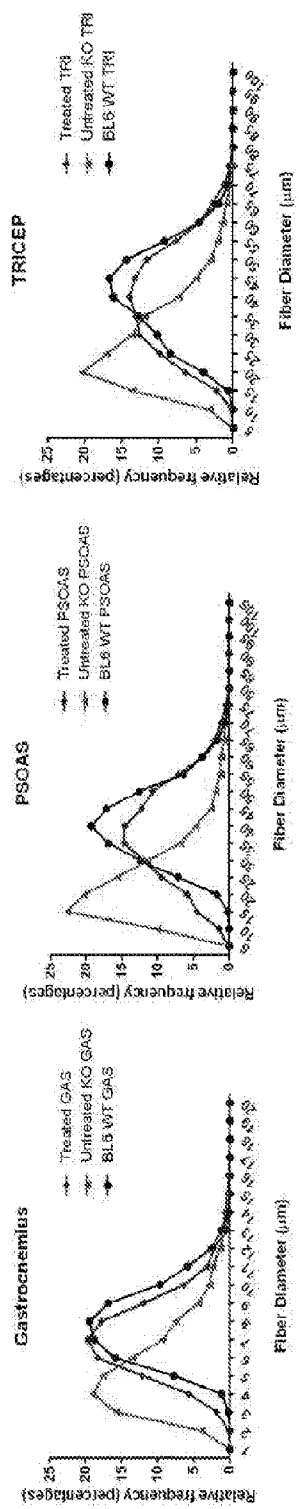
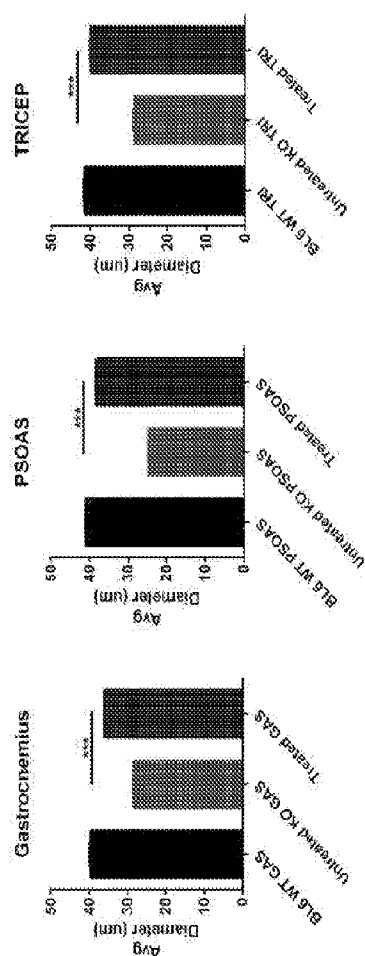
Figure 13C**Figure 13D**

Figure 14A

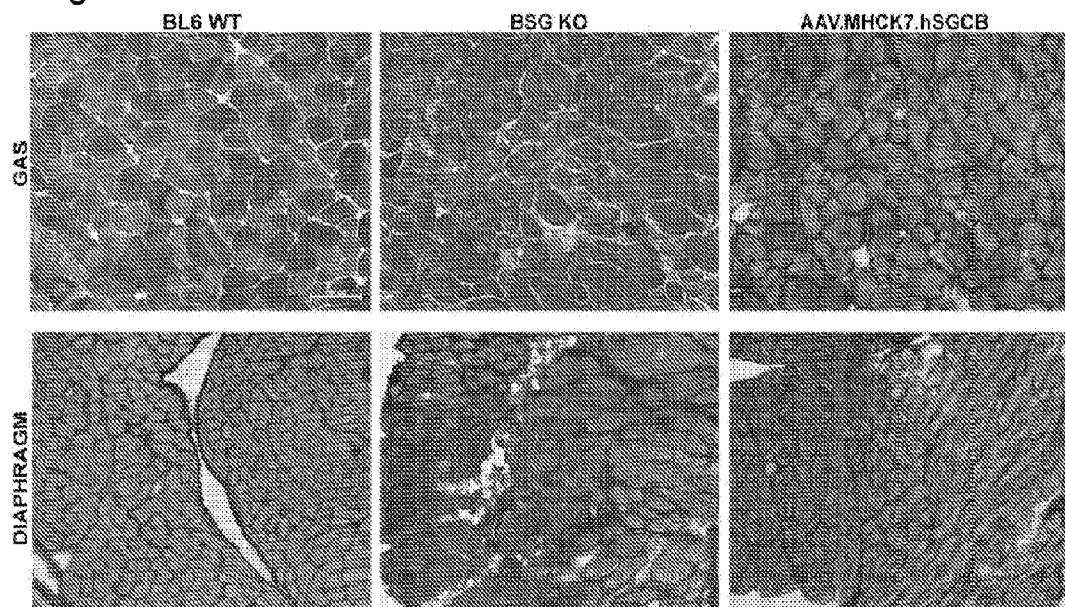


Figure 14B

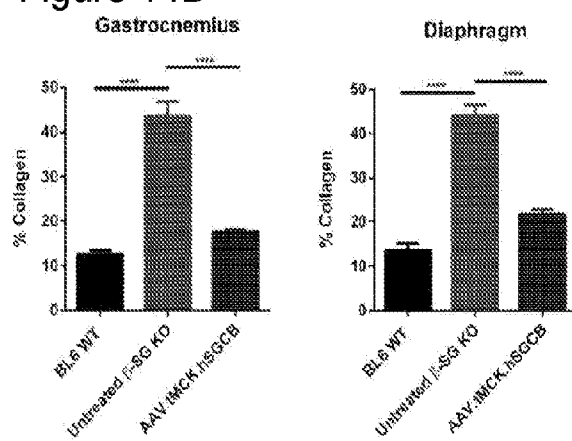


Figure 15

MHCK7.hSGC6 6 month IV 1e12vg

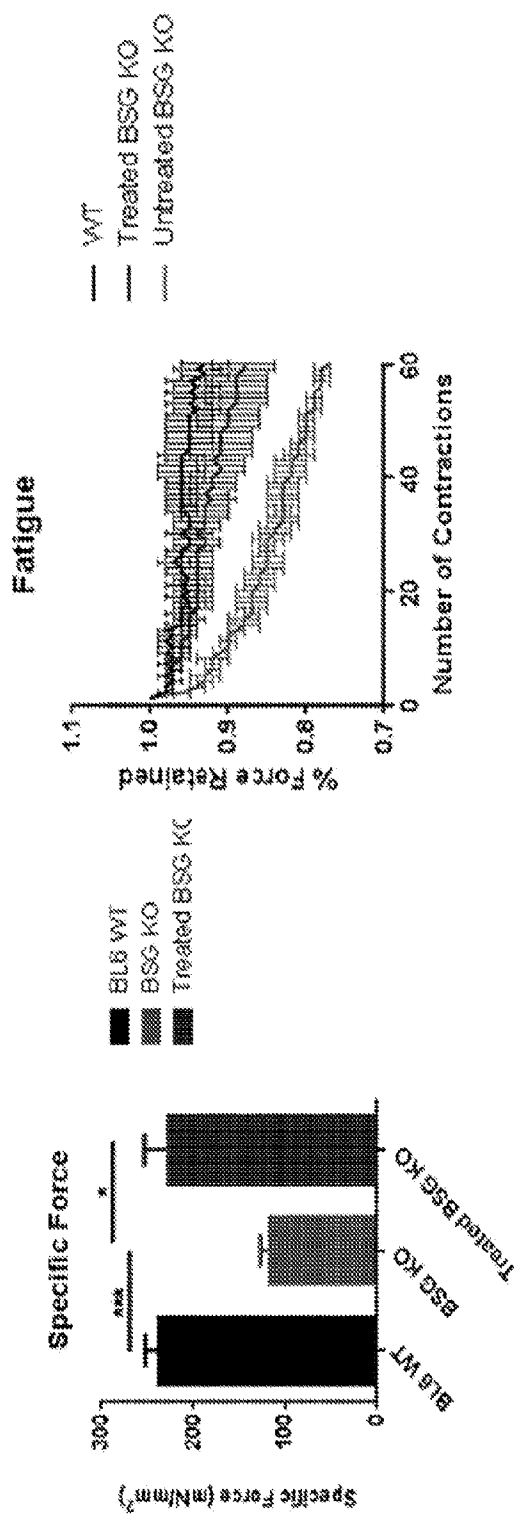


Figure 16



SEQ ID NO: 9: miR-29C IN A miR-30 BACKBONE

Figure 17

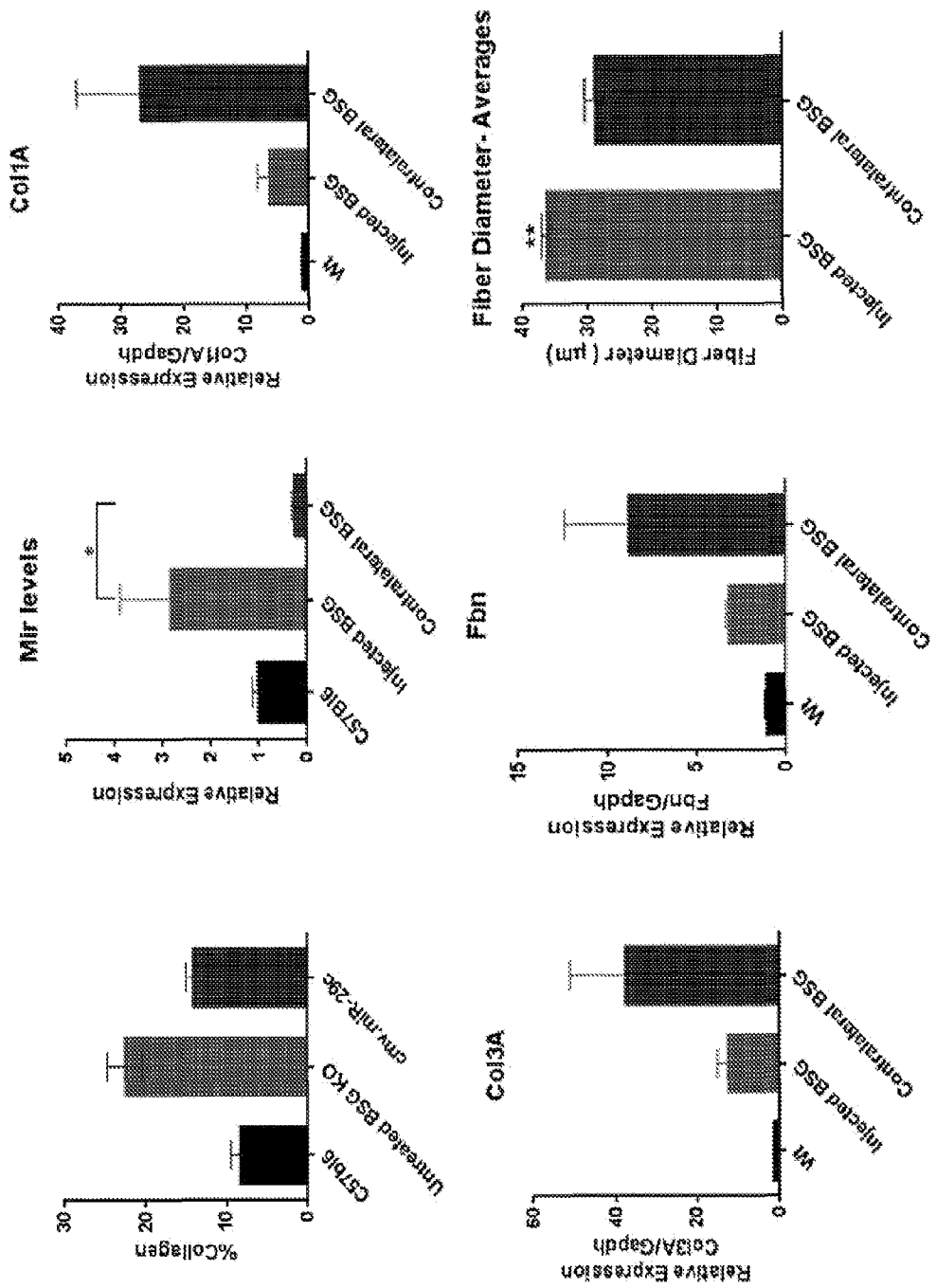
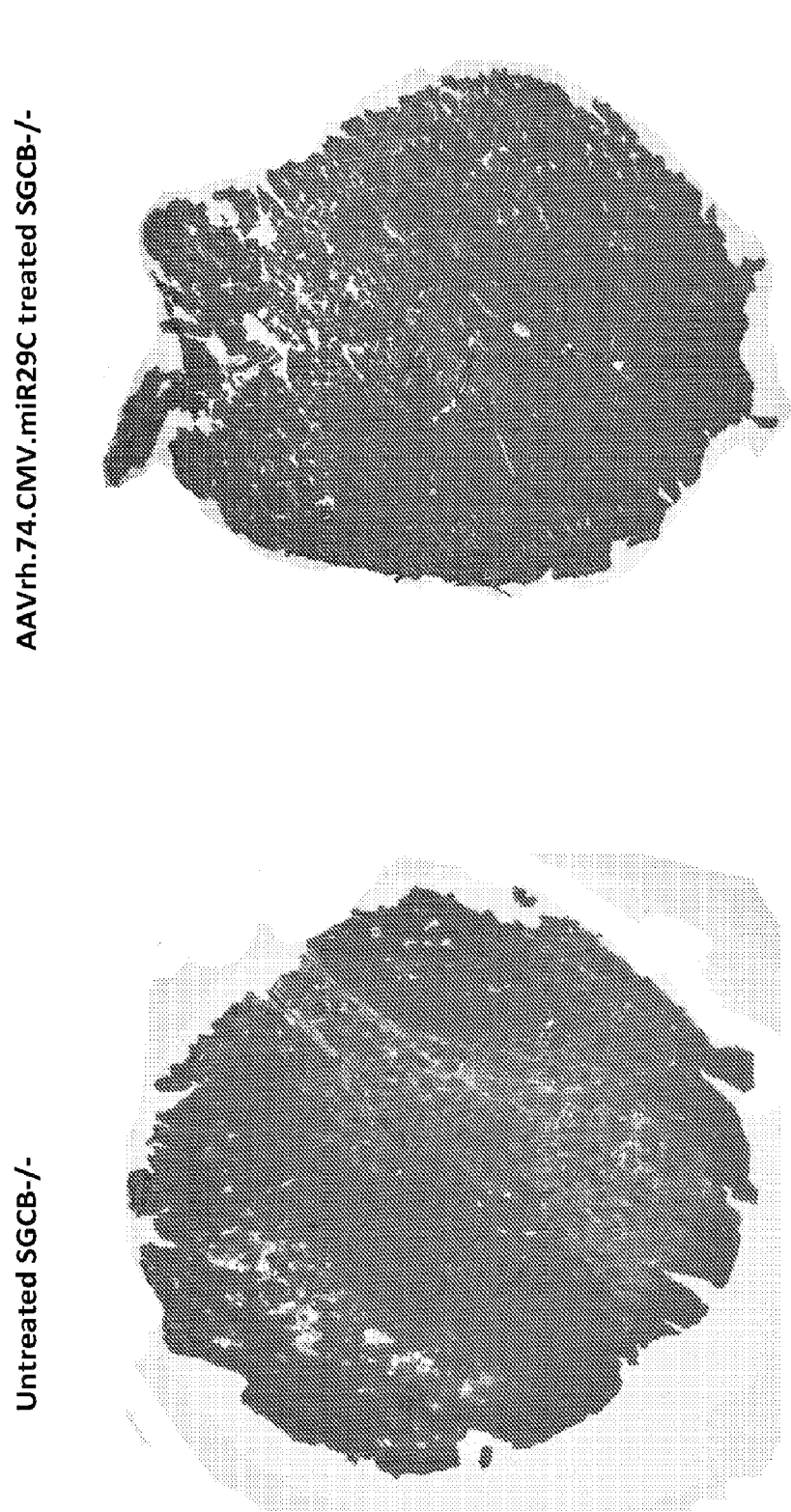


Figure 18



AAVrh.74.CMV.miR29C treated SGCB-/-

Figure 19A



Figure 19B

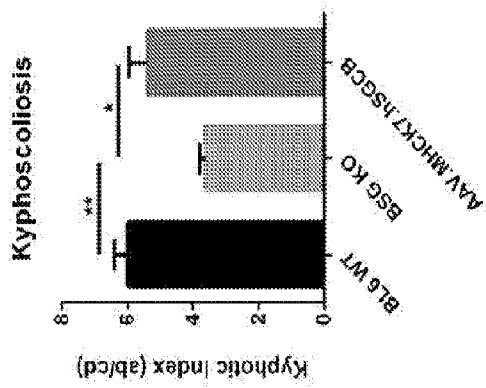


Figure 20A

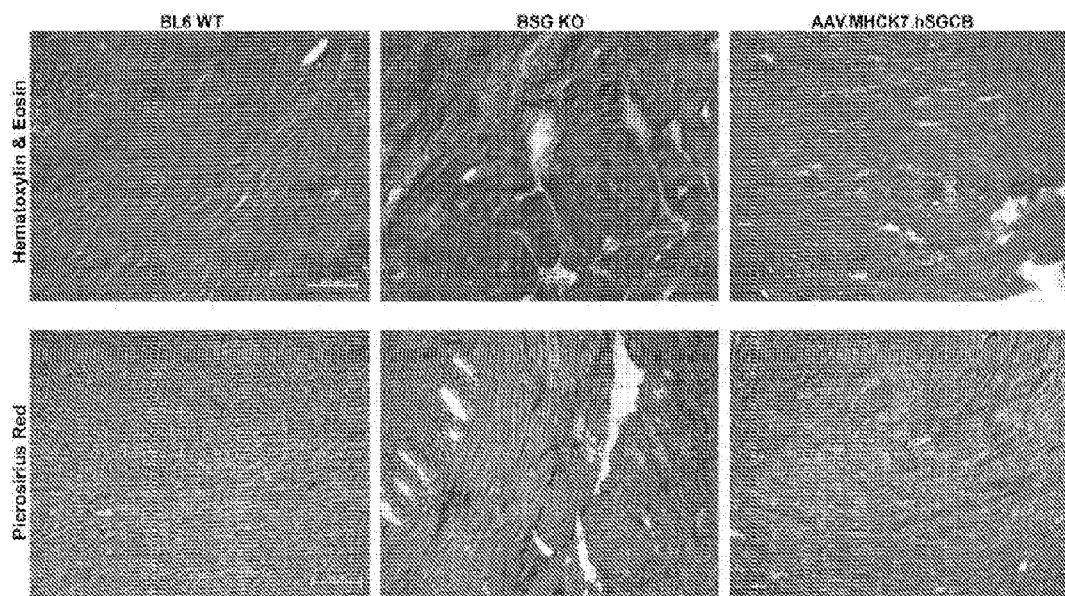


Figure 20B

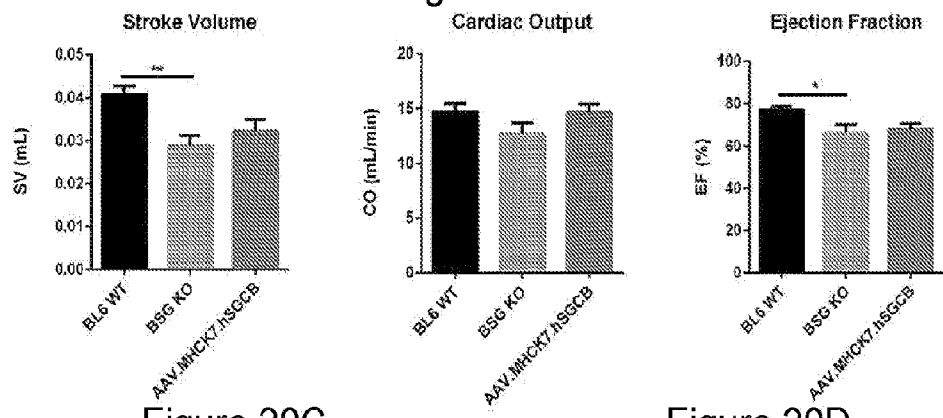


Figure 20C

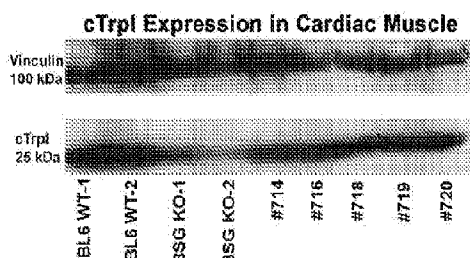


Figure 20D

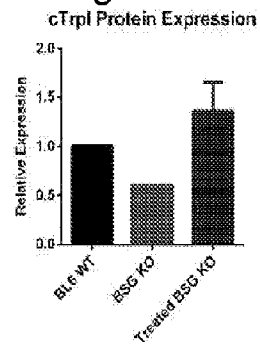


Figure 21A

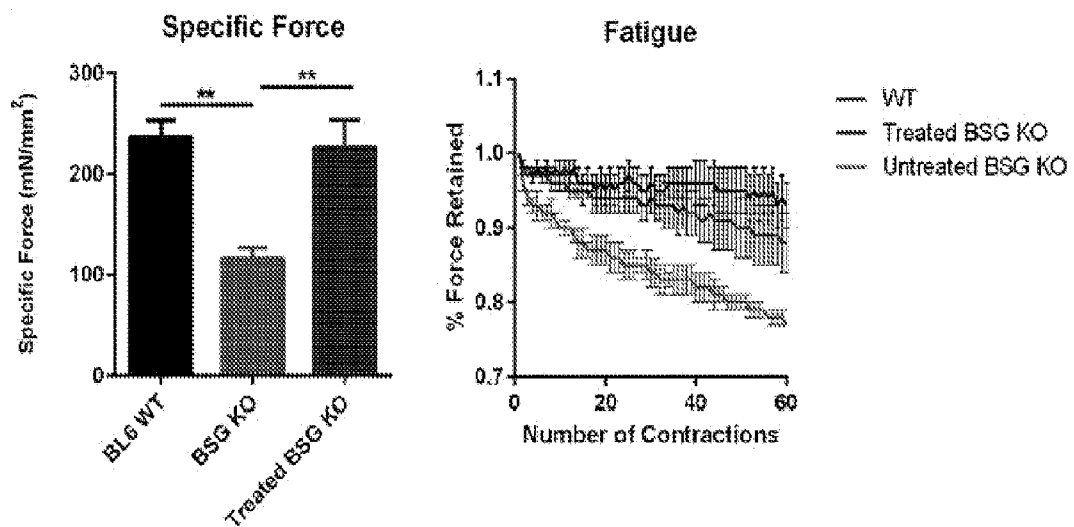


Figure 21B

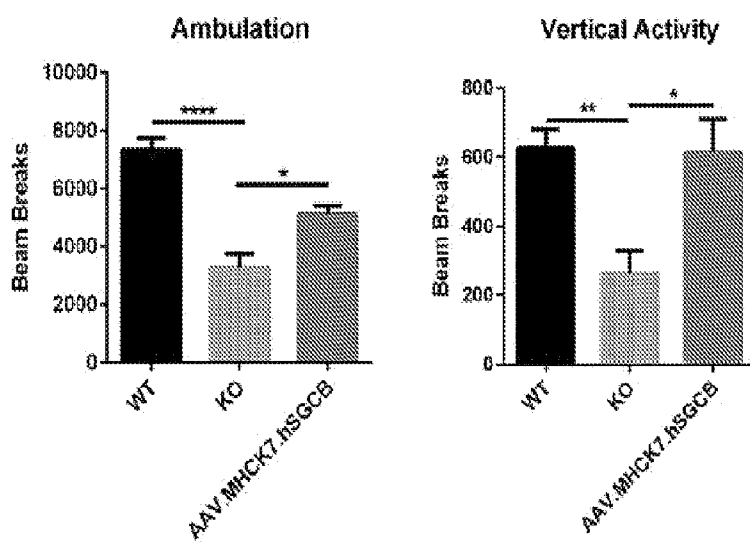


Figure 22A

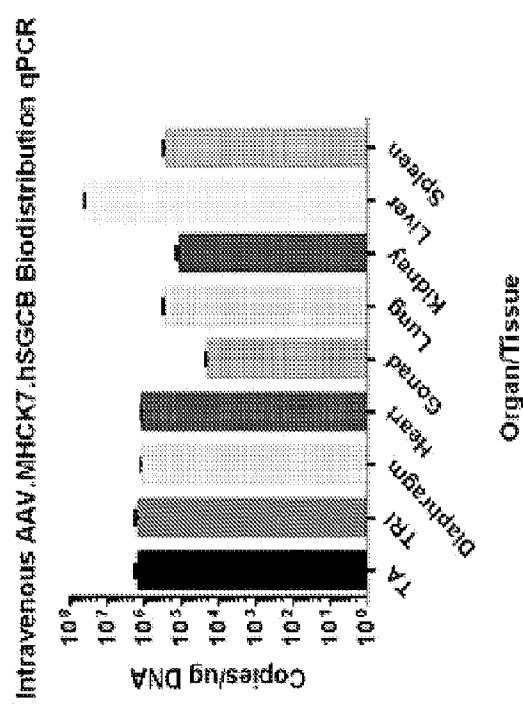
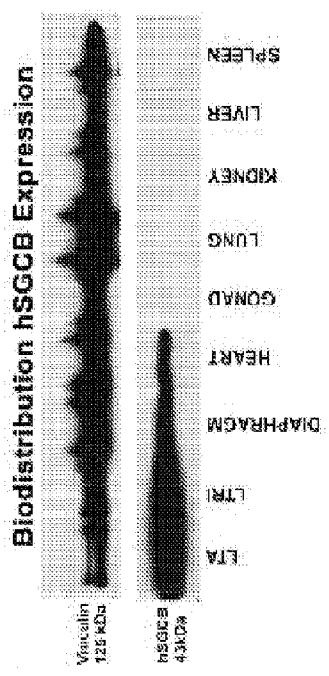


Figure 22B



SEKVENSLISTE

Sekvenslisten er udeladt af skriftet og kan hentes fra det Europæiske Patent Register.

The Sequence Listing was omitted from the document and can be downloaded from the European Patent Register.

